SYNOPTIC RÉGIMES IN THE LOWER ARCTIC TROPOSPHERE

DURING 1955

A Thesis

Presented to

The Faculty of Graduate Studies and Research

McGill University

In Partial Fulfillment

of the Requirements for the Degree

Master of Science

by

Cynthia V. Wilson, B.A.

Montreal, Que.

May 1958

TABLE OF CONTENTS

		PAGE
Preface		
List of Figures		(ii)
List of Tables		(iii)
List of Appendices		(iv)
Abstract		(v)
SYNOPTIC RÉGIMES IN THE LOWER ARCTIC TROPOSPHERE DURING 1955		1
1.	Introduction	2
2.	The Data	5
3.	Method: Specification and Comparison of Daily Charts	8
4.	Investigation over the Arctic During 1955	14
	(a) The Persistent Periods	19
	(b) Limited Value of Individual Terms in Expansion	30
5.	Discussion	35
6.	Summary	51
BIBLIOGRAPHY		55
Acknowledgments		58
APPENDIX A	Values of the Inter-Map Correlation Coefficients for One- and Two-Day Lags (January 1st, 1955 to January 6th, 1956)	
APPENDIX B	Periods of Persistence During 1955	
APPENDIX C	An Attempt to Relate Geomagnetic Indices to Sea-Level Circulation Changes	

LIST OF FIGURES

FIGURE		PAGE
1	The extent of the area and the orientation of the grid.	6
2	Monthly mean percent reductions based on mean yearly thresholds of 70%, 80%, 85% and 90%.	11
3	Monthly mean values of the estimated population variance	12
4(a)(b)	Percentage of the variance of the pressure patterns for day t_1 associated with the variance for day t_o	17-18
5	Daily percent reduction of variance, Z_{10}	31
6	Annual and seasonal mean percent reduction of variance from the individual coefficients	32
7	Annual and seasonal mean percent reduction of variance by polynomial degree	33
8(a)	Normal pressure distribution, April	40
8(b)	Thirty-day mean pressure distribution, April, 1955	40
9	Mean persistence correlations for days minus 12 to plus 19, for all 47 years (564 cases for each mean).(After Shapiro.)	44
10	Behaviour of $\bar{\hat{r}}_1$ before and after a sudden rise in C_i of ≥ 1.00	46
11	Barometric tendency during the 48-hour interval from March 12th - 14th	49
12	Barometric tendency during the 48-hour interval from April 5th - 7th	50
13	Behaviour of $\bar{\hat{r}}_1$ after Quiet and Disturbed key days	52
14	Behaviour of $\bar{\hat{r}}_1$ after Quiet and Disturbed key days (February data omitted)	53

LIST OF TABLES

TABLE		PAGE
I	Monthly and seasonal mean values of $\hat{r}_1^{\ 2}$ and $\hat{r}_2^{\ 2}$ (scaled by 100)	15
II	Dates of the periods of persistence and change during 1955	20-21
III	The frequency of the various lengths of run of persistence and change	22
IV	Mean length of run of persistence and change for the seasons and the year; percentage of total number of days in the seasons and for the year which are 'persistent'	23
V	Values for ($\hat{r}_\ell$) between the initial and subsequent days of each period compared with hypothetic values from the relationship $r_\ell = r_1^{\ell}$.	25-27
VI	Dates of the key days (when C_i increased by ≥ 1.00) and the 14th day after each key day	45

LIST OF APPENDICES

APPENDIX A

Table 1 Inter-map correlation coefficients, one-day lag ($\hat{r}_1$), January 1st, 1955 to January 6th, 1956.

Table 2 Inter-map correlation coefficients, two-day lag ($\hat{r}_2$), January 1st, 1955 to January 6th, 1956.

Fig. 1 Graphs showing the change with time of the inter-diurnal correlation coefficients $\hat{r}_1$ and $\hat{r}_2$.

APPENDIX B

Maps 1-28 Mean maps for periods of persistence over the Arctic at sea-level in 1955.

APPENDIX C

Table 1 Mean persistence correlations (one-day lag) from 12 days before to 19 days after the key days.

Table 2 Key days in 1955: the five Quietest and five Most Disturbed key days for each month during 1955.

Table 3 Behaviour of $\bar{\hat{r}}_1$ after the five Quietest days of each month.

Table 4 Behaviour of $\bar{\hat{r}}_1$ after the five Most Disturbed days of each month.

SYNOPTIC RÉGIMES IN THE LOWER ARCTIC TROPOSPHERE

DURING 1955

Synoptic Régimes in the Lower Arctic Troposphere During 1955

1. Introduction

During the past five years the continuous flow of data from the Arctic region has made possible a more reliable daily synoptic analysis both for the surface and upper levels. Much work has already been done to establish the monthly and seasonal broad-scale features of the lower and mid-troposphere, and to study in greater detail the perturbations.

In 1952[1] the Extended Forecasting Section of the United States Weather Bureau published a revised version of their monthly normal maps for the northern hemisphere. The previously hypothetical analysis over the Arctic had been modified in this new edition by the incorporation of the more reliable 1946-50 mean values and by checks against the maps of Baur (1929), Dzerdzeevskii (1946) and Dorsey (1949) — maps drawn up after careful consideration of all previous expedition data. As a further check, in 1956[2] this Section compiled eight-year (1948-55) mean maps for January, April, July and November, for the surface and 700 mb. levels, to study deviations from the 1952 normals. The chance of climatic fluctuations in so short a period and the greater weight of the observations from 1952-55 make such deviations difficult to interpret. The results showed one to four mb. differences in intensity, especially over the polar basin, where observations are at a minimum, but the major features were not significantly different from those of the 1952

---

[1] Normal Weather Charts for the Northern Hemisphere. Technical Paper No. 21, U.S. Department of Commerce, Weather Bureau, Washington, D.C., October,1952.

[2] Namias, J., "General Circulation of the Lower Troposphere over Arctic Regions and its Relation to the Circulation Elsewhere". Paper delivered before the AGARD Symposium on Polar Atmosphere, Oslo, Norway, July 2-7, 1956.

normals. Within these limits the monthly broad-scale features of the pressure field in the lower troposphere are considered to be well established over the Arctic, especially in winter when the major features are more deeply set.

Observers in the Arctic before World War II had reported a high degree of variability in the elements recorded. They had concluded that in spite of certain preconceived ideas concerning a polar anticyclone, there was, in fact, great variety of synoptic activity, and that storms similar to those of mid-latitudes were present at all seasons. The new data have substantiated these ideas. It was possible to make a tentative climatological estimate of the arctic circulation before the early 1950's, but there was no chance of breaking down these mean distributions into their components. Since 1952 case studies have been made, such as those on polar vortices by Reed and Tank (1956) and on anticyclogenesis in Alaska by Bodurtha (1952). On a broader scale, Keegan (1957) has examined the surface frequency of cyclones and anticyclones north of 60°N, their development and motion over a period of nine winter months, December, January and February, 1952-55. Separate maps showing the frequency of centres of highs and lows are presented, which are then divided into zones, each containing a cyclonic or anticyclonic frequency maximum; the synoptic features in each of these regions and their displacements are carefully analysed and classified, and interrelationships are considered.

One question which is not covered by any of these approaches is whether these synoptic situations tend to group themselves into régimes or whether there is in fact a normal fluctuation about the mean. In averaging over arbitrary periods it may happen that significant large-scale patterns in time are being lost. Furthermore, if these régimes do exist in the Arctic, what is the nature of the change from one régime to the next? In mid-latitudes, Baur (1951) introduced the idea of a Grosswetterlage, which he defines as "the mean pressure distribution (at sea-level) for a time interval during which the position of the stationary (steering) cyclones and anticyclones and the steering within a special circulation region remain essentially unchanged". Baur divided the northern hemisphere into five cells and for each he isolated a number of Grosswetterlagen. The mid-tropospheric circulation is broken down into three zonal and four meridional types, which apply to every zone. Other mid-latitude evidence of the tendency for the circulation to persist in certain overall patterns, then to break down, is given by the index cycle as described by Willett (1944), the phenomenon of blocking (Rex, 1950, 1951) and the many studies both from Europe and America on singularities.

Sutcliffe (1954), writing on predictability in meteorology, points out that many natural systems are open, "defined by coherence in structure or organization", that they have a finite life span and they are complex, in that "each system may be broken down into natural sub-systems of smaller scale and, generally, with shorter individual lives".[3] He then selects from a hierarchy of systems and sub-systems, five of increasing scale:

(a) micro-meteorological systems
(b) sub-synoptic systems
(c) small synoptic systems
(d) large synoptic systems
(e) the atmospheric system as a whole.

The Grosswetterlagen of Baur, like the centres of action of Tesserenc de Bort, the natural periods of Multanovsky, the five-day mean patterns used by the Extended Forecasting Group in Washington and the large-scale circulation of Bjerknes are all on the scale of Sutcliffe's large synoptic systems, that

[3] Sutcliffe, R.C., "Predictability in Meteorology", Archiv für Meteorologie, Geophysik und Bioklimatologie, Serie A, Vol. 7, 1954, p. 7.

is, large-scale components of the general circulation. Considering them further, Sutcliffe continues:

> "Although there is no clear-cut break in the spectrum of scale of synoptic systems, it is generally possible, in extra-tropical latitudes, to distinguish two scales at any one time with the smaller-scale systems moving through the larger-scale. This fact of organization is largely responsible for the conception of large-scale synoptic types which persist usually for a few days and may persist for weeks."[4]

In studying these large synoptic systems, the main problem is that of defining them both in space and time. It is a question of finding

(i) an objective means of isolating and describing the systems from the daily charts;

(ii) a quantitative measure over the area as a whole, which will filter out the periods in which these large-scale patterns persist from periods of change, and if possible give some indication of the nature of the breakdown.

Mean circulation patterns can then be set up for the more stable situations, with the addition of tracks of the main high and low centres to indicate small-scale synoptic activity within that time.

This study is an attempt to tackle this problem over the Arctic, using 1955 as a test year.[5] As yet this work has been restricted to sea-level, but data have already been prepared for the 500 mb. level over the same period of time. These have not yet been analysed, but it is hoped to extend the investigation to these data shortly. Fig. 1 shows the area under consideration.

2. The Data

The data consisted of the daily synoptic weather charts for sea-level

---

[4] *Ibid.*, p. 10.

[5] Owing to the labour involved in data preparation, 1955 formed the basis of most of the work by the Group.

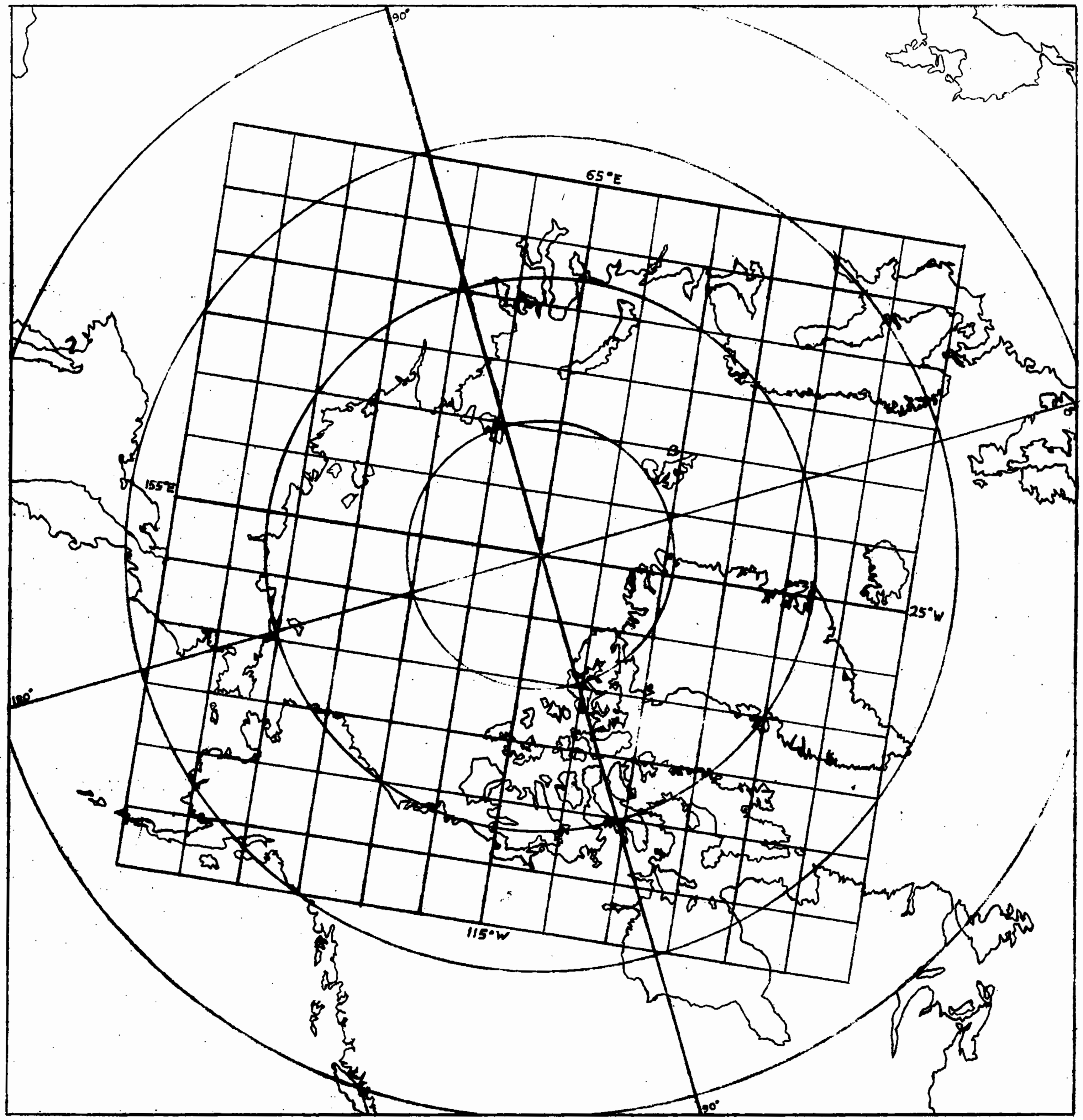

Figure 1. The extent of the area and the orientation of the grid.

and 500 mb., analysed by the Arctic Forecast Team of the Canadian Meteorological Division in Edmonton, for the year 1955. With the almost daily increase in the amount of synoptic data over the Arctic, it was considered more reasonable to work on a current basis when the McGill Group was set up at the end of 1954 than to use the checked Historical Series for earlier years. The Edmonton analysts focus their attention on the arctic area, and the Group considered their maps excellent. However, these maps are an operational series, and as such are liable to occasional omissions of data. Keegan (1957) has shown effectively how much importance is to be placed, for example, on ice island data, and that considerable error can be introduced when there is no such observation over the central Arctic. During the period studied there was at least one report from the central Arctic on each chart, although there were some twenty days, mainly in winter, when East Siberian coastal stations between Chetyrekhstolbowyi (965) and Kap Tscheljuskin (292) were missing. The poorest coverage at all seasons is over eastern and central continental Siberia.

In such areas there must be considerable dependence on historical continuity in the analysis, and the resulting circulation patterns are often broad. This may be just a reflection of the more uniform surface conditions over large continental expanses, but in a study of persistence it is debatable to what extent it is historical continuity rather than true persistence that is being shown. When verifying his Arctic forecasts, Estoque (1957) computed the interdiurnal correlation coefficients for the Siberian European Sector and the American zone separately; on the six occasions when the values were lower over Siberia, there were more observations than usual, and the circulation patterns were more complex. The direct use of station data would overcome this dependence on the analysis, but the method used in this investigation demanded observations from equally spaced grid points.

3. Method: Specification and Comparison of Daily Charts

The grid employed (Fig. 1) was orientated to extend furthest south into the major centres of the winter normal patterns (Hare, Scientific Report No. 3, 1957). The charts are on a Polar Stereographic projection 1:12,500,000, true at 60°N., and the grid interval averages 300 miles. Keegan found that the size[6] of cyclones north of 60°N. averaged about 550 miles in diameter with a mean speed of 400 nautical miles (460 miles) a day, with corresponding figures for the average anticyclone of 890 miles and 310 nautical miles (350 miles) a day. From these evaluations it seemed reasonable to expect a good representation of the large-scale synoptic patterns, but the grid was too coarse for a consistently reliable specification of the small-scale synoptic systems. A comparison using various grid sizes would be interesting, but in this region, the use of a narrow mesh would probably not be statistically sound with so few observations.

Within these limits a comparison between any two charts can then be obtained in a single variable by computing the correlation coefficient between the two sets of values, where

$$r_\ell = \frac{\left[\overline{W_{ij}(t_o)\, W_{ij}(t_\ell)} - \overline{W_{ij}(t_o)}\ \ \overline{W_{ij}(t_\ell)}\right]}{\sigma W_{ij}(t_o)\ \ \sigma W_{ij}(t_\ell)} \tag{1}$$

W_{ij} = the pressure (or geopotential) reading at grid point $x_i\ y_j$;

t_o = the initial day's chart;

t_ℓ = a subsequent chart of lag ℓ.

[6] Keegan (1957) defines size as the "average diameter of the largest closed sea-level isobar of the cyclone or anticyclone".

This is, however, a very laborious task if the correlation is to be computed over any reasonable period of time and for more than one lag, and the possibility of making this study really depended on the easier methods employed in the main specification programme of the McGill Group.

For the year 1955, the series of daily surface and 500 mb. charts had already been specified, using a technique first applied by Wadsworth, Bryan and Gordon (1948) at Massachusetts Institute of Technology. The method and performance in relation to the arctic area are described in detail in Scientific Report No. 3 (1957) and Supplement No. 1 to that report (1957).

The aim in specifying these maps was to describe them analytically, so that they could be handled more simply and efficiently. This was done by calculating the correlation coefficient between the pressure topography of each chart and a series of hypothetical surfaces. In this programme the surfaces were those of the terms of a Tchebycheff orthogonal expansion of two space variables.

Once these coefficients had been evaluated, they could be used to compute the correlation coefficient between any two charts. Since the space mean had already been removed and the coefficients had been divided by a measure of the standard deviation, equation (1) could be replaced by

$$r_{\ell} = \sum_{r=0}^{n-1} \sum_{s=0}^{n'-1} Z_{rs}(t_o)\, Z_{rs}(t_{\ell}) \qquad (2)$$

(the product applying to like powers only), in which

r, s, are the degrees of the polynomial in x and y;

n, $n' = 13$;

Z_{rs} is the standardised coefficient of the orthonormal functions.

However, a good approximation to the daily pressure patterns had been obtained by computing only the first 48 Z_{rs} out of the possible 168, so that

$$\hat{r}_\ell = \sum_{r=0}^{6} \sum_{s=0}^{6} Z_{rs}(t_o)\, Z_{rs}(t_\ell) \tag{3}$$

and equation (3) forms the basis of this study.

The chief advantage of this method over the point-by-point correlation (equation (1)) is that far less computation is involved. On the other hand, the estimates of $\hat{r}_\ell$ must be interpreted with some caution. These approximations depend, for example, on:

(i) the total reduction of variance of the daily pressure patterns concerned. Since the number of Z_{rs} has been reduced to 48,

$$\sum_{r=0}^{6} \sum_{s=0}^{6} {Z_{rs}}^2 \neq 1 \tag{4}$$

(ii) the number of the Z_{rs} which were statistically significant for each chart;

(iii) the over-all variability, S^2, of the pressure surface on each occasion.

Considering these points in relation to the surface charts:-

(i) From the 48 Z_{rs} the daily percent reduction of variance (equation (4) scaled by 100) averaged 95 for the year, and only in June did the monthly mean value fall below 90 (Fig. 2). Eight days in the year lay below the 85% threshold, including three below 80%, the minimum value being 69. Wadsworth, Bryan and Gordon reversed the process and reconstructed a series of charts to test the effect of the approximation. Their results showed that the large-scale patterns, although somewhat simplified, were quite adequately represented when the reduction of variance was 80%.

(ii) In this study a standard number of Z_{rs} was employed and it may well be that many of the higher powers were not significant (Lorenz, 1956), bearing in mind the coarse grid that was used and the paucity of observations over

Figure 2

SURFACE
Monthly Mean Percent Reductions Based on
Mean Yearly Thresholds of 70%, 80%, 85%, 90%.

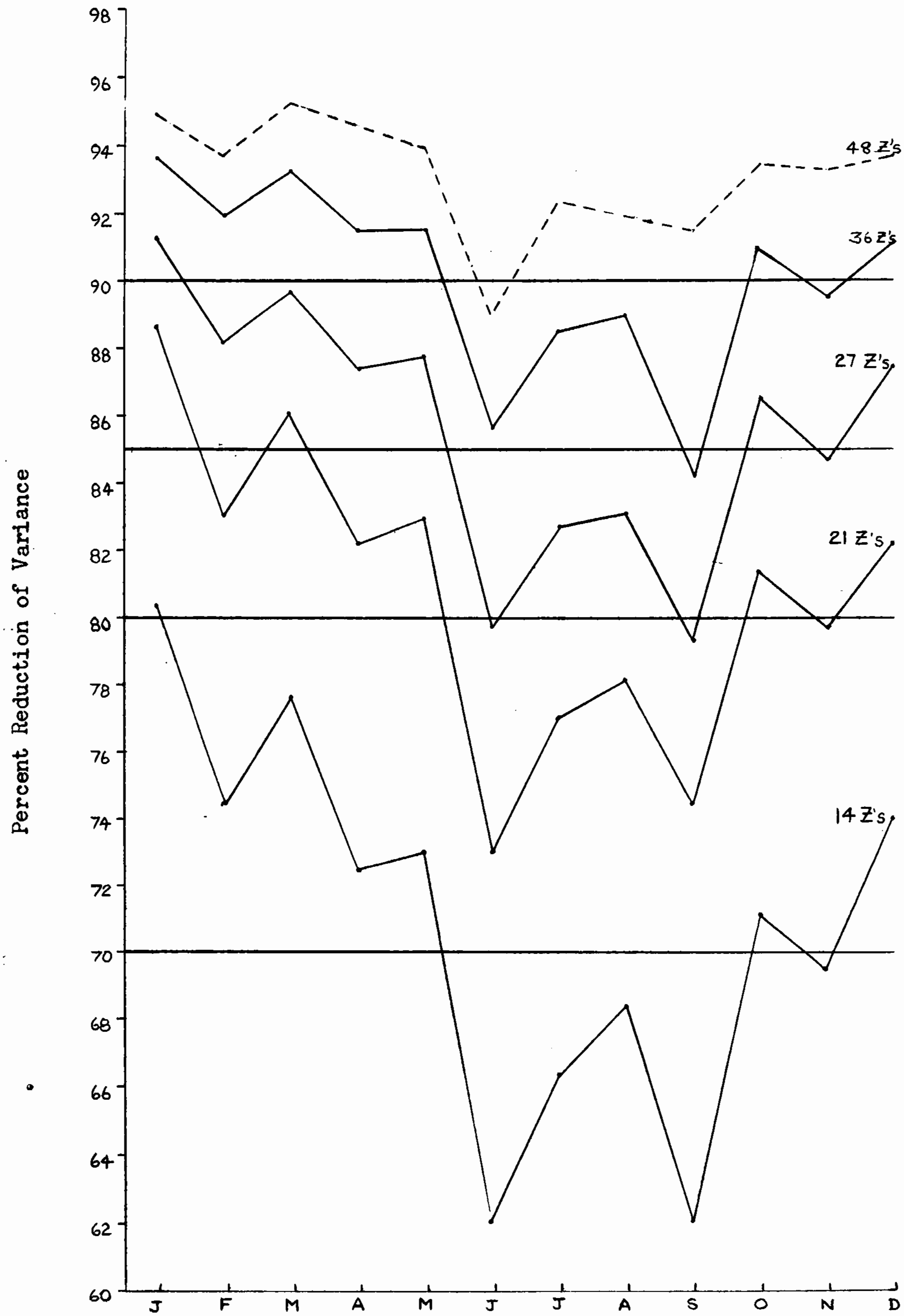

(Reprinted from Supplement No. 1 to Scientific Report No. 3 (15)).

much of the arctic area. Fig. 2 shows the monthly mean percent reductions based on mean yearly thresholds of 70%, 80%, 85% and 90%. From this analysis, it is suggested that the use of 36 Z_{rs} might have been sounder statistically.

(iii) The poorest specification appears to be associated with the flatter and/or more cellular pressure patterns. For example, the June charts reveal a series of rather amorphous features. This raises the question of the relationship between the degree of specification and the variance of the pressure pattern. Fig. 3 shows the strong seasonal trend in the curve of the monthly mean variance, the values ranging from 226 mb.^{2} in January to 54 mb.^{2} in both June and July.

Fig. 3

Monthly mean values of σ^2, the estimated population variance;

$$(\sigma^2 = S^2/nn'-1 = S^2/168)$$

Since the coefficients were standardised by dividing by S, where

$$S = \left[\sum_{i=1}^{13}\sum_{j=1}^{13} (W_{ij} - \overline{W_{ij}})^2\right]^{\frac{1}{2}} \quad = \text{the root sum-squared deviation (5)}$$

the $\hat{r}_\ell$ estimates should perhaps have been weighted at least seasonally with respect to the variance. In this respect, Wadsworth, Bryan and Gordon suggest that an interdiurnal correlation of 0.600 in summer may be less significant than 0.400 in winter, when the patterns are bolder. "With the usual flat summer map, it is very easy to distribute the residual variance in such a way as to obtain many entirely different looking maps all with the same reasonably high correlation with the base maps."[7]

An attempt was made to begin to correct the $\hat{r}_\ell$ values, but there were so many unknown factors involved in this approximation, that it was considered best to leave them uncorrected rather than to introduce further possible discrepancy. To a certain extent errors caused by (i) and (ii) might have compensated. However, the summer values should be handled with reservation.

Within these limitations $\hat{r}_\ell$ is a rough measure of the persistence of the circulation patterns from time t_o to t_ℓ. By calculating a time series of values for ℓ = 1 day, ℓ = 2 days, etc. throughout the year, it should be possible to filter out objectively periods when the large-synoptic systems persist from those characterised by breakdown and change. Once the beginning and end of each period of high autocorrelation has been established, the coefficients between the initial and subsequent days in each case should give some indication of the rate of the internal fall in persistence with respect

---

[7] Wadsworth, G.P., Bryan, J.G. and Gordon, C.H., "Short Range and Extended Forecasting by Statistical Methods", Air Weather Service Tech. Rep. No. 105-38, 1948, p. 186.

to time.

In summary, the advantages of this method for this particular study include:-

(i) the small number of parameters required to describe the charts and the ease with which the inter-map correlation coefficients can be computed;

(ii) the opportunity to filter out the large-scale patterns through the approximation itself, for only the simpler surfaces are fitted;

(iii) a chance to break down the total correlation into components — the individual Z_{rs}, and the column (x) and row (y) and interaction (x,y) groups of Z_{rs} — to analyse the nature of the persistence and change. It was hoped that the observed cellularity of the patterns over the Arctic might have resulted in these particular surfaces being especially suitable;

(iv) other surfaces can be specified for comparison.

However, the general efficiency of the method depends ultimately on the applicability of the particular surfaces to the regional pressure systems. Are these polynomial surfaces suited to the states and changes of the arctic circulation? For mid-latitudes, these coefficients $\hat{r}$ have been used in extensive analogue studies by Wadsworth, Bryan and Gordon, and by Shapiro (1954, 1956) in an investigation of the effect of extraterrestrial impulses on the atmospheric circulation. The McGill Group's experience is that they function at least as well in high latitudes, in spite of the different (i.e., non-zonal) nature of the organized circulations.

4. Investigation over the Arctic during 1955

The inter-map correlation coefficients $\hat{r}_\ell$ were computed at the surface level for a one-day lag (i.e., $\ell = 1$) and plotted through the year (Appendix A). Perhaps the degree of persistence implied by these coefficients is more graphically expressed by

$$\left[\hat{r}_{\ell}^{\,2}\right]100 \qquad (6)$$

i.e., the percentage of the variance of the chart for t_{ℓ} which is dependent on the variance of the pressure pattern for t_o. Therefore a correlation coefficient of 0.800 produces a similarity between maps of 64%, whilst

$$\left[1 - \hat{r}_{\ell}^{\,2}\right]100 \qquad (7)$$

i.e., 36% of the variance in t_{ℓ} is independent of t_o and represents change. Table I gives the monthly and seasonal mean values of $\left[\hat{r}_1^{\,2}\right]100$.

Table I

	J	F	M	A	M	J	J	A	S	O	N	D
$\left[\hat{r}_1^{\,2}\right]100$	68	51	57	56	56	43	51	46	47	46	44	53
$\left[\hat{r}_2^{\,2}\right]100$	51	29	31	30	31	18	26	21	21	20	19	27

	Summer (May-Sept)	Winter (Oct-April)	June-November	December-May	Annual
$\left[\hat{r}_1^{\,2}\right]100$	49	54	46	57	52
$\left[\hat{r}_2^{\,2}\right]100$	23	30	21	33	27

The curve shows several interesting features:-

(i) The high level of correlation throughout the year (annual mean $\left[\hat{r}_1^{\,2}\right]100 \doteq 52$), possibly reflecting the stabilising effect of predominantly anticyclonic conditions over the area as a whole, although 1955 was a year of considerable cyclonic activity over the central Arctic.

(ii) The tendency for the arctic circulation to persist during 1955 at a high level of interdiurnal correlation, and then to change rapidly; this suggests that there may be certain preferred states to which the atmosphere may return and/or certain preferred paths which the small-scale systems may take.

(iii) The absence of low plateaus in the curve, the steepness of the troughs showing a sudden rapid change to the next period of persistence.

(iv) The difference in the curve between the first half of the year (January to early June) and the latter half. Table I shows lower average values from June to November and there is a lack of the very clear-cut plateau and trough pattern of the first six months. This latter half of the year coincides to a considerable extent with the period of change in snow and ice cover, the season of maximum heating followed by gradual cooling when conditions are least stable.

(v) An approximate 14-15 day period can be seen in the January to May season, but during the latter six months of the year there is little hint of any regularity.

(vi) The only approach to a run of low values occurs in mid-June. The lowest value of $\hat{r}_1$ for the year is that for June 25th-26th. It is interesting that this should occur during the period of monsoonal change in other regions of the northern hemisphere. It is hoped that it will be possible to consider this further when the upper air data are analysed.

Fig. 4(a) shows the frequency of $\left[\hat{r}_1^{\,2}\right]100$ during the seasons and for the year, while Fig. 4(b) shows for comparison the first and second six months of the year. There is an intensification of the "summer" and "winter" distributions — a continuation of the summer conditions into November. The form of the curve for the one-day lag was encouraging; therefore, in order to attempt to find a measure of the beginning and end of each run of high persistence, the two-day inter-map correlation coefficient $\hat{r}_2$ was computed over the same period of time. The curve has been plotted above the one-day lag values in Appendix A, and Table I shows the monthly, seasonal and annual means of $\left[\hat{r}_2^{\,2}\right]100$.

This curve paralleled that for the one-day lag, at a lower level of

Fig. 4(a)
Percentage of the Variance of the Pressure Patterns for Day t_1
Associated with the Variance for Day t_o

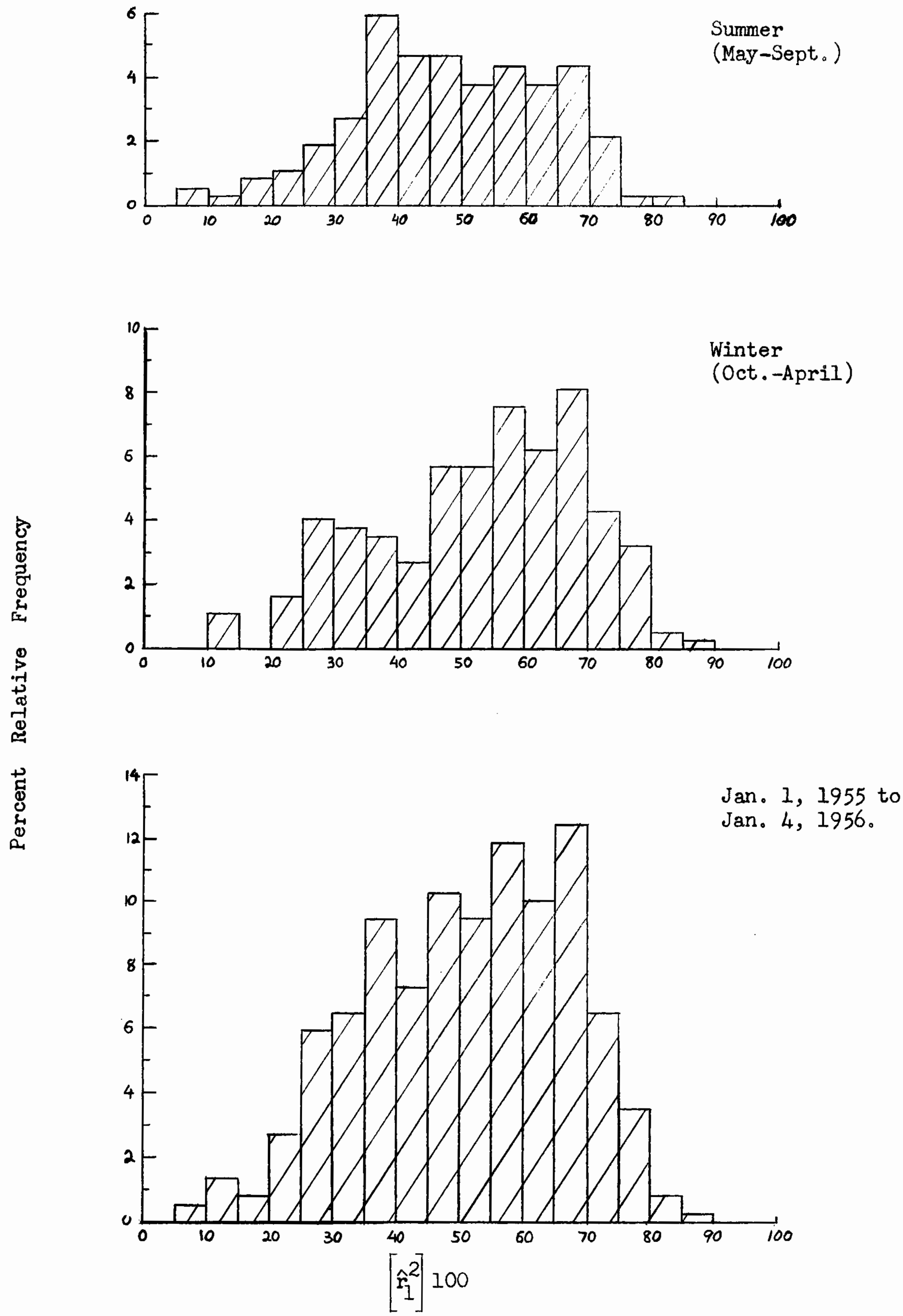

Fig. 4(b)
Percentage of the Variance of the Pressure Patterns for Day t_1
Associated with the Variance for Day t_o

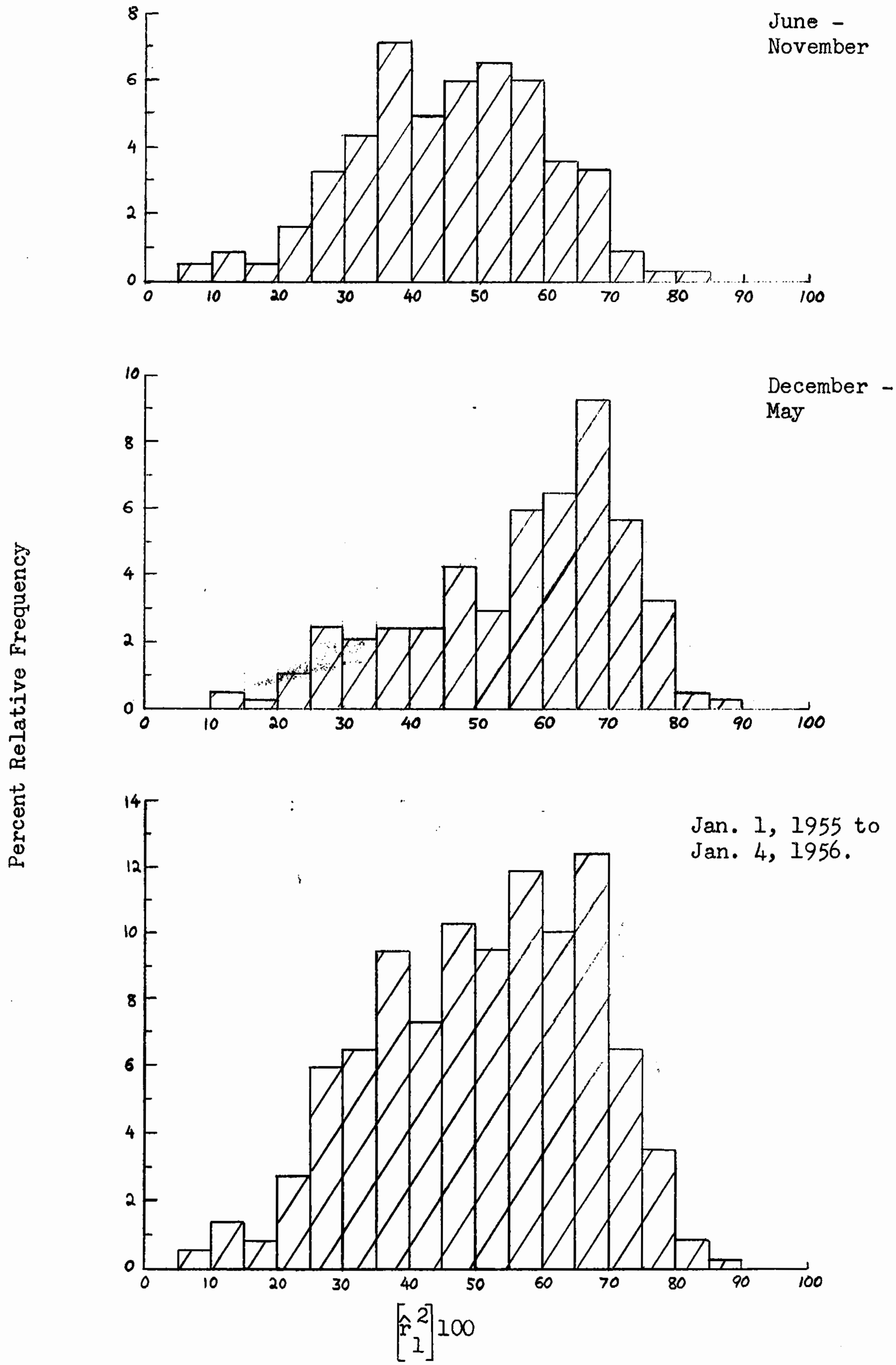

persistence, and it would have been interesting to compare values for $\hat{r}_3 \ldots\ldots \hat{r}_n$ where n is the number of days at which the curve breaks down. Owing to the amount of computation involved, three arbitrary definitions of persistence were set up, differing in degree, which use the first two lags only.

Type[8] A where $\hat{r}_1 \geq 0.800$ and $\hat{r}_2 \geq 0.700$

Type B where $\hat{r}_1 \geq 0.700$ and $\hat{r}_2 \geq 0.600$

Type C where $\hat{r}_1 \geq 0.700$ and $\hat{r}_2 \geq 0.500$

The lower thresholds of $\hat{r}_1$ and $\hat{r}_2$ coincided approximately with the year's mean and the 0.700 level for $\hat{r}_1$ was felt to be reasonably conservative (Figs. 4(a) and 4(b)). The lower level for $\hat{r}_2$ allowed a 75% change between maps, which might have been too low; however, Wadsworth, Bryan and Gordon set a lower limit of $\hat{r}$ at 0.38 in their analogue study and this proved to be practical. A minimum duration of four days above these thresholds was set.

(a) The Persistent Periods

Based on these criteria, twenty-eight periods of persistence of the large-scale pressure systems were isolated (Table II). For each of these runs the mean circulation patterns were set up by computing the mean pressure values at each grid point for the days concerned. The twelve-hourly positions of the main centres of highs and lows were then superimposed to indicate the synoptic activity during each period. Appendix B comprises this set of mean pressure distributions together with a brief commentary.

Throughout the year and seasonally the average run of persistence lasted about six days (Tables III and IV), the longest duration being eleven days

---

[8] These types refer only to the thresholds reached and not to the synoptic patterns.

<u>Table II</u>

PERSISTENCE CHANGE

MAP NO.*	DATES		TYPE	LENGTH OF RUN	DATES		LENGTH OF RUN
					Jan.	1-10	10
1	Jan.	11-20	A	10			
					Jan.	21-23	3
2	Jan.-Feb.	24- 3	A	11			
					Feb.	4	1
3	Feb.	5- 8	A	4			
					Feb.	9-15	7
4	Feb.	16-19	B	4			
					Feb.	20-26	7
5	Feb.-Mar.	27- 4	C	6			
					Mar.	5-7	3
6	Mar.	8-11	C	4			
					Mar.	12-15	4
7	Mar.	16-25	B	10			
					Mar.	26-29	4
8	Mar.-Apr.	30- 5	B	7			
					Apr.	6	1
9	Apr.	7-10	B	4			
					Apr.	11-18	8
10	Apr.	19-22	B	4			
					Apr.	23-26	4
11	Apr.-May	27- 5	B	9			
					May	6-8	3
12	May	9-19	B	11			
					May	20-22	3
13	May	23-27	C	5			
					May	28-31	4
14	June	1- 4	B	4			
15	June	5-10	C	6			
					June	11-26	16
16	June-July	27- 1	C	5			
					July	2-5	4
17	July	6-11	B	6			
					July	12-17	6
18	July	18-21	B	4			
					July	22-27	6
19	July	28- 3	C	7			
					Aug.	4-7	4
20	Aug.	8-11	C	4			
					Aug.	12-18	7
21	Aug.	19-23	A	5			
					Aug.-Sept.	24- 2	10
22	Sept.	3-7	B	5			
					Sept.	8-26	19

(*Appendix B)

(continued)

Table II (continued)

PERSISTENCE CHANGE

MAP NO.	DATES		TYPE	LENGTH OF RUN	DATES		LENGTH OF RUN
23	Sept.	27-30	C	4			
					Oct.	1-2	2
24	Oct.	3-7	B	5			
					Oct.	8-28	21
25	Oct.-Nov.	29-1	B	4			
					Nov.-Dec.	2-5	34
26	Dec.	6-10	B	5			
					Dec.	11-14	4
27	Dec.	15-20	C	6			
					Dec.	21-27	7
28	Dec.-Jan.	28-4	A	8			

. . . .

in January and again in May. The highest consecutive values (Type A) occurred in December, January and February, with an isolated summer case in August. During the three winter months there is the combined effect of the ice acting as a stabiliser and the polar night, while in 1955 these months were also characterised by strong blocking activity. August, however, was a month when these conditions were reversed. The August 19th-23rd period of high inter-map correlation occurred during a time when the polar vortex had contracted abnormally and the polar westerlies reached record values.

In general (Table IV), there appeared to be no seasonal difference in the relative number of periods of persistent situations. It is interesting to note the high percentage of days (almost 50%) of both the year as a whole and of the seasons, on which there was apparently so little change in the large-scale systems. Again, the sharper contrast was between the first and second six months rather than the seasons. The spring month of May revealed

Table III

The Frequency of the Various Lengths of Run of Persistence and Change

PERSISTENCE

Length of Run	Oct/Apr Winter	May/Sept Summer	Dec/May	June/Nov	Year
4	6	4	5	5	10
5	2	4	2	4	6
6	2	2	2	2	4
7	1	1	1	1	2
8	1	0	1	0	1
9	1	0	1	0	1
10	2	0	2	0	2
11	1	1	2	0	2

CHANGE

Length of Run	Oct/Apr Winter	May/Sept Summer	Dec/May	June/Nov	Year
1	2		2		2
2	1			1	1
3	2	2	4		4
4	4	3	5	2	7
5					
6		2		2	2
7	3	1	3	1	4
8	1		1		1
9					
10	1	1	1	1	2
16		1		1	1
19		1		1	1
21	1			1	1
34	1			1	1

These frequencies are biased by the arbitrary lower limit of 4 days in defining the periods of persistent situations.

Table IV

	Oct/Apr Winter	May/Sept Summer	Dec/May	June/Nov	Year
Number of days in the season	* 221	* 148	186	183	* 369
Number of days of persistence	101	66	108	59	167
% days in the year or season which are persistent	46	44	58	32	45
Total number of runs	16	12	16	12	28
Mean length of run (days)	6	6	7	5	6
Mean length of periods of change (days)	8	7	5	12	8

* Period 11, April 27th-May 5th, has been included in the winter total.

high values for $\hat{r}_1$ and $\hat{r}_2$ (Table I; also Appendix A, Tables 1 and 2) with a sudden fall in June, whereas the late autumn months October and November were characterised by considerable fluctuation in the circulation patterns with only a gradual reinstatement of more stable winter conditions.

To investigate the amount of internal change within each period, the initial day was next correlated with the subsequent days, $\hat{r}_{12}$, $\hat{r}_{13}.....\hat{r}_n$ where n = the final day of the run. These values are given in Table V. In general these sequential correlation coefficients remained high, but there were four cases where either a sudden drop occurred or where the correlation between the first and last day had almost reached zero. Godson suggested two models by means of which the degree and type of persistence might have been analysed, but owing to the number of approximations that were inherent in the $\hat{r}_\ell$ values and the comparatively small numerical changes involved in the test, it was decided that the results would be very difficult to assess. As a rough check on internal persistence the simple relationship[9]

$$r_\ell = r_1^{\ \ell} \tag{8}$$

was applied, where the values between the initial and subsequent days were assumed to depend only on the first 24-hour lag. If this were a valid assumption for spatial autocorrelations, then an approximate guide to the degree of persistence in each period could be obtained by comparing the actual sequential values of $\hat{r}_\ell$ with those values resulting from equation (8) where $\hat{r}_1$ assumed the threshold values of 0.800 for Type A and 0.700 for Types B and C. These values are given at the top of Table V. With the exception of March 8th-11th, May 23rd-27th and June 5th-10th, all Type C, the actual $\hat{r}_\ell$ values were well above these levels.

Using the same relationship but substituting the individual $\hat{r}_1$ values for the first day lag of each period in place of the threshold values, the actual sequential coefficients were again mostly above or close to the hypothetical figures (Table V). There were four cases in which the actual differed from the latter by ≥ -0.100. These included the three periods mentioned above and in addition December 15th-20th, another Type C run.

Perhaps the only check of this filter was to study the series of synoptic charts day by day.

In general $\hat{r}_\ell$ proved sensitive to the large-scale changes in that the

---

[9] Brooks, C.E.P., and N. Carruthers, Handbook of Statistical Methods in Meteorology. Her Majesty's Stationery Office, London, 1953, p. 323.

Table V

VALUES FOR ($\hat{r}$) BETWEEN THE INITIAL AND SUBSEQUENT DAYS OF EACH PERIOD COMPARED WITH HYPOTHETICAL VALUES FROM THE RELATIONSHIP $r = r_1$

DATE	TYPE	$r = r_1$ where r_1 =	= 1	2	3	4	5	6	7	8	9	10
	A	0.800	0.800	0.640	0.512	0.410	0.328	0.262	0.210	0.168	0.134	0.107
	B, C	0.700	0.700	0.490	0.343	0.240	0.168	0.118	0.083	0.058	0.040	0.028
		0.849		0.720	0.611	0.520	0.441	0.374	0.318	0.270	0.229	
Jan. 11-20	A		0.849	0.804	0.757	0.745	0.751	0.749	0.762	0.794	0.595	
		0.819		0.671	0.549	0.450	0.368	0.302	0.247	0.202	0.166	0.136
Jan. 24-Feb. 3	A		0.819	0.808	0.769	0.654	0.684	0.664	0.597	0.562	0.570	0.551
		0.883		0.780	0.688							
Feb. 5-8	A		0.883	0.744	0.765							
		0.777		0.604	0.469							
Feb. 16-19	B		0.777	0.607	0.498							
		0.818		0.669	0.547	0.448	0.366					
Feb. 27-Mar. 4	C		0.818	0.655	0.550	0.549	0.406					
		0.814		0.662	0.539							
Mar. 8-11	C		0.814	0.540	0.374							
		0.853		0.728	0.621	0.529	0.452	0.385	0.328	0.280	0.241	
Mar. 16-25	B		0.853	0.738	0.712	0.726	0.633	0.611	0.688	0.646	0.568	
		0.792		0.627	0.497	0.393	0.312	0.247				
Mar. 30-Apr. 5	B		0.792	0.627	0.486	0.482	0.439	0.208				
		0.824		0.679	0.559							
Apr. 7-10	B		0.824	0.656	0.566							
		0.750		0.562	0.422							
Apr. 19-22	B		0.750	0.650	0.534							
		0.783		0.613	0.480	0.376	0.294	0.230	0.180	0.141		
Apr. 27-May 5	B		0.783	0.626	0.535	0.479	0.404	0.464	0.497	0.334		
		0.768		0.590	0.453	0.348	0.267	0.205	0.158	0.121	0.093	0.072
May 9-19	B		0.768	0.664	0.680	0.655	0.602	0.616	0.633	0.498	0.401	0.380

Table V (continued)

DATE	TYPE	r =r_1 where r_1 =	= 1	2	3	4	5	6	7	8	9	10
		0.785		0.616	0.484	0.380						
May 23-27	C		0.785	0.513	0.331	0.502						
		0.834		0.696	0.580							
June 1-4	B		0.834	0.756	0.579							
		0.819		0.671	0.549	0.450	0.368					
June 5-10	C		0.819	0.658	0.436	0.349	0.162					
		0.758		0.574	0.436	0.330						
June 27-July 1	C		0.758	0.556	0.509	0.556						
		0.862		0.743	0.640	0.552	0.476					
July 6-11	B		0.862	0.686	0.587	0.519	0.571					
		0.779		0.607	0.473							
July 18-21	B		0.779	0.626	0.561							
		0.734		0.539	0.395	0.290	0.213	0.156				
July 28-Aug. 3	C		0.734	0.576	0.521	0.552	0.513	0.403				
		0.745		0.555	0.413							
Aug. 8-11	C		0.745	0.561	0.435							
		0.843		0.711	0.599	0.506						
Aug. 19-23	A		0.843	0.761	0.777	0.646						
		0.763		0.582	0.444	0.339						
Sept. 3-7	B		0.763	0.597	0.555	0.482						
		0.772		0.596	0.460							
Sept. 27-30	C		0.772	0.679	0.517							
		0.834		0.696	0.580	0.484						
Oct. 3-7	B		0.834	0.699	0.490	0.422						
		0.785		0.616	0.484							
Oct. 29-Nov. 1	B		0.785	0.717	0.621							
		0.752		0.566	0.425	0.320						
Dec. 6-10	B		0.752	0.633	0.539	0.574						

Table V (continued)

DATE	TYPE	r = r_1 where r_1 =	= 1	2	3	4	5	6	7	8	9	10
		0.818		0.669	0.547	0.448	0.366					
Dec. 15-20	C		0.818	0.513	0.357	0.290	0.175					
		0.864		0.746	0.645	0.557	0.481	0.416	0.359			
Dec. 28-Jan. 4	A		0.864	0.757	0.670	0.635	0.604	0.742	0.635			

initiation and end of each run of persistence had been defined in agreement with a subjective estimation. The correlation coefficient was computed, however, over the whole area, and since this area was large and contained the complete longitudinal range, occasional regional breakdowns within the grid were liable to occur, counterbalanced as far as $\hat{r}_{\ell}$ was concerned by strong persistence elsewhere. Three of the four weak cases isolated above appeared to fall into this category.

(i) March 8th-11th (Map 6, Appendix B)

Persistence was a regional characteristic applying only to the Siberian sector. Over the arctic basin, eastern Canada and Europe large-scale changes occurred and in these sectors the mean map had less value.

A very intense storm (central value 952 mb.) had just invaded Labrador on March 8th, while a ridge of high pressure extended from the Atlantic across Greenland to an anticyclone centred over Ellesmere Island. By March 9th the cyclone (969 mb.) covered much of Greenland and the archipelago, and the Atlantic ridge was displaced to the east. By 12:30 on March 10th, cyclonic flow existed over the whole of the Canada-Greenland quadrant of the chart and the Atlantic high now extended over north-west Europe linked by an eastern ridge to the Siberian anticyclone. At 500 mb. the major cyclonic vortex lay over the Barren Lands and Labrador during the first two days, but by March 11th the orientation had changed with an extension towards the pole, over the western archipelago. During the same time interval a surface low (1000 mb.) had developed beneath the upper air cyclonic vortex near T-3 and the March 11th chart revealed a deep trough across the polar basin.

On closer inspection the one-day lag exceeded 0.800 throughout while the two-day lag was very little above 0.500. It is very doubtful whether this period can be called persistent.

(ii) May 23rd-27th (Map 13, Appendix B)

In this case, the low sequential correlations were probably due to the rather flat patterns throughout the period. The daily variance was small on each day. The mean map can be considered representative of these rather weak large systems except across Canada where a low moved in from the Pacific, and there was an eastward shift in high pressure from central Canada to Labrador.

(iii) June 5th-10th (Map 15)

This was another series of very low summer pressure variance. Weak fluctuating patterns with a number of rather feeble centres characterised most areas over the Arctic. In general it was the Asiatic sector which demonstrated persistence in the circulation patterns, on this occasion dominated by strong zonal flow at 500 mb. Again the arctic basin and eastern Canada showed most change. The high over the basin was weak and contracting, while the tracks over eastern Canada showed well the fluctuation in that area between anticyclonic and cyclonic flow. A weak cold low developed over the basin and moved towards Greenland.

The large-scale patterns were not sufficiently well defined on the daily charts to give a reliable mean map, and this situation should be viewed conservatively.

(iv) December 15th-20th (Map 27)

The one-day lag between December 17th/18th showed a drop from 0.818 (December 16th/17th) to 0.702, then rose to 0.800 (December 18th/19th), but the two-day lags never reached 0.600. This change between December 17th/18th, although not great in itself, proved to be highly significant over a longer period, marking the beginning of a reversal of circulation over the arctic basin (Keegan, 1958) from one of predominantly anticyclonic flow which had lasted since mid-October, to a circulation predominantly cyclonic due to persist into January. These six days comprised three days of both régimes. But here again the breakdown in persistence, viewed within the period, was regional over the E. Siberian-Alaskan quadrant. The period mean map indicates this. The area of high pressure over the arctic basin moved rapidly southwards towards Alaska and a low centre was steered into the polar basin under strong flow aloft. On December 20th, a cold low at 500 mb. was centred over the surface low and the latter had intensified.

This mean map is not representative over at least a third of the area and must be rejected.

One other mean map requires comment:

(v) January 24th-February 3rd (Map 2)

Although the correlation coefficients remained high,

> subjectively there did appear to be a slackening of general persistence from January 31st. This was brought about by an acceleration in the westward movement of the large-scale centres during the first three days of February. During these three days there was a marked change in the position of the polar high, while a low centre developed over the arctic basin. As a result of this westerly shift of the major systems, the low centre over Novaya Zemlya, which predominated during the last few days in January, tended to be smoothed out in the mean, through filling, at the beginning of February. After February 3rd westward regression took place much more rapidly. In general the map can nevertheless be considered to give a valid representation of the major centres of action during this period.

With the exceptions indicated above, the mean maps in Appendix B are believed to represent on a large synoptic scale, periods of relative stability in the shifting circulation patterns of 1955.

(b) Limited Value of Individual Terms in Expansion

In Section 3 it was suggested that one of the advantages of using these Z_{rs} might have been the opportunity of breaking down the correlation coefficient into physically significant components, so that the patterns of both persistence and change could be investigated objectively. As was feared, these surfaces did not prove well suited to this purpose over the arctic area.

Fig. 5, reprinted from Supplement No. 1 to Scientific Report No. 3, shows the frequency of the daily reduction of variance by Z_{10}, one of the three dominant surfaces. The high frequency of very low values is remarkable. The other two dominant coefficients, Z_{11} and Z_{01}, displayed similar distributions, each of the three accounting for only 9% of the reduction of variance on a yearly average. Fig. 6 shows the annual and seasonal values of the 48 Z_{rs}, and it can be seen just how widely spread the variance was. Furthermore, combinations of the daily dominant and second dominant coefficients showed a maximum of only nine days in any one group (Z_{11}, Z_{21}). Owing to this internal

Daily Percent Reduction of Variance (Surface)

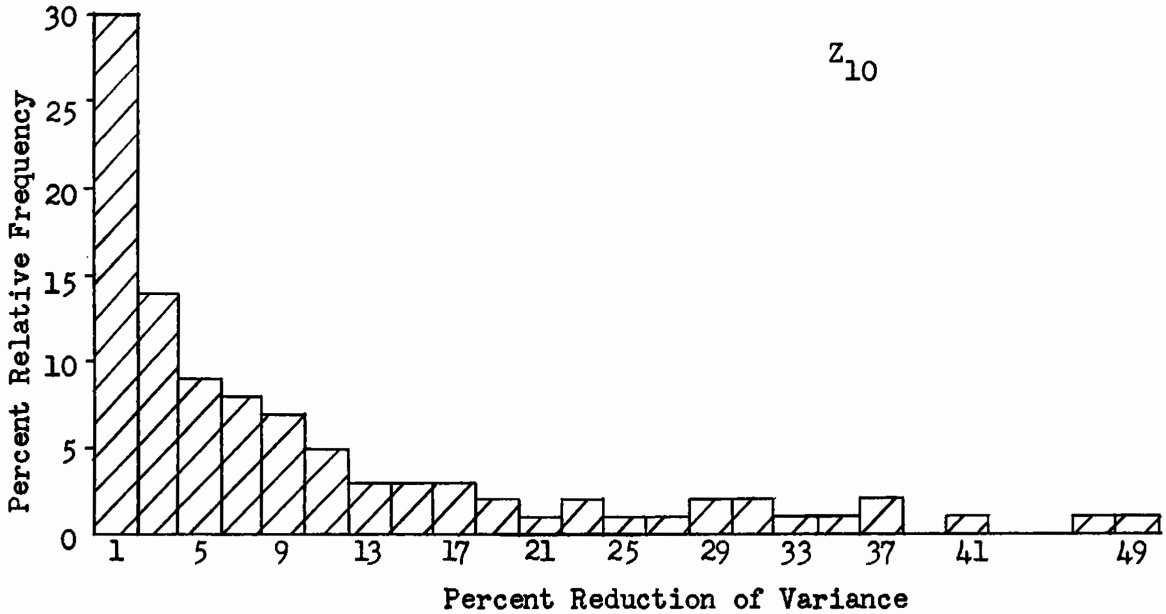

Fig. 5

distribution of the variance it was not easy to handle or to interpret these parameters.

In general the same Z_{rs} were dominant in both seasons, the winter values tending to be higher than the summer (Fig. 6). Z_{02} was the only important coefficient to show a higher average value in the summer season, although this often occurred with the higher powers (Fig. 7), while the two seasonal means for Z_{10} were almost identical. However, this similarity masked a change in the frequency of the sign of the coefficient. The most striking case was Z_{11} which underwent a complete reversal from January (entirely positive) to July (entirely negative), with sharp changes in the monthly frequency of sign from 81% positive in May to 7% in June and from 43% in September to 87% in October. Both Z_{10} and Z_{02} also showed a seasonal reversal in sign from negative to positive.

In mid-latitudes the row and column component variances and coefficients

Annual and Seasonal Mean Percent Reduction of Variance from Individual Coefficients

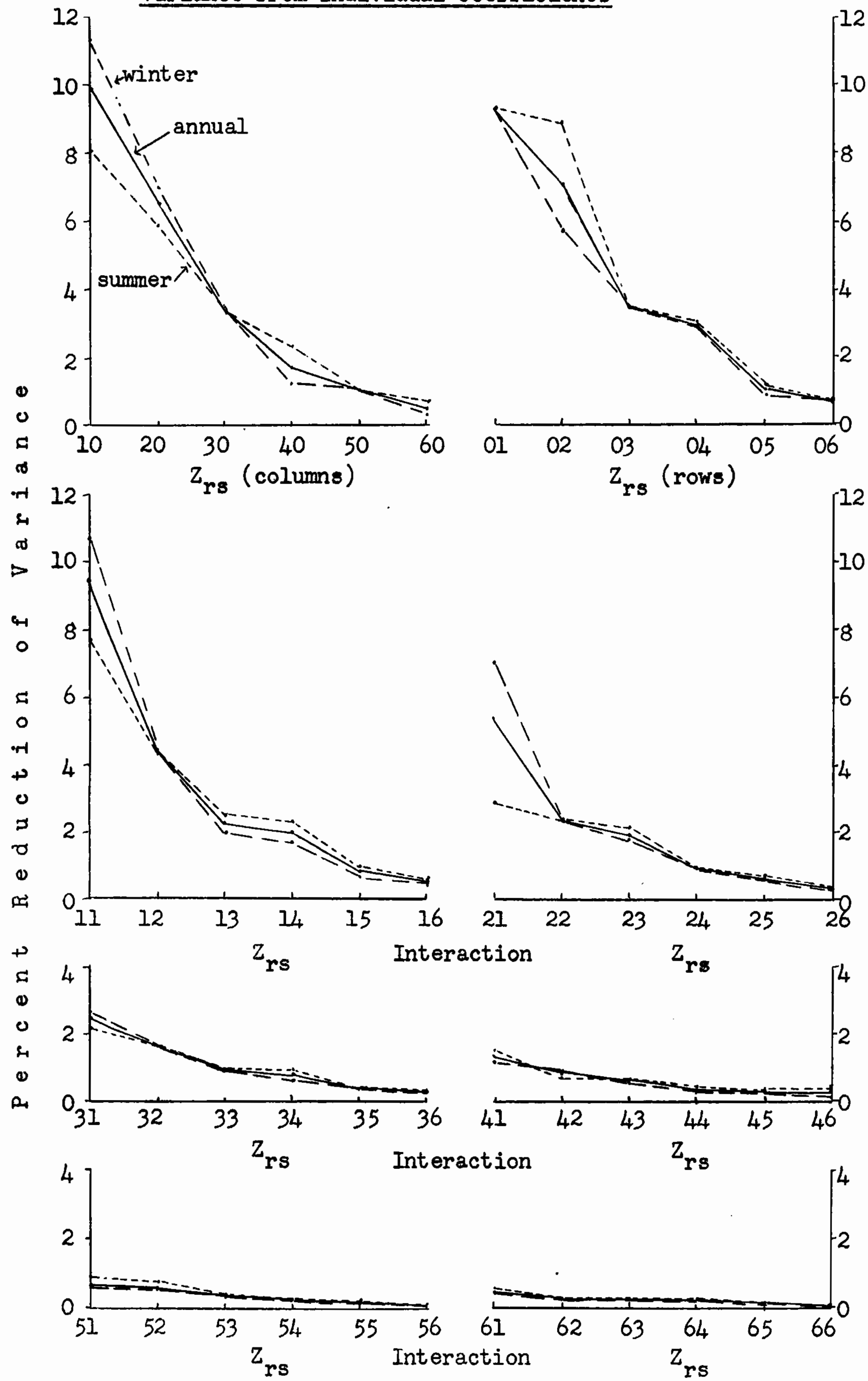

Fig. 7

Annual and Seasonal Mean Percent Reduction of Variance

by Polynomial Degree

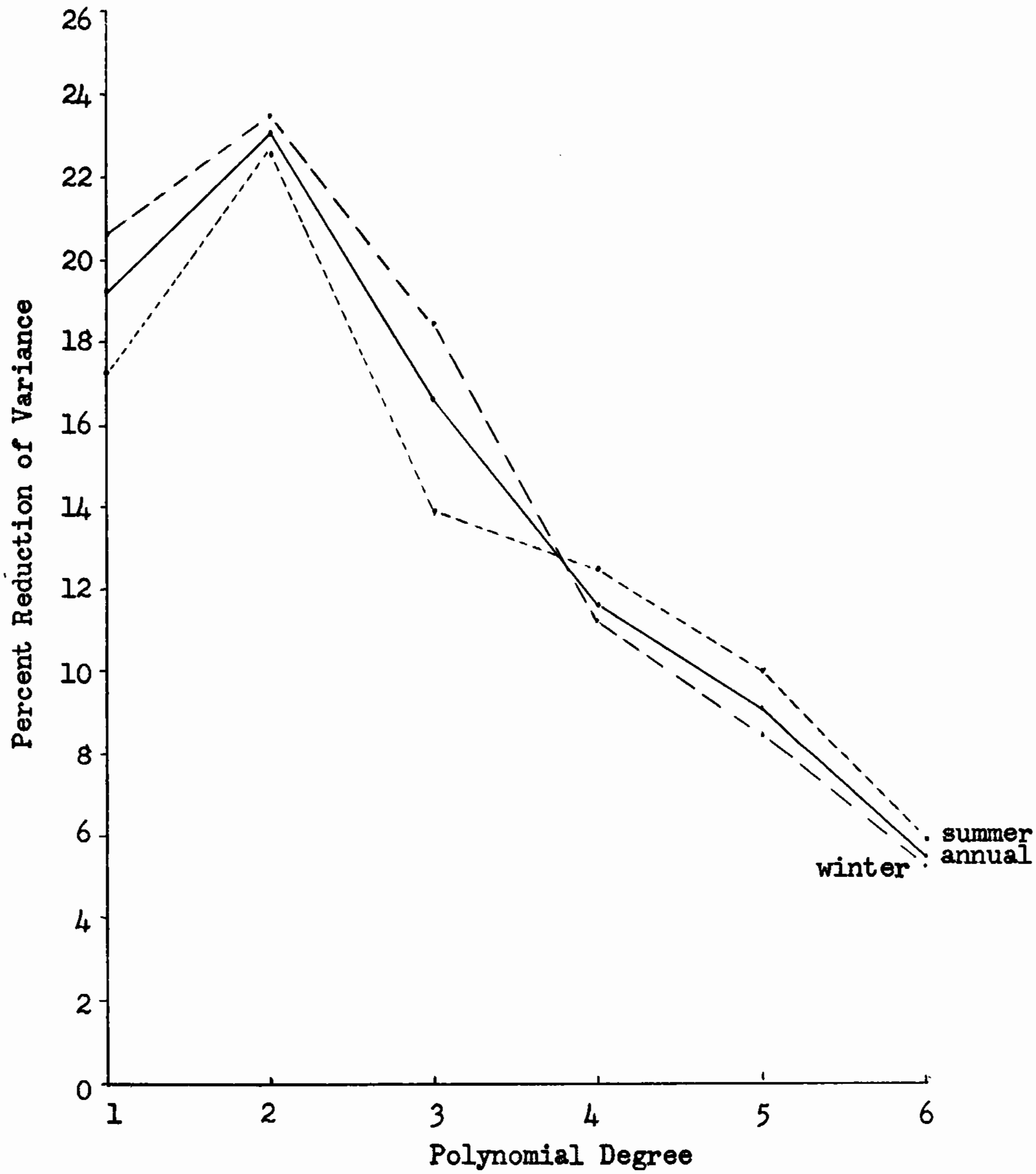

were interpreted in terms of zonal and meridional flow. This advantage was lost over the Arctic, but owing to the orientation of the grid it would have been possible to consider the column coefficients as rough indicators of mass transfer between the two major continental regions, and the row components as a measure of the mass exchange between the two oceans. During 1955, however, the interaction variance accounted for 50% of the total internal variance, on the average, the remainder being divided equally between the rows and columns.

It was even more difficult to discover any physically significant change in the values of the individual Z_{rs} with respect to time, except a general change from a comparatively few dominant coefficients describing well-defined large-scale systems to a wider dispersal of the variance associated with the dissolution of these systems and increase in cellularity. Breakdown in persistence can be due to rapidity of movement and reorientation of the main centres of action, but inasmuch as it is often due to a true breakdown in the large-scale circulation, this measure of cellularity might have been useful. In this study the great drawback was the difficulty in handling so many variables. Using a Cartesian grid over the Polar area was perhaps too rigid. A slight change of orientation in the patterns — insignificant synoptically — might bring a different surface into prominence. Only where large-scale systems were very simple and almost stationary (for example, January 11th-20th (Z_{11}), February 5th-8th (Z_{10}), or June 1st-4th (Z_{10})) was there a run of high values for one particular surface, the highest value being 64% (Z_{10}) on June 1st. In addition the grid was centred on the pole, whereas eccentricity and asymmetry were often apparent in the daily and mean maps. It is hoped that the study of the components of the variance in the Godson orthogonal harmonic method will give a more direct means of effectively analysing the daily changes.

Three months' data from 1955 are now being computed for both the surface and 500 mb. levels using this latter technique.

Thus the individual coefficients in the specification expansion proved, as expected, to be of little value. Taken together, however, the complete roster of coefficients seemsto fulfil the main need of this paper — a filter to isolate the persistent large-scale systems from the complex daily maps.

5. Discussion

During 1955 it was possible to isolate some twenty-five periods of persistence of the large-scale synoptic patterns, varying in length from four to eleven days and averaging six days. These periods could be recognised as those in which

(i) the large systems remained steady, with no significant interdiurnal change;

(ii) there was a slow systematic change in orientation of the large-scale systems, including slow progression or retrogression, but without fundamental change.

It follows that a breakdown in persistence occurred when a rapid acceleration of these processes took place. The main types of change could be subjectively described as

(i) a general breakdown of the circulation, both at 500 mbs. and at the surface, when the large-scale patterns disintegrated and gave place to a large number of weak centres and small-scale ridges and troughs. (Examples of this could be detected following the flow patterns represented by Maps 3, 12, 13, 15, 19 and 20);

(ii) a regional change associated with slackening and strengthening of the zonal flow at 500 mb., especially over north Asia. This affected the surface extension of ridges and the passage of cyclones (Maps 5, 6, 7, 10, 16, 25, and 26);

(iii) rapid reorientation of the large-scale systems through eastward progression or westward retrogression (such as occurred following periods presented by Maps 1, 2, 4, 9, 21, 23, 24 and 28).

Since the interdiurnal correlation coefficient measured the degree of persistence over the whole area, covering the complete longitudinal range of circulation, it might have been anticipated that any tendency to persistence over the arctic basin would have been ironed out by less stable patterns over the peripheral regions. It was interesting therefore to find stable conditions existing throughout the whole range of longitude during most of these periods of persistence, although the type of circulation pattern often differed with respect to longitude. An example of this could be seen during May 9th-19th (Map 12) when there was a blocking situation over the western hemisphere, with zonal flow persisting over Siberia.

One year is naturally too short a period to determine whether there is a finite number of persistent circulation types or Grosswetterlagen over the Arctic. There was, however, a strong similarity between the situations given in Maps 1 and 28 (the only slight overlap in time), showing the characteristic ridge from Siberia to Canada of the normal January map. The only other important resemblances between the maps that could be clearly seen were in March and June. Maps 7 and 8 simply showed the continued persistence of the warm high over the Arctic interrupted by a temporary eastward acceleration of the peripheral patterns, but the June maps 15 and 16 are worth a comment. Separated by just over two weeks of feeble and restless circulation, including the lowest value of interdiurnal persistence for the year (June 25th-26th), these patterns were very similar both to each other and to the normal map for June.[10]

Since the data were limited to one year, it was important to compare the

---

[10] Normal Weather Charts for the Northern Hemisphere. Technical Paper No. 21, U.S. Department of Commerce, Weather Bureau, Washington, D.C., Oct.1952, pp.7,12.

particular synoptic conditions for 1955 with the normals when considering the results. This was a year of two major abnormalities.[11] The mid-tropospheric circulation in ten months of the year was characterised by strong blocking situations in middle-high latitudes over the western hemisphere, while the remaining two months (July and August) showed a complete reversal. During these two months the polar vortex contracted to a greater extent than normal; the mean maximum value of the westerly wind component occurred near 52°N., that is, to the north of the seasonal normal, the the polar westerly index reached some of the highest values on record. Considering that both June and January were months of blocking, the difference in the respective values for $\hat{r}_\ell$ was very great. Furthermore, the strong zonal flow of mid-August (Map 21) resulted in persistence almost as high as that during the blocking situation of mid-January (Map 1). The "summer" season of low persistence (June to November) extended through both "blocking" and "non-blocking" situations. Perhaps in summer, when the north-south hemispheric temperature gradient was at a minimum, and the amount of incident solar radiation was at a maximum in polar areas, the regional instability caused by differential heating over ice, open water and land minimised the effect of dynamic stability induced by blocking situations. (Over North America Namias (1952) found that persistence in the monthly height anomaly patterns at 700 mbs. was greater in summer than in winter, but that during the cold season persistence was more marked at times of low index.)

The daily zonal indices for the surface and 700 mb. levels computed over 35° to 55°N. and 175°E. to 5°W. were made available to the McGill Group.[12]

---

[11] Klein, W.H., "The Weather and Circulation of 1955", Weatherwise, Vol. 9, No. 1, 1956, pp. 5-10.

[12] Our thanks are due to Dr. Namias for this courtesy.

The curve for the surface was drawn up and inspected in relation to the curves of persistence. Although this index was to a certain extent a key to the incidence of blocking situations over the western hemisphere during 1955, it was not uniformly so, since the actual blocking highs occasionally occurred outside the range of this particular sample. No simple systematic relationship could be found, although one or two cases deserve mention. For example, the periods represented by Maps 1, 2 and 3 were isolated through reorientation rather than true breakdown, and these periods were found to be associated with a run of high index values. In addition, in one or two cases where breakdown in persistence was caused by a general slackening or tightening of the gradient of the polar westerlies, there was a possible relationship with this index (e.g., the patterns illustrated by Map 16 break down after July 2nd when the flow becomes more meridional at mid-latitudes).

One of the difficulties in relating the flow at mid-latitudes to that over the Arctic is the problem of finding a representative parameter for the arctic circulation. Over such an area zonal and meridional flow cannot be simply defined, not only owing to the convergence of the meridians, but also because of the nature of the circulation. At 500 mb., strong gradients often flank the individual cells of the polar vortex; split jets occur north of blocking highs of middle and high latitudes, while the general asymmetry and eccentricity of the flow patterns form a basic complication. Within the McGill Group work has recently been done to establish a statistical relationship between the variance of height of the daily 500 mb. surfaces and kinetic energy.[13] Though real, this relationship is not precise enough for analytical

---

[13] Godson, W.L., and MacFarlane, M.A., Pressure-contour Variance and Kinetic Energy over the Arctic. Scientific Report No. 5, McGill Arctic Meteorology Research Group, Contract No. AF 19(604)-1141. McGill University, Montreal, 1958.

purposes. Visual comparison of their time series shows some resemblance between the behaviour of the mid-latitude westerly index and this variance parameter. In addition, the wave component variances from the Godson orthogonal harmonic specification technique will offer further possibilities of setting up an index for the arctic circulation. As yet, however, this work has not been brought to fruition.

At the surface, one of the most outstanding features of 1955 was the amount of cyclonic activity over the central Arctic. The summer of that year revealed large negative pressure anomalies and the circulation during this season was marked by almost continual cyclonic disturbance. Cyclones were also conspicuous during other periods of the year. During early January, mid-February, early March and mid-April, cyclones were continually present over the arctic basin. During the latter month especially, the circulation over the arctic was for some ten days (Map 9) a complete and persistent reversal of the normal conditions for April (Fig. 8(a)). The thirty-day mean pressure distribution for April (Fig. 8(b)) showed a low pressure anomaly over the basin, in spite of anticyclonic conditions at the beginning and end of April which have smoothed the values. In 1955 these lows over the central Arctic area appeared to be almost without exception cold lows related to the shifting pools of cold air of the major tropospheric circumpolar vortex.

It was suggested earlier in this report that the high values of the persistence correlation over the arctic area may be a reflection of the stabilising influence of anticyclonic conditions. Intense and, for the most part, warm anticyclones prevailed over the central Arctic in (a) late January, early February, (b) most of March and early April, and (c) late April through May. During June

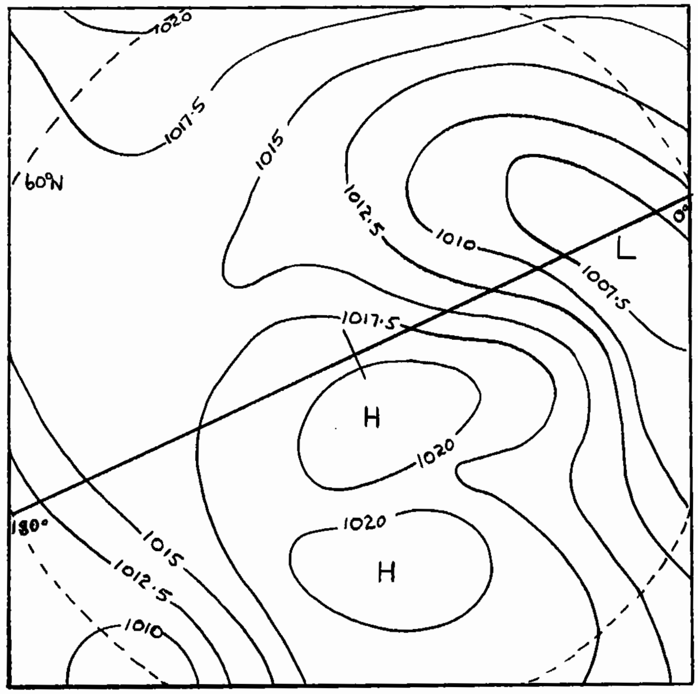

Fig. 8(a)
Normal Pressure Distribution - April
(This map is the revised normal map for the Arctic based on the short period 1948-55. This was discussed on page 1.)

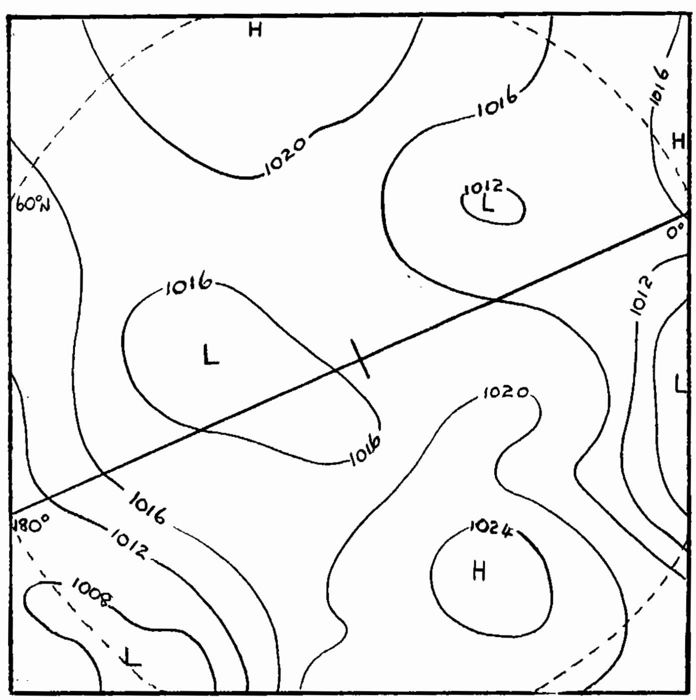

Fig. 8(b)
Thirty-day Mean - April, 1955

the frequency, extent and intensity of these anticyclones rapidly decreased, to increase once again in late October. By early December (Map 26) a major central anticyclone was once again a temporary feature of the arctic circulation. These highs were mostly below warm ridges at 500 mb., extensions of the major oceanic and continental high pressure systems. The surface centres apparently moved in over the basin most frequently from Alaska and Siberia. Table 1 in Appendix A has shown the higher values of $\hat{r}_1$ and $\hat{r}_2$ for the six month period December-May. Since 1955 showed a high frequency of cyclonic activity over the Arctic, the values of the inter-map correlation coefficients may in fact be a conservative estimate, especially during the months June to November.

It is hoped that the 500 mb. level analysis and case studies will shed a little more light on the nature of the change. From an inspection of the charts the most interesting feature connected with the stability of the surface circulation is the circumpolar vortex. The cold pools associated with this vortex were so frequently reflected in closed centres of low pressure on the surface chart that there appeared to be a direct relationship between the amount of asymmetry or eccentricity of this major centre of action and the existence of high pressure or low pressure over the arctic basin, while the degree of cellularity was linked with its intensity and degree of ramification. Sudden changes in the position of this upper air feature were associated with breakdown and change in surface circulation patterns. One of the most interesting examples of this could be seen during April, 1955. A comparison of Maps 8 and 9 gave a fascinating reversal of pattern, occurring for the most part within the 24 hours of April 6th. From March 16th to April 5th the central Arctic had been dominated by a very intense anticyclone (Map

7, mean central value 1048 mb.; Map 8, 1036 mb.). By April 7th this circulation had been replaced by an equally intense and persistent cyclone (mean central value 992 mb.) which continued as the outstanding feature of the arctic circulation until April 17th, after which time almost a second reversal took place. Referring to the 500 mb. charts, for the same period of time, during the end of March and early April, the vortex was centred over the Canadian archipelago. Between April 5th and 7th there was a rapid displacement of the upper air low to a new position over the polar basin. At the same time the geometry of the vortex was simplified to form one major unit centred over the pole. Within these 24 hours from April 5th to 7th the surface pressure changed over the basin by as much as 27 mb. A further example of the relationship between this vortex and surface persistence appeared in the June 11th-26th run, which gave the lowest set of $\hat{r}_\ell$ values for the year. During this time a series of low centres at the surface, revitalised at the Siberian coastal-ice-water margin, moved around the arctic basin under a rotating upper air vortex. In Germany, Scherhag (1956) and Flohn (1952) have studied the distribution, movement and properties of the cold poles of the mid-troposphere and emphasised the asymmetry and eccentricity of the circumpolar vortex and its importance, not only in regional studies of the Arctic, but in the general circulation of the atmosphere.

The abrupt quality of the change in the inter-map correlation coefficients suggested some trigger effect. Since "persistence" occurred in both sluggish and swift circulation patterns with considerable regularity in the winter months, it might have been the effect of large-scale instability, such as that associated with the hemispheric change from zonal to meridional flow when the temperature gradient between the equator and pole had increased to some critical value. This trigger effect was certainly less clearly marked in those months when the north-south gradient was at a minimum.

On the other hand the impulsive quality of the changes suggests a consideration of possible extraterrestrial effects. Evans (1956), speaking at the 146th National Meeting of the American Meteorological Society in Boulder, Colo. (July 25th-27th, 1956), made the following comments:-

> "The sun affects the state of the earth by means of its electromagnetic and corpuscular radiations. The overwhelming influence is that of the steady-state solar radiation, which maintains the temperature of the earth and drives the steady-state system of atmospheric circulation. Superposed on this tremendous background radiation are variations which are comparatively small in terms of energy, but are in such a critical region of the spectrum or are of such a corpuscular nature that they produce terrestrial effects, sometimes quite out of proportion to the energy involved."[14]

Considering an increase in corpuscular radiation as a possible cause of the change in the atmospheric circulation patterns, Shapiro (1956) assumed a direct relationship between this form of solar energy, which is believed to occur as charged particles, and the earth's magnetic field. He then tried to establish a further relationship between the $\hat{r}_\ell$ values and the International Geomagnetic Character Index, C_i. He found a statistically significant drop in the mean inter-map correlation values fourteen days after a sudden increase in the disturbance of the earth's magnetic field.

The great advantage in using the $\hat{r}_\ell$ values as a measure of the atmospheric fluctuations is two-fold. Firstly, these parameters merely record that a change has taken place; and secondly, the one variable takes into consideration the change over a large area. The C_i index is a measure of the geomagnetic activity, ranging from 0.0 (quiet) to 2.0 (very disturbed). The key days were defined as those when the daily values of C_i increased by ≥ 1.0.

Shapiro considered forty-seven years of surface data (1899-1945) over an

---

[14] Evans, J.W., Variations of the Sun. Technical Report No. 2, Institute for Solar-Terrestrial Research, High Altitude Observatory of the University of Colorado, 1956, p. 1.

area extending from 30°N. to 60°N. and 65°W. to 125°W., employing the $\hat{r}_\ell$ values for three-day running mean pressure distributions. During this time he isolated 564 key days, and by means of the superposed epoch method computed mean $\hat{r}_\ell$ values from twelve days prior to the key days to nineteen days beyond (Fig. 9).

Fig. 9[15]

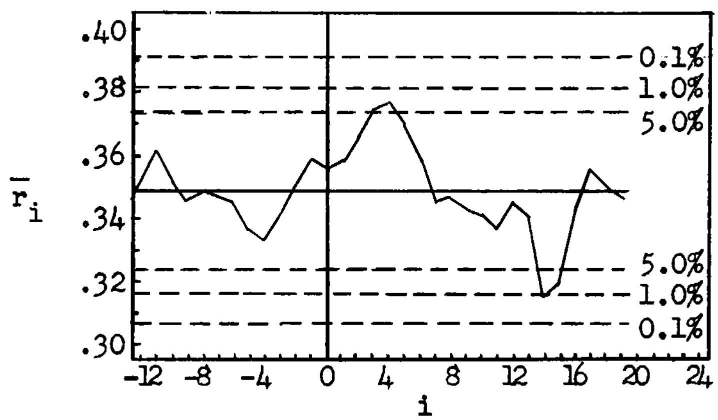

Mean persistence correlations for days minus 12 to plus 19, for all 47 years (564 cases for each mean).

In testing the significance of these values Shapiro assumed:-

(i) that the population mean was that of the coefficients, since the sample was so large;

(ii) a normal distribution for $\hat{r}_\ell$.

The mean values displayed random fluctuation before the sudden geomagnetic disturbances, but revealed a statistically significant (1.0% level Student's t-test) negative departure from the assumed population mean on Day 14. With the omission of the years of maximum sunspots, the significance of the deviation on Day 14 became better than the 0.1% level and a division

15 Shapiro, R., "Further Evidence of a Solar-Weather Effect", J. Meteor., Vol. 13, 1956, p. 336, Fig. 1.

of the data into the earlier and later years still showed a similar trend on Day 14. Random key days gave no such result.

Assuming that the earth's magnetic field funnels this solar energy into high latitudes, this effect, if real, might be expected to reach a maximum over the polar regions. A similar study was therefore attempted for the arctic area, using the very limited quantity of data for 1955.

The C_i[16] index was adhered to, rather than the more reliable K_p index (Ward, 1954) to allow comparison, and the key days were defined as in Shapiro's analysis. During 1955 there were only fourteen day days, with a rather uneven distribution through the year (Table VI) since the summer months of June, July and August were undisturbed to this extent.

Table VI

KEY DAYS 24 hr. $\Delta C_i \geq 1.00$	DAY +14	KEY DAYS 24 hr. $\Delta C_i \geq 1.00$	DAY +14
January 11	January 25	August -	-
January 17	January 31	September 27	October 11
February 28	March 14	October 25	November 8
March 22	April 5	November 4	November 18
March 30	April 13	November 8	November 22
April 24	May 8	November 15	November 29
May 25	June 8	November 18	December 2
June -	-	December 1	December 15
July -	-		

The one-day lag coefficients were chosen to represent the circulation changes.

Fig. 10 illustrates the resulting mean values, $\bar{r}_1$; one of the most striking features was in fact the substantial decrease in the mean persistence

[16]These indices were kindly made available to us through the courtesy of the United States Department of Commerce, National Bureau of Standards, Boulder, Colorado.

Fig. 10

Surface 1955

Behavior of $\bar{\bar{r}}_1$ Before and After a Sudden Rise in C_i of ≥ 1.00

(14 Key Days)

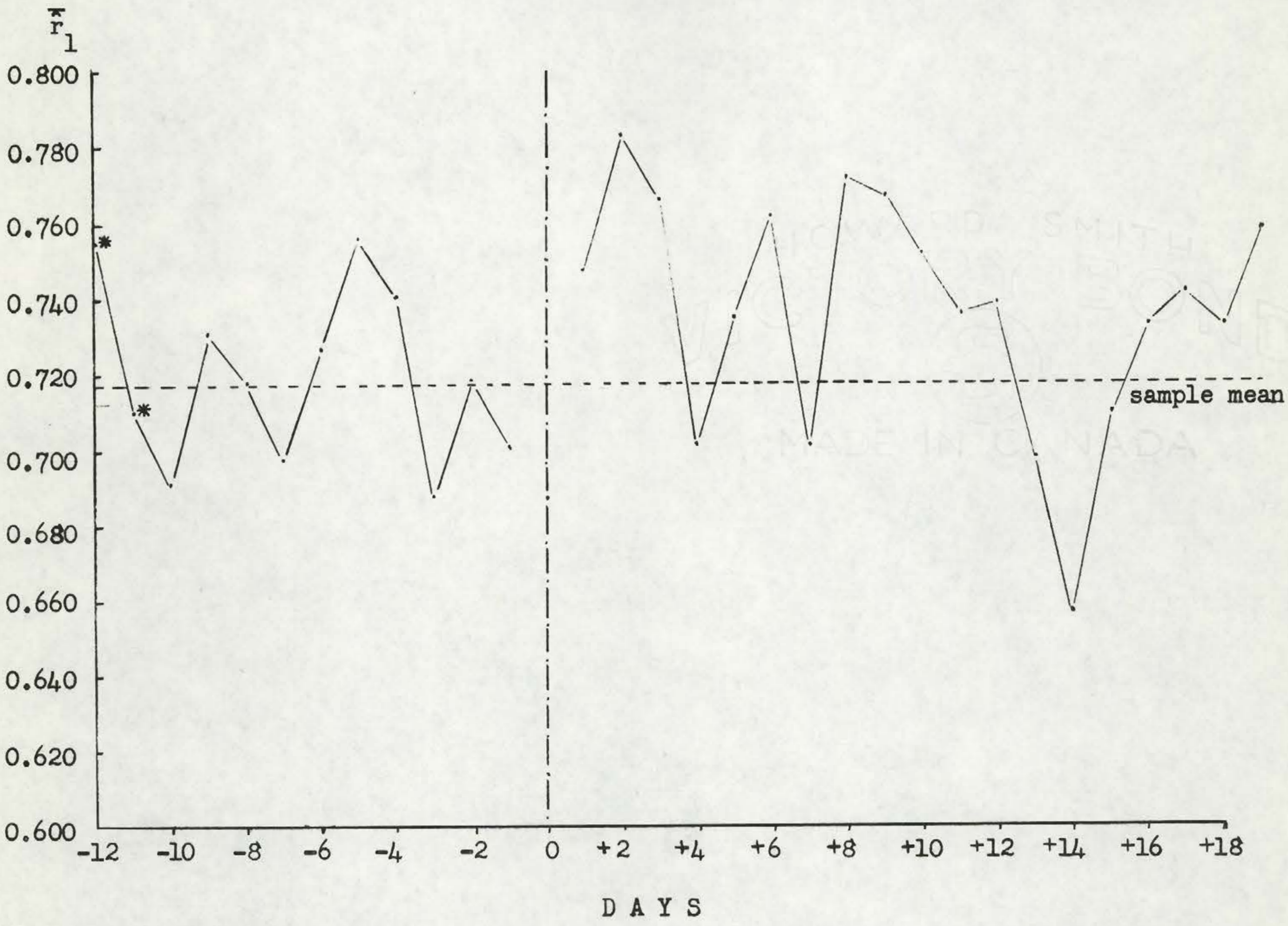

N.B.: The sample mean was computed by means of Fisher's z transformation.
The $\bar{\bar{r}}_1$ values are tabulated in Appendix C.
* = 13 Key Days only.

function on the fourteenth day after the key day.[17] However, direct comparison with Shapiro's results through the use of the t-test for significance was not possible, since the present samples are smaller by an order of magnitude and he employed three-day mean values; meanwhile these $\bar{\hat{r}}_1$ values are presented merely as an interesting suggestion of confirmation of Shapiro's results.

The fourteenth day after each key day was then tabulated (Table VI) so that the synoptic charts and individual $\hat{r}_1$ values could be studied for those particular times. January 25th, January 31st and June 8th actually occurred within so-called periods of persistence, although the significance of the June 5th-10th run has already been doubted and January 31st was noted as a time of acceleration in the retrogression of the large-scale systems.

Perhaps the most dramatic large synoptic changes of the year occurred around March 14th and April 5th, both these dates coinciding with a decrease in the persistence function fourteen days following a sudden geomagnetic disturbance. (The April 5th reversal in the flow patterns has already been mentioned on page 41 in connection with a rapid change in the 500 mb. polar vortex.) The circulation over the arctic during the week prior to March 14th had been dominated by cyclonic activity (Map 6). However, during the forty-eight hour period between March 12th-14th an anticyclone moved into the arctic basin under a warm ridge aloft. This system intensified and persisted until the beginning of April (Maps 7 and 8). The barometric tendency for the 48-hour interval March 12th-14th (Fig. 11) represented a change which amounted to a sudden reversal in the flow patterns (Maps 8 and 9). Moreover, these anticyclonic conditions prevailed until early April when this system

[17] Since the number of key days was so few the mean correlation coefficients were obtained through Fisher's z' transformation. This was carried out on the E101 computer at Canadair by the Electrodata division of Burroughs.

was replaced equally suddenly by a cyclone below a cold cyclonic vortex at 500 mb., which was to persist for just over a week. Fig. 12 illustrates the 48-hour barometric tendency between April 5th-7th. By April 19th a hint of another reversal was suggested in a return to anticyclonic flow (Maps 9 and 10), but the changeover was not so spectacular, although April 13th, another significant date (Table 6), was associated with low $\hat{r}_{\ell}$ values.

Considering Figs. 11 and 12, the most remarkable feature is the reversal of the tendency. If the irregular emission of solar corpuscular radiation is a cause of these changes, the regional effect must depend on a number of other variables, including the initial state of the circulation. For this reason, the use of $\hat{r}_{\ell}$ proves to be exceptionally valuable.

However, it is still not known how this additional corpuscular radiation can trigger off the release of sufficient energy to bring about fluctuations of this magnitude. There are in addition so many uncertain measurements involved in a study of this nature that these results can only be put forward as an interesting suggestion of a relationship.

A further analysis was carried out using the five Quietest and five Most Disturbed days in each month[18] as key days, and $\hat{r}_1$ as before. Duell and Duell (1948) analysed the behaviour of sea-level pressure at a number of stations in N.W. Europe before and after these key days, and found that during the winter months of years of low sunspot number, pressure fell three days after disturbed key days and rose to a maximum three or four days after quiet key days. Craig (1952) followed this up by extending the area to cover the whole northern hemisphere between 30° and 70°N. He considered the same

---

[18] The five days of least and five days of greatest disturbance in the geomagnetic field are published for each month by the Bureau of Standards (see footnote 16). These days are tabulated for 1955, together with values of $\bar{\hat{r}}_1$, in Appendix C.

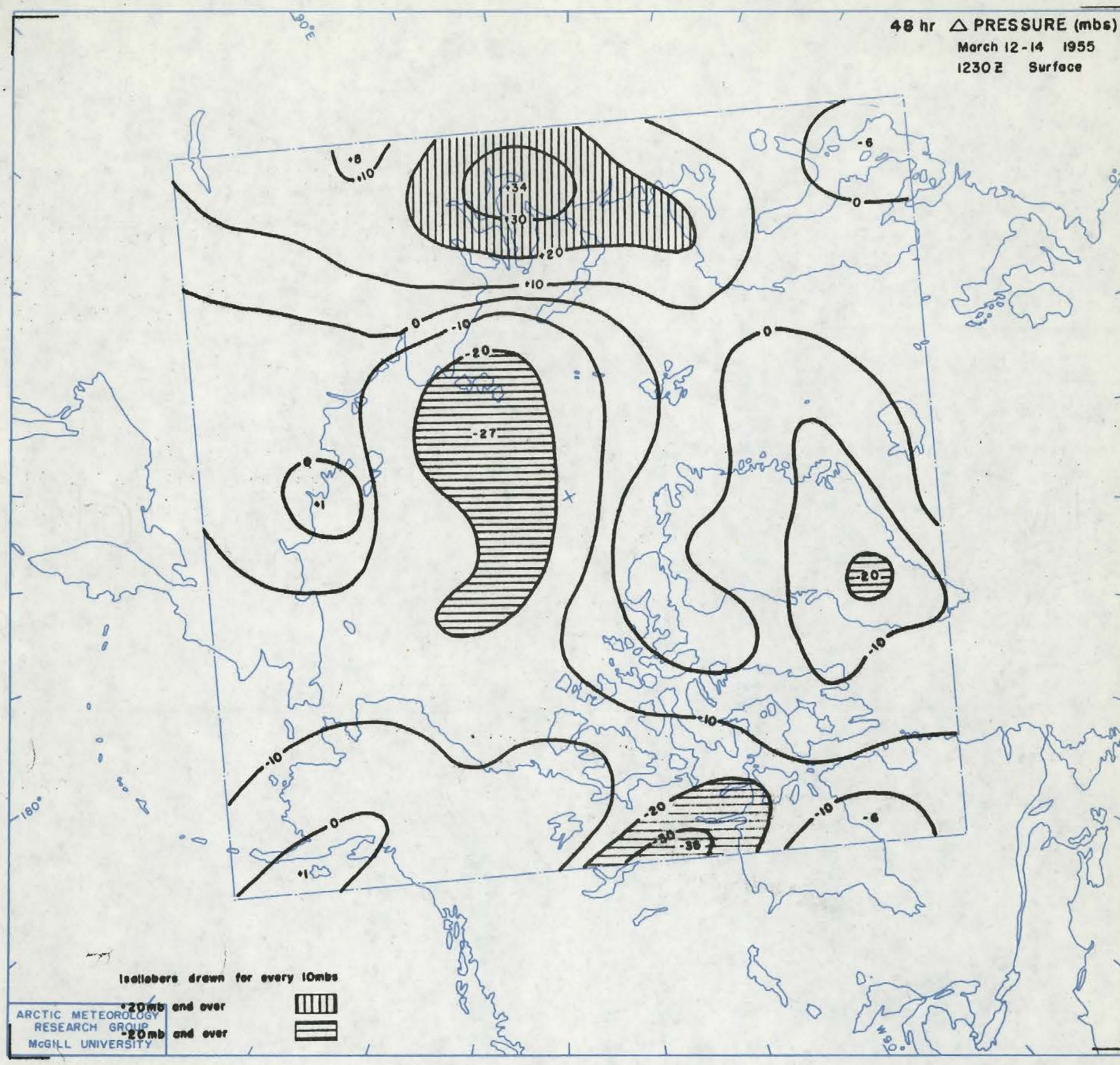

Fig. 11

Barometric Tendency During the 48-hr. interval from March 12th-14th.

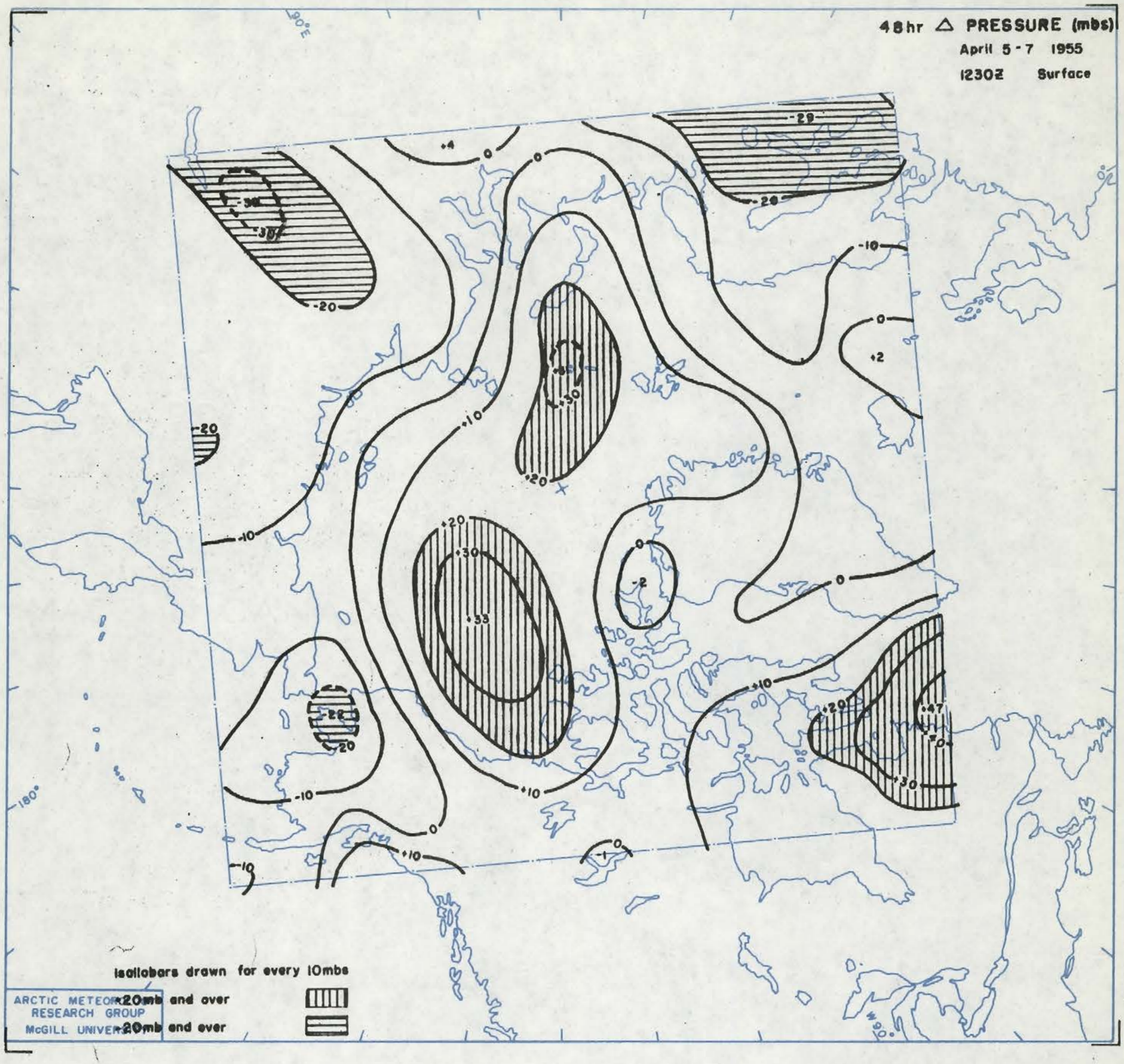

Fig. 12

Barometric Tendency During the 48-hr. interval from April 5th-7th.

period of time and similar key days, but the results were disappointing. His main conclusion was that at any one station for the surface level there was a tendency towards a negative correlation between the pressure behaviour after quiet and disturbed key days.

The results of this study, illustrated in Figs. 13 and 14, were disappointing and no conclusions could be suggested. It so happened that at the beginning of this analysis the key days for February were missing and work was carried out on the 55 remaining key days in each case. The graph of these results is given as Fig. 14, and shows an interesting point. When the February 1955 data were not included a very interesting annual and seasonal rise in the values of $\hat{r}_1$ fourteen days after quiet key days was suggested, with a slight hint of a reversal of this result after disturbed key days. However, these graphs emphasize the danger of attempting to draw conclusions from the data for one year only.

6. Summary

The sea-level large-scale circulation over the arctic during 1955 showed the following features:-

(i) A generally high degree of stability with 45% of all the days defined as persistent.

(ii) A tendency for these high levels of persistence to be maintained for periods averaging six days, followed by an abrupt breakdown and rapid return to more stable conditions.

(iii) A winter-spring régime where the degree of persistence was consistently high, with a hint of regularity in breakdown every fourteen to fifteen days, followed by a sharp change at the beginning of June to a new régime. During the summer and autumn conditions were generally less stable, changes less well defined with a gradual transition to the more stable winter régime through November into early December.

Fig. 13

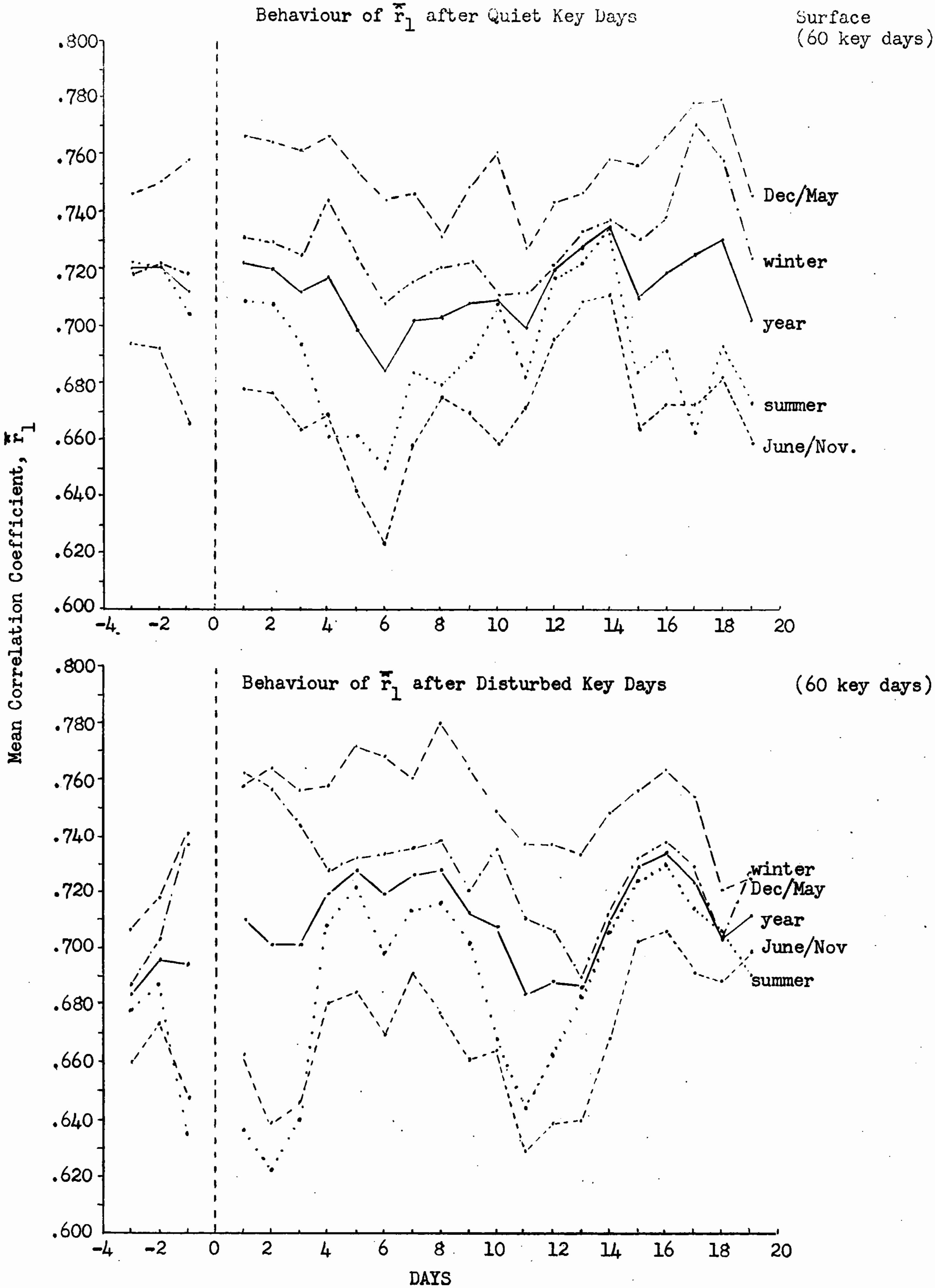
Behaviour of $\bar{\bar{r}}_1$ after Quiet Key Days
Surface
(60 key days)
Dec/May
winter
year
summer
June/Nov.
Mean Correlation Coefficient, $\bar{\bar{r}}_1$
.800
.780
.760
.740
.720
.700
.680
.660
.640
.620
.600
-4
-2
0
2
4
6
8
10
12
14
16
18
20
Behaviour of $\bar{\bar{r}}_1$ after Disturbed Key Days
(60 key days)
winter
Dec/May
year
June/Nov
summer
DAYS

Fig. 14

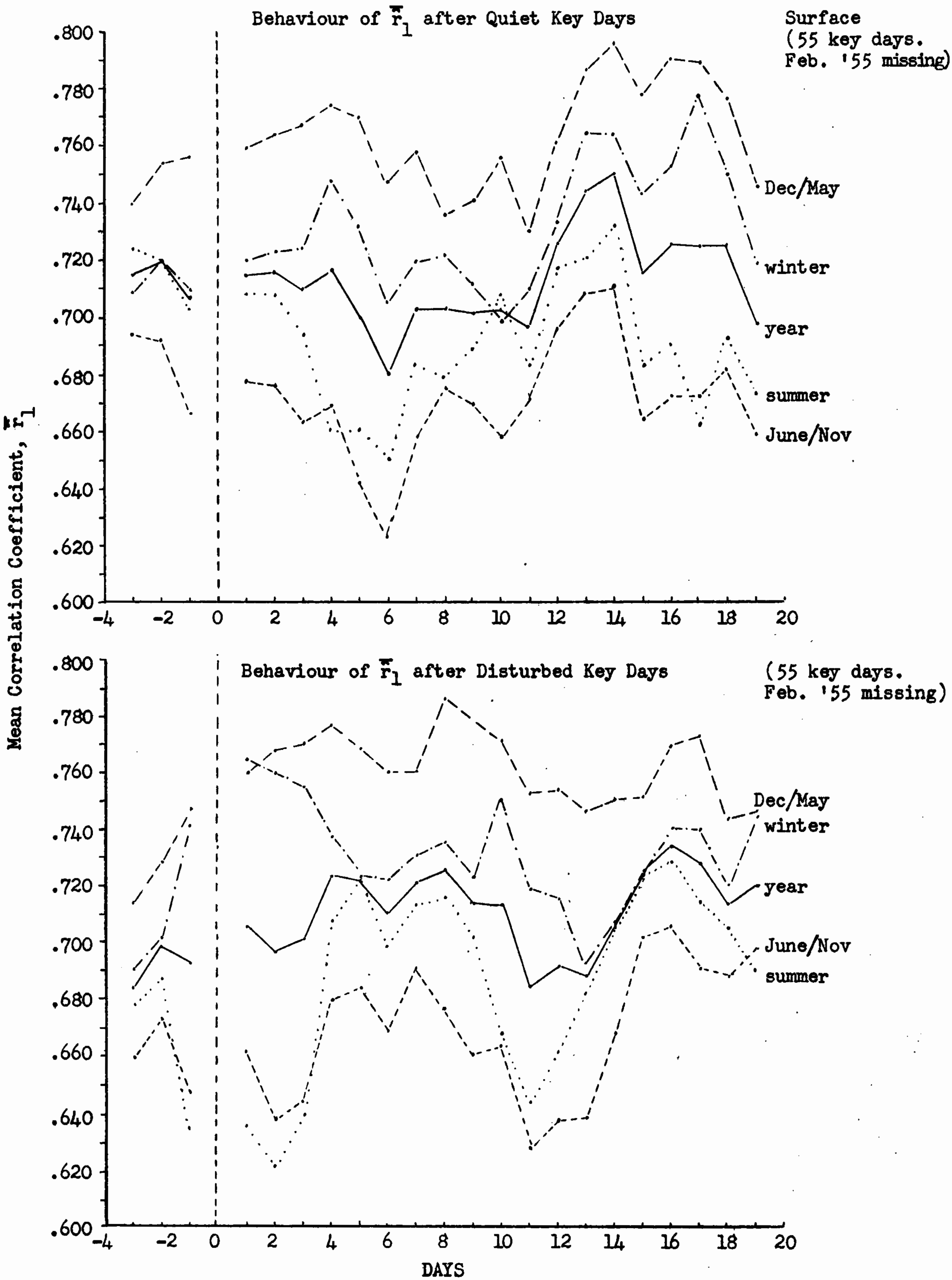
Behaviour of $\bar{\bar{r}}_1$ after Quiet Key Days
Surface
(55 key days.
Feb. '55 missing)
Dec/May
winter
year
summer
June/Nov
Behaviour of $\bar{\bar{r}}_1$ after Disturbed Key Days
(55 key days.
Feb. '55 missing)
Dec/May
winter
year
June/Nov
summer
Mean Correlation Coefficient, $\bar{\bar{r}}_1$
.800
.780
.760
.740
.720
.700
.680
.660
.640
.620
.600
-4
-2
0
2
4
6
8
10
12
14
16
18
20
DAYS

Taking into consideration the strong development of blocking situations in middle high latitudes in 1955, when the circulation might have been more sluggish than normal, the high level of persistence might have been a phenomenon of this particular year. However, stable periods also occurred during the run of abnormally strong polar westerlies in July and August, whilst unstable conditions prevailed during the blocking situations of October and November. Furthermore the apparent relationship between strong anticyclonic conditions over the arctic and high degree persistence suggested that the summer-autumn values for 1955, seasons marked by abnormal cyclonic activity, might in fact be conservative.

The abrupt nature of the changes suggested some trigger effect. Since "persistence" occurred in both sluggish and swift circulation patterns with considerable regularity in the winter months, it might have been the effect of large-scale instability such as that associated with the hemispheric change from zonal to meridional flow when the temperature gradient between the equator and pole had increased to some critical value. This effect was certainly less clearly marked in those months when the north-south gradient was at a minimum.

A subjective study of the 500 mb. maps showed an interesting relationship between surface instability and changes in the degree of asymmetry, eccentricity, intensity and ramification of the circumpolar vortex. Sudden changes in the position of this feature were associated with breakdown and change in the surface circulation patterns. There were two outstanding examples of this during March and April, which occurred some fourteen days after a sudden geomagnetic disturbance, suggesting in the light of Shapiro's results and the impulsive quality of the change, a trigger effect possibly caused by additional solar corpuscular radiation.

BIBLIOGRAPHY

(1) Baur, F., 1929: "Das Klima der bisher erforschten Teile der Arktis", Arktis, 2, pp. 77-89, 110-120.

(2) ——, 1951: "Extended-Range Weather Forecasting", Compendium of Meteorology. T. F. Malone, editor; American Meteorological Society, Boston, Mass., pp. 814-33.

(3) Bodurtha, F.T., 1952: "An Investigation of Anticyclogenesis in Alaska", J. Meteor., 9, pp. 118-25.

(4) Craig, R.A., 1952: "Surface-pressure Variations following Geomagnetically Disturbed and Geomagnetically Quiet Days", J. Meteor., 9, pp. 126-38.

(5) Dorsey, H.G., Jr., 1949: "Meteorological Characteristics of Northern Arctic America". Unpublished Master's Thesis, Department of Meteorology, Massachusetts Institute of Technology, Cambridge, Mass.

(6) Duell, B. and Duell, G., 1948: "The Behavior of Barometric Pressure During and After Solar Particle Invasions and Solar Ultraviolet Invasions", Smithsonian Misc. Collection, Vol. 110, No. 8. 34 pp.

(7) Dzerdzeevskii, B.L., 1946: "On the Distribution of Atmospheric Pressure over the Central Arctic", Meteorologia i Gidrologia, No. 1, pp. 33-8. Translated by I. Tone, University of California at Los Angeles, Scientific Report No. 3, Contract AF 19(122)-228.

(8) Estoque, M.A., 1957: Dynamical Prediction of the Arctic Circulation. Scientific Report No. 4, Contract AF 19(604)-1141, Arctic Meteorology Research Group, McGill University, Montreal.

(9) Evans, J.W., 1956: Variations of the Sun. Technical Report No. 2, Institute for Solar-Terrestrial Research, High Altitude Observatory of the University of Colorado, pp. 1-10.

(10) Flohn, H., 1952: "Zur Aerologie der Polargebiete", Met. Rundschau, 5, pp. 81-7, 121-8. Translated as "The Aerology of the Polar Regions", Arctic Meteorology Research Group, McGill University, Appendix to Status Report No. 4, Contract AF 19(604)-1141, March, 1955.

(11) Hare, F. Kenneth, Godson, W.L., MacFarlane, M.A. and Wilson, C.V., 1957: Specification of Pressure Fields and Flow Patterns in Polar Regions. Theories and Techniques. Scientific Report No. 3, Contract AF 19(604)-1141, Arctic Meteorology Research Group, McGill University, Montreal.

(12) Keegan, T.J., 1957: "Synoptic Climatology of the Arctic". Unpublished Master's Thesis, Department of Meteorology, Massachusetts Institute of Technology, Cambridge, Mass. 51 pp.

BIBLIOGRAPHY (continued)

(13) Keegan, T.J., 1958: "The Wintertime Circulation in the Arctic Troposphere", in Contributions to the Study of the Arctic Circulation. Scientific Report No. 7, Contract AF 19(604)-1141, Arctic Meteorology Research Group, McGill University, Montreal.

(14) Lorenz, E.N., 1956: Empirical Orthogonal Functions and Statistical Weather Prediction. Scientific Report No. 1, Contract AF 19(604)-1566, Statistical Forecasting Project, Massachusetts Institute of Technology, Cambridge, Mass. 49 pp.

(15) MacFarlane, M.A., 1957: The Wadsworth Orthogonal Polynomial Technique over the North Polar Area during 1955. Supplement No. 1 to Scientific Report No. 3, Contract AF 19(604)-1141, Arctic Meteorology Research Group, McGill University, Montreal.

(16) Miller, R.G., and Sellers, W.D., 1956: "Part II: Theory and Methods of Application", in Studies in Climatology. W.D. Sellers, editor; Final Report, Contract N5 ori-07883, M.I.T., Cambridge, Mass., pp.10-31.

(17) Namias, J., 1952: "The Annual Course of Month-to-Month Persistence in Climatic Anomalies", Bull. Am. Met. Soc., 33, No. 7, pp. 279-385.

(18) Reed, R.J., and Tank, W.G., Miscellaneous Studies of Polar Vortices. Occasional Report No. 4, Scientific Report No. 1, Contract AF 19(604)-1298, Department of Meteorology and Climatology, University of Washington. May, 1956.

(19) Rex, D.F., 1950: "Blocking Action in the Middle Troposphere and its Effect on Regional Climate. Part I: An Aerological Study of Blocking Action," and "Part II: The Climatology of Blocking Action". Tellus, 2, pp. 196-211 and pp. 275-301.

(20) ——, 1951: "The Effect of Atlantic Blocking Action upon European Climate", Tellus, 3, pp. 100-12.

(21) Scherhag, R., "The Rôle of Tropospheric Cold Air Poles and of Stratospheric High Pressure Centers in the Arctic Weather". Paper delivered before the AGARD Symposium on Polar Atmosphere, Oslo, Norway, July 2-7, 1956.

(22) Shapiro, R., 1954: "A Possible Solar-Weather Effect", J. Meteor., 11, pp. 424-5.

(23) ——, 1956: "Further Evidence of a Solar Weather Effect", J. Meteor., 13, pp. 335-40.

(24) Sutcliffe, R.C., 1954: "Predictability in Meteorology", Archiv. für Meteorologie, Geophysik und Bioklimatologie, Serie A, vol. 7, pp.1-15.

BIBLIOGRAPHY (continued)

(25) Wadsworth, G.P., Bryan, J.G., and Gordon, C.H., 1948: "Short Range and Extended Forecasting by Statistical Methods", Air Wea. Serv. Tech. Rep. No. 105-38, 207 pp.

(26) Ward, W.W., Jr., 1956: Solar, Geomagnetic and Ionospheric Phenomena as Indices of Solar Activity. Geophysical Research Paper No. 54, Geophysics Research Directorate, Cambridge, Mass.

(27) Willett, H.C., 1944: Descriptive Meteorology. New York, N.Y.: Academic Press, Inc. 310 pp.

ACKNOWLEDGMENTS

I should like to thank Professor F. Kenneth Hare for his direction and encouragement, and Dr. W.L. Godson, Dr. M.A. Estoque and Dr. S. Orvig for their advice and help.

APPENDIX A

Surface Level

<u>Values of the Inter-map Correlation Coefficients</u>

<u>for One- and Two-day Lags</u>.

(January 1st, 1955 to January 6th, 1956)

INTER-MAP CORRELATION COEFFICIENTS, ONE-DAY LAG ($\hat{r}_1$)

DAY	JAN	FEB	MAR	APR	MAY	JUN	JUL	AUG	SEPT	OCT	NOV	DEC	JAN
1 - 2	0.665	0.833	0.895	0.856	0.861	0.834	0.604	0.819	0.516	0.676	0.748	0.602	0.86*
2 - 3	0.835	0.887	0.826	0.819	0.793	0.823	0.733	0.746	0.433	0.680	0.586	0.671	0.81*
3 - 4	0.794	0.764	0.743	0.827	0.833	0.744	0.734	0.598	0.763	0.834	0.749	0.639	0.80*
4 - 5	0.834	0.866	0.782	0.837	0.785	0.648	0.670	0.538	0.787	0.828	0.802	0.637	0.84*
5 - 6	0.880	0.883	0.704	0.680	0.711	0.819	0.665	0.605	0.786	0.751	0.611	0.655	0.70*
6 - 7	0.772	0.858	0.529	0.698	0.661	0.819	0.862	0.266	0.832	0.749	0.745	0.752	
7 - 8	0.747	0.817	0.689	0.824	0.506	0.754	0.841	0.627	0.667	0.727	0.366	0.851	
8 - 9	0.838	0.801	0.814	0.809	0.452	0.781	0.782	0.745	0.698	0.718	0.476	0.818	
9 -10	0.828	0.839	0.821	0.768	0.768	0.743	0.827	0.724	0.706	0.545	0.728	0.738	
10-11	0.778	0.773	0.801	0.754	0.829	0.709	0.756	0.709	0.745	0.561	0.718	0.606	
11-12	0.849	0.723	0.581	0.495	0.819	0.490	0.767	0.605	0.716	0.637	0.720	0.527	
12-13	0.894	0.616	0.527	0.585	0.821	0.474	0.608	0.688	0.512	0.676	0.560	0.666	
13-14	0.925	0.489	0.583	0.739	0.864	0.386	0.702	0.581	0.634	0.593	0.787	0.630	
14-15	0.807	0.361	0.749	0.710	0.846	0.462	0.630	0.718	0.628	0.723	0.635	0.721	
15-16	0.880	0.646	0.775	0.591	0.801	0.426	0.741	0.597	0.702	0.736	0.678	0.818	
16-17	0.852	0.777	0.853	0.730	0.821	0.547	0.670	0.562	0.668	0.685	0.665	0.702	
17-18	0.825	0.806	0.805	0.769	0.853	0.635	0.687	0.565	0.628	0.569	0.538	0.800	
18-19	0.912	0.778	0.876	0.715	0.813	0.539	0.779	0.678	0.647	0.509	0.726	0.784	

* extra days computed directly from equation (1)

Table 1

INTER-MAP CORRELATION COEFFICIENTS, ONE-DAY LAG ($\hat{r}_1$)
(continued)

DAY	JAN	FEB	MAR	APR	MAY	JUN	JUL	AUG	SEPT	OCT	NOV	DEC
19-20	0.834	0.700	0.812	0.750	0.624	0.699	0.749	0.843	0.649	0.613	0.734	0.718
20-21	0.701	0.553	0.795	0.839	0.633	0.615	0.783	0.885	0.664	0.798	0.631	0.578
21-22	0.740	0.531	0.813	0.790	0.639	0.567	0.559	0.906	0.686	0.327	0.574	0.676
22-23	0.776	0.558	0.768	0.771	0.683	0.619	0.618	0.831	0.681	0.535	0.656	0.688
23-24	0.767	0.545	0.756	0.698	0.785	0.693	0.672	0.820	0.693	0.553	0.766	0.479
24-25	0.819	0.536	0.835	0.465	0.762	0.492	0.725	0.727	0.667	0.602	0.504	0.596
25-26	0.850	0.373	0.781	0.685	0.847	0.244	0.592	0.632	0.646	0.687	0.611	0.750
26-27	0.855	0.572	0.710	0.784	0.785	0.640	0.595	0.630	0.690	0.706	0.781	0.824
27-28	0.877	0.818	0.702	0.783	0.634	0.758	0.627	0.517	0.772	0.713	0.749	0.841
28-29(1)	0.885	0.876	0.529	0.849	0.672	0.736	0.734	0.612	0.800	0.645	0.567	0.864
29-30	0.895		0.724	0.814	0.730	0.771	0.817	0.560	0.765	0.785	0.655	0.886
30-31(1)	0.858		0.792	0.791	0.807	0.806	0.762	0.594	0.667	0.744	0.505	0.852
31-1	0.816		0.858		0.555		0.723	0.767		0.752		0.910*

* extra days computed directly from equation (1)

(1) - first day of the following month.

Table 1 (continued)

Table 2

INTER-MAP CORRELATION COEFFICIENTS, TWO-DAY LAG ($\hat{r}_2$)

DAY	JAN	FEB	MAR	APR	MAY	JUN	JUL	AUG	SEPT	OCT	NOV	DEC	JAN
1 - 3	0.614	0.740	0.520	0.664	0.713	0.756	0.519	0.591	0.112	0.367	0.259	0.413	0.786*
2 - 4	0.669	0.594	0.591	0.694	0.689	0.641	0.568	0.369	0.358	0.431	0.206	0.397	0.818*
3 - 5	0.595	0.572	0.446	0.616	0.661	0.447	0.648	0.151	0.597	0.699	0.592	0.375	0.673*
4 - 6	0.686	0.447	0.687	0.464	0.444	0.483	0.394	0.348	0.696	0.626	0.549	0.364	0.353*
5 - 7	0.657	0.744	0.358	0.277	0.310	0.658	0.544	0.043	0.727	0.651	0.446	0.232	
6 - 8	0.666	0.791	0.420	0.435	0.398	0.519	0.686	0.157	0.540	0.566	0.338	0.633	
7 - 9	0.701	0.620	0.592	0.656	0.329	0.584	0.691	0.453	0.449	0.407	0.083	0.784	
8 -10	0.767	0.644	0.540	0.639	0.142	0.578	0.660	0.561	0.504	0.220	0.139	0.618	
9 -11	0.676	0.633	0.564	0.545	0.664	0.465	0.615	0.532	0.506	0.209	0.361	0.402	
10-12	0.670	0.531	0.394	0.551	0.787	0.242	0.563	0.327	0.478	0.335	0.511	0.300	
11-13	0.804	0.524	0.226	0.369	0.665	0.219	0.445	0.416	0.332	0.459	0.412	0.291	
12-14	0.806	0.507	0.083	0.388	0.631	0.062	0.417	0.338	0.403	0.372	0.493	0.323	
13-15	0.830	0.324	0.393	0.437	0.765	-0.016	0.403	0.303	0.421	0.407	0.504	0.293	
14-16	0.789	0.414	0.416	0.612	0.661	-0.042	0.361	0.276	0.447	0.491	0.249	0.408	
15-17	0.800	0.431	0.576	0.472	0.687	-0.017	0.463	0.221	0.442	0.575	0.507	0.513	
16-18	0.741	0.607	0.738	0.517	0.686	0.264	0.477	0.304	0.218	0.492	0.364	0.512	
17-19	0.756	0.635	0.715	0.470	0.688	0.197	0.643	0.390	0.325	0.118	0.388	0.592	

* extra days computed directly from equation (1)

INTER-MAP CORRELATION COEFFICIENTS, TWO-DAY LAG ($\hat{r}_2$)
(continued)

DAY	JAN	FEB	MAR	APR	MAY	JUN	JUL	AUG	SEPT	OCT	NOV	DEC
18-20	0.722	0.455	0.702	0.494	0.451	0.263	0.626	0.530	0.355	0.287	0.571	0.555
19-21	0.544	0.251	0.616	0.650	0.295	0.381	0.631	0.761	0.345	0.537	0.615	0.602
20-22	0.557	0.375	0.720	0.680	0.282	0.312	0.422	0.849	0.297	0.158	0.423	0.327
21-23	0.659	0.381	0.651	0.533	0.272	0.229	0.240	0.782	0.368	0.215	0.298	0.503
22-24	0.627	0.458	0.636	0.460	0.433	0.372	0.232	0.683	0.450	0.191	0.432	0.096
23-25	0.548	0.422	0.643	0.112	0.513	0.411	0.501	0.556	0.482	0.053	0.529	0.418
24-26	0.808	-0.065	0.575	0.189	0.580	-0.139	0.519	0.511	0.319	0.207	0.516	0.459
25-27	0.857	0.237	0.424	0.546	0.750	-0.039	0.172	0.563	0.444	0.458	0.478	0.614
26-28	0.744	0.526	0.710	0.591	0.566	0.540	0.299	0.419	0.587	0.552	0.526	0.707
27-29(1)	0.834	0.655	0.398	0.626	0.464	0.556	0.274	0.121	0.679	0.388	0.514	0.667
28-30(2)	0.779	0.764	0.120	0.690	0.457	0.543	0.576	0.172	0.556	0.485	0.434	0.757
29-31(1)	0.709		0.590	0.649	0.523	0.620	0.578	0.129	0.367	0.717	0.332	0.748
30-1 (2)	0.739		0.627	0.663	0.338	0.422	0.492	0.388	0.554	0.631	0.367	0.822*
31-2	0.815		0.713		0.333		0.524	0.314		0.465		0.732*

* extra days computed directly from equation (1)

(1) first day of the following month.
(2) second day of the following month.

Table 2 (continued)

Graphs Showing the Change with Time of the Interdiurnal Correlation Coefficients $\hat{r}_1$ and $\hat{r}_2$

The one-day lag ($\hat{r}_1$) has been plotted midway between the days concerned.

The two-day lag ($\hat{r}_2$) has been plotted midway between the two days correlated and as a double curve (i.e., $\hat{r}_2$'s for January 1-3, 3-5, 5-7, etc. have been plotted on days 2, 4, 6, etc. and joined. Similarly, coefficients between charts for January 2-4, 4-6, 6-8, etc. have been plotted at January 3, 5, 7, etc. and joined.


JANUARY
FEBRUARY
MARCH
APRIL
MAY
JUNE
JULY
AUGUST
SEPTEMBER
OCTOBER
NOVEMBER
DECEMBER
JANUARY


JANUARY
FEBRUARY
MARCH
APRIL
MAY
JUNE
JULY
AUGUST
SEPTEMBER
OCTOBER
NOVEMBER
DECEMBER
JANUARY

APPENDIX B

Surface Level

Periods of Persistence During 1955

Mean Maps for Periods of Persistence over the Arctic at Sea-Level in 1955

The mean maps comprise one map a day throughout each period.

The centres and tracks are plotted at 12-hour intervals, but have been dated only at the 24-hour interval used in the mean map.

·——·——→ centres and apparent displacement of cyclones

·——·······→ regeneration or doubtful displacement

·- - - -·- - - -→ centres and apparent displacement of anticyclones

TYPE A: where $\hat{r}_1 \geqq .800$; $\hat{r}_2 \geqq .700$

TYPE B: where $\hat{r}_1 \geqq .700$; $\hat{r}_2 \geqq .600$

TYPE C: where $\hat{r}_1 \geqq .700$; $\hat{r}_2 \geqq .500$

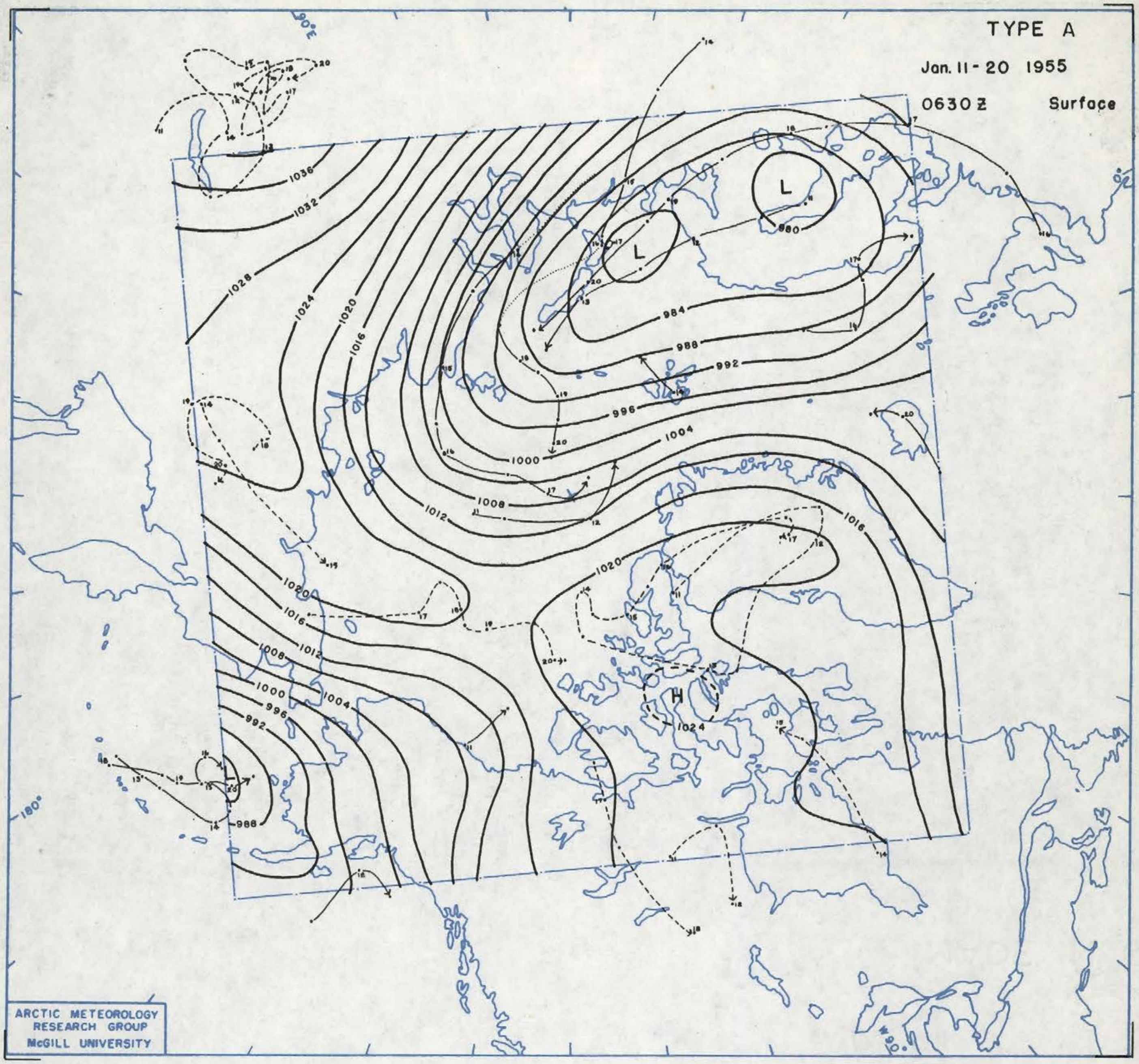

Map 1

During this period these large-scale systems are remarkably persistent, but on the synoptic scale there is a great deal of activity associated with the strong upper air vortex centred over the Svalbard-Scandinavia area. Prior to the 9th January, a high situated over the Atlantic and Western Europe has prevented Atlantic storms from entering the Polar regions, while the end of persistence is marked by the breakdown of the Siberian ridge and shift of the major high into the Arctic basin. At 500 mb. this is associated with the westward movement of the upper vortex to a position over Greenland.

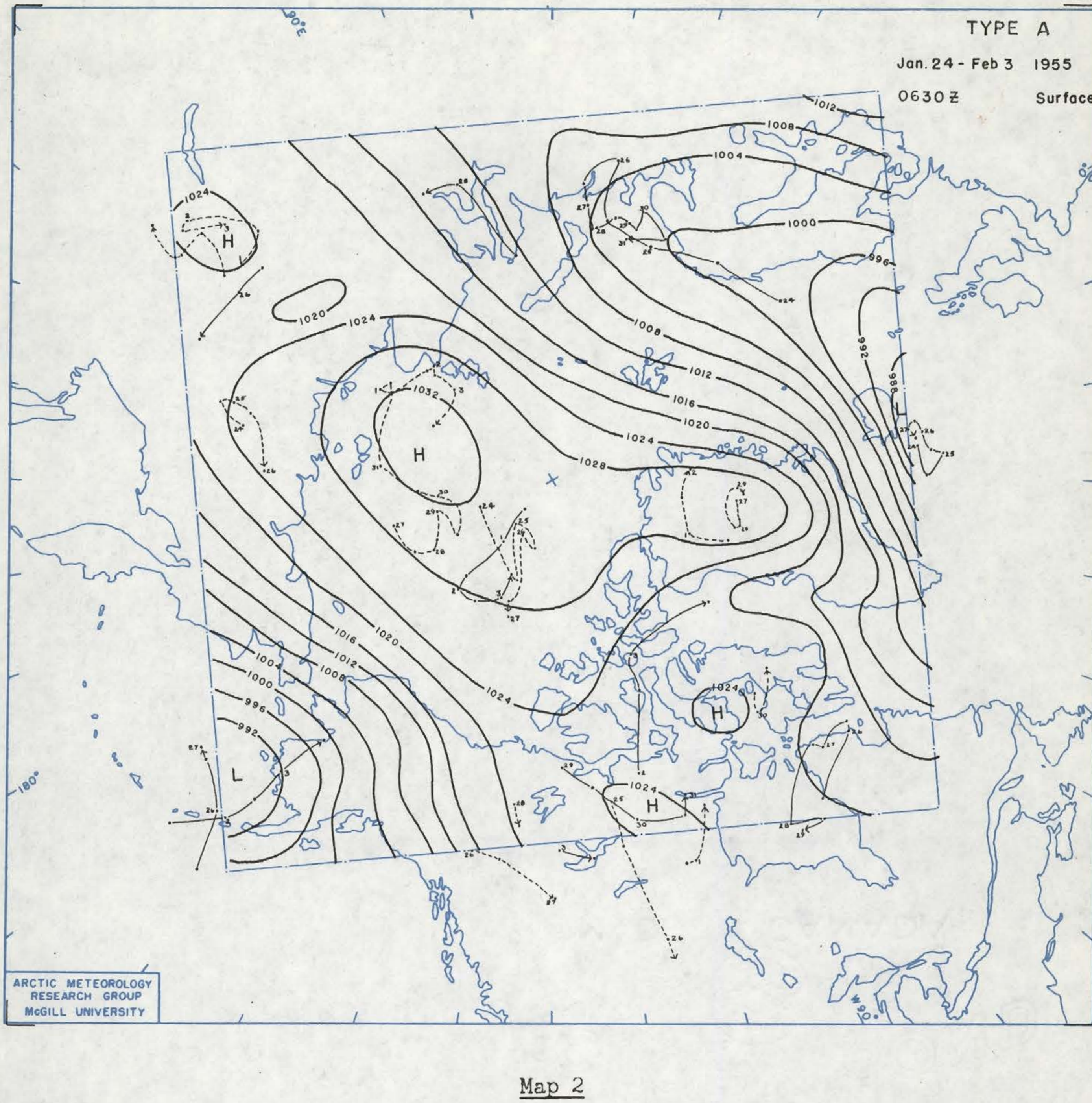

Map 2

Following the breakdown of the Siberian ridge after January 20, the large-scale systems were temporarily realigned to allow free movement of cyclones from Scandinavia to E. Siberia. By January 24, the main area of high pressure had migrated westwards to cover the Arctic basin, while pressure had fallen considerably over the Atlantic. The most outstanding changes from Map 1 appear to be connected with this general westward shift of the large-scale systems, both at the surface and 500 mb. levels. On February 1 a low develops over the Polar basin and the high gradually begins to change its position with a continued westerly motion. At the same time the strong cyclonic system near Novaya Zemlya fills. After February 3 the westward regression takes place more rapidly.

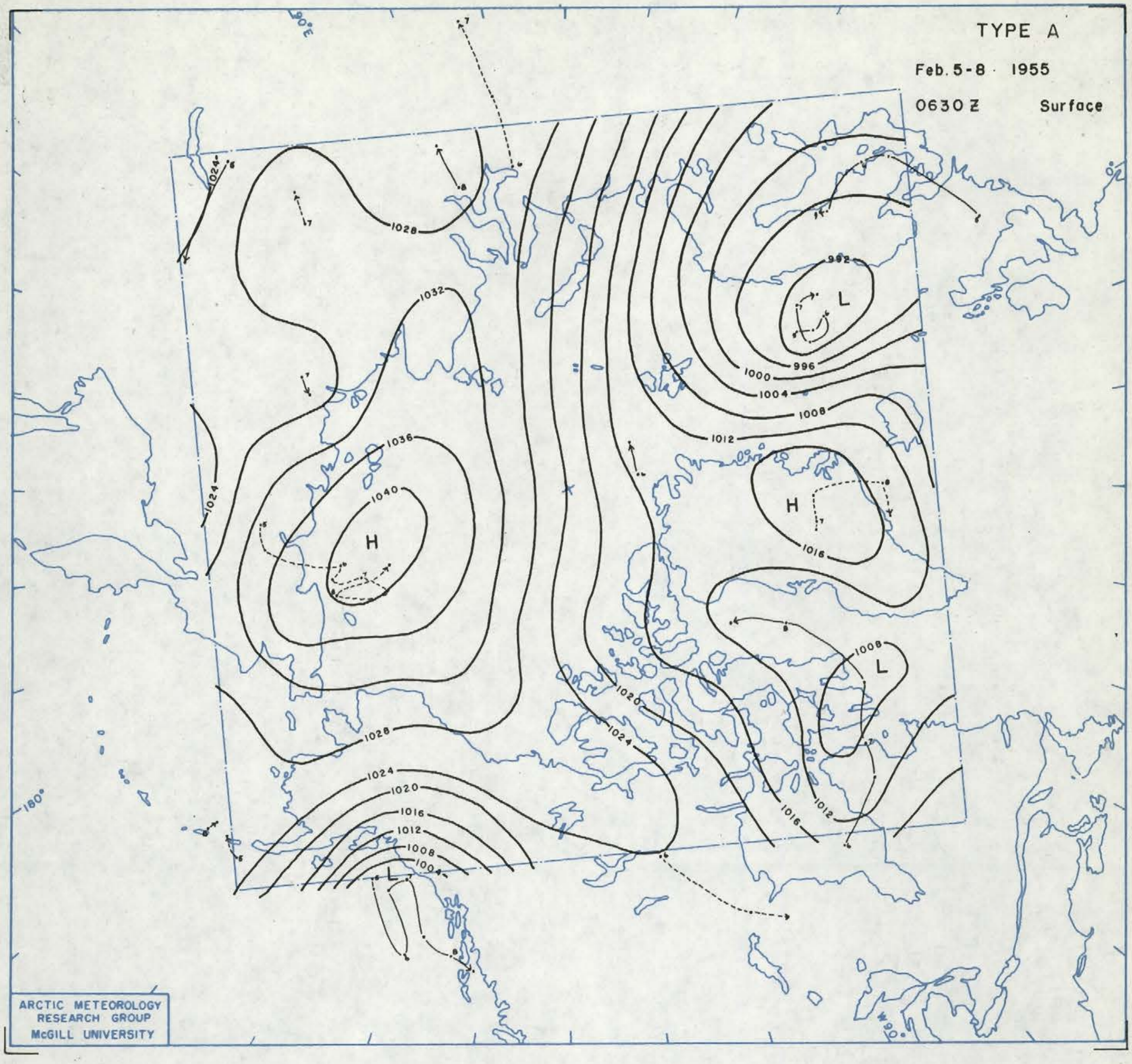

Map 3

February 5 to 8 represents another pause in this westward migration of the large-scale systems. This period is remarkably stable. The main synoptic activity appears to be connected with two low centres at 500 mb., one major vortex over the Canadian Archipelago, around which storms are being steered into Baffin Bay, and a small centre near the Scandinavian coast. The breakdown after February 8 shows up in a more cellular structure with intricate troughs and ridges. A low develops over Franz Josef Land and crosses the Polar basin to the American coast. Over Greenland a ridge of high from the Atlantic builds up into a considerable block associated with strong upper level gradients.

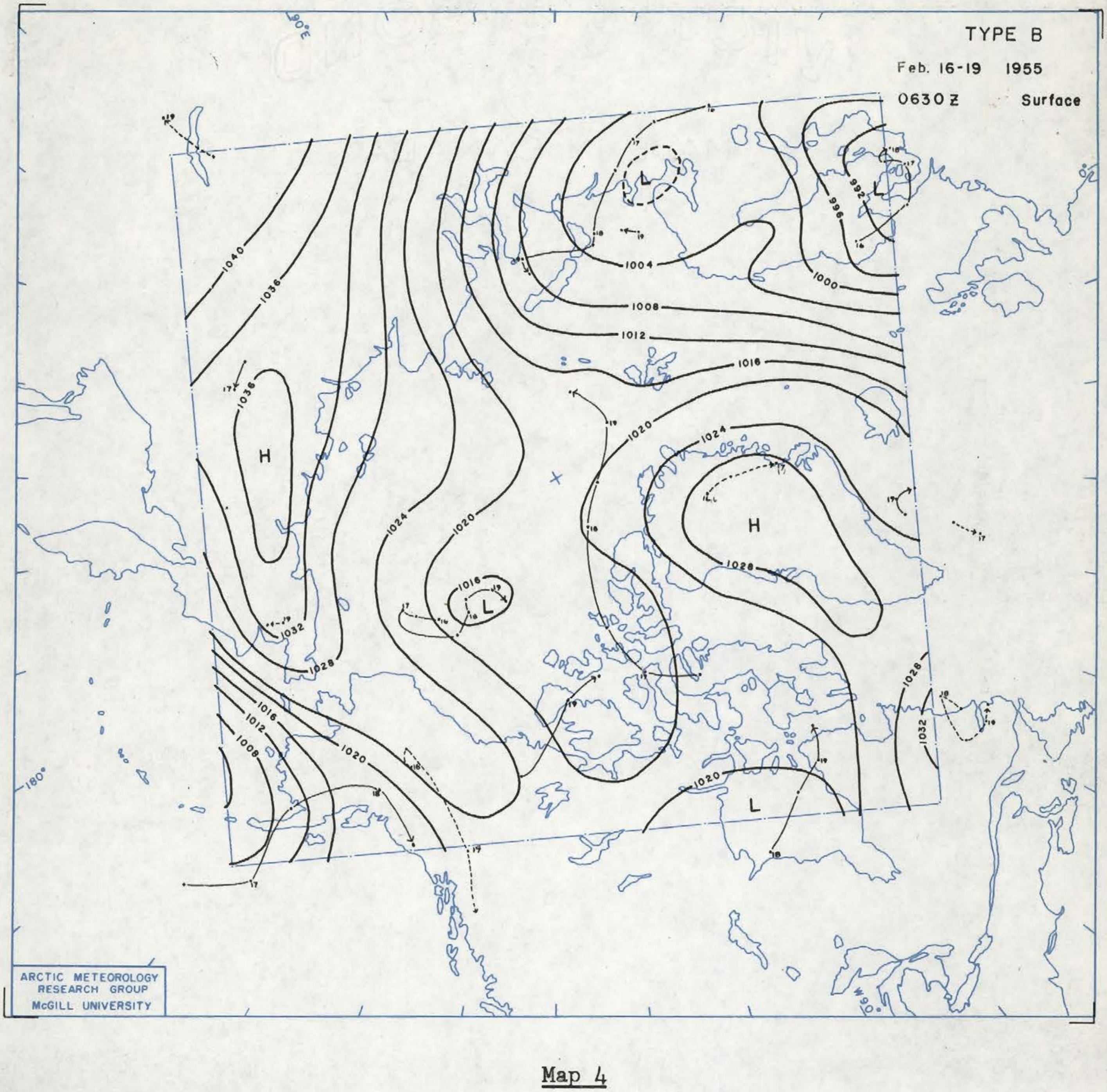

Map 4

Following nine days of lower persistence, the large-scale systems are now more clearly defined and stable. The trough over the Arctic has become well established and the Siberian high is again a major feature. The 500 mb. map is reflected to a high degree in these surface patterns, the synoptic systems over Europe and the Arctic basin lying beneath upper air lows, whilst the cyclonic tracks around N. Greenland and the Bay of Alaska are in the path of strong upper air westerlies around the Atlantic and Pacific ridges. From the end of this period there is a rapid eastward change in the orientation of the major high-level vortex as the ridge over Greenland weakens and shifts to the east.

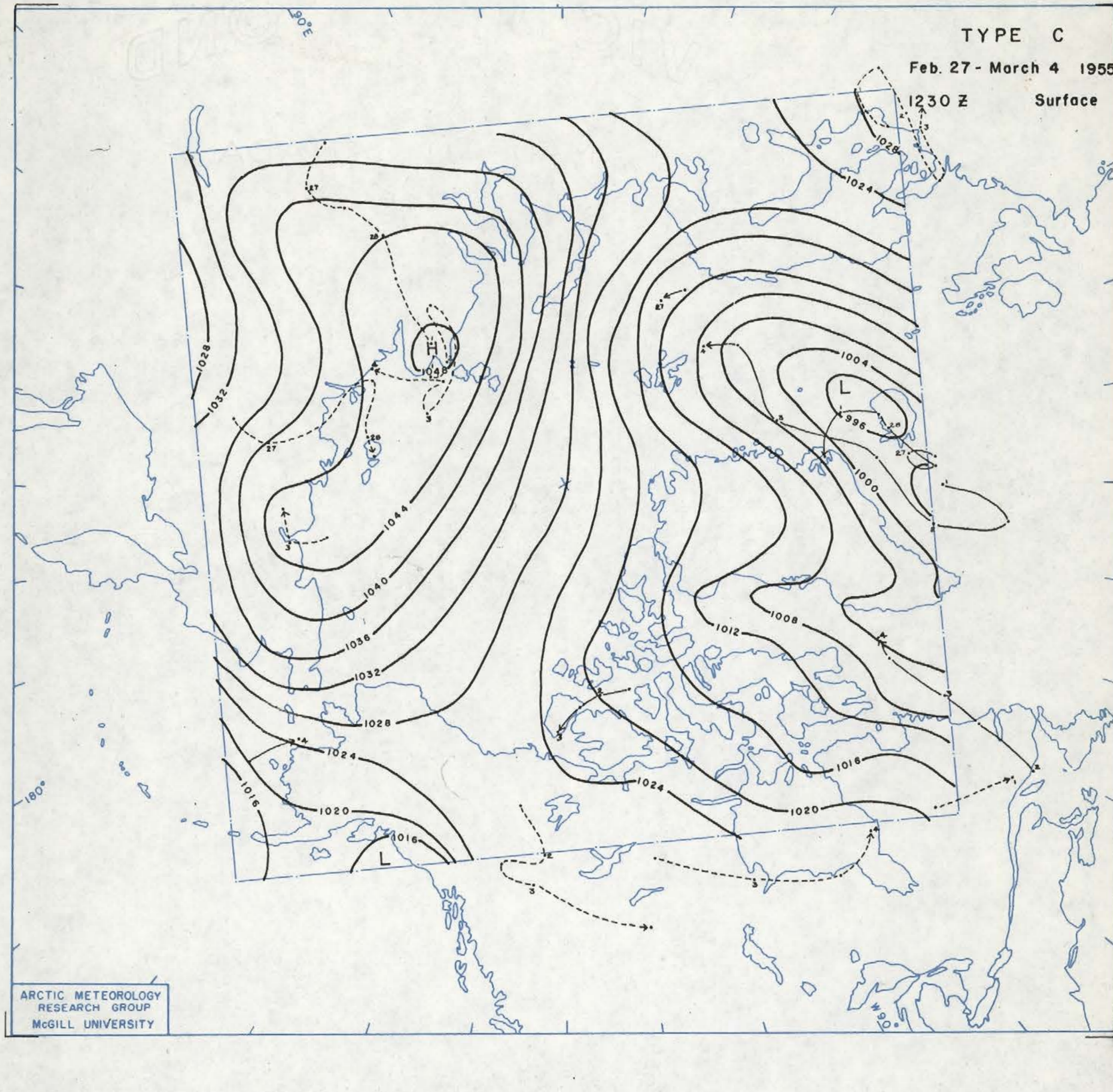

Map 5

Between February 19 and 27 the patterns changed rapidly. The Pacific high extended poleward and later retreated as the Siberian high moved northwards to cover the whole basin. During these six days cyclonic activity is associated with strong upper air gradients over Labrador and E. Greenland, while the major anticyclone gradually moves towards the Laptev Sea. By March 5 the Siberian high has declined in extent and magnitude.

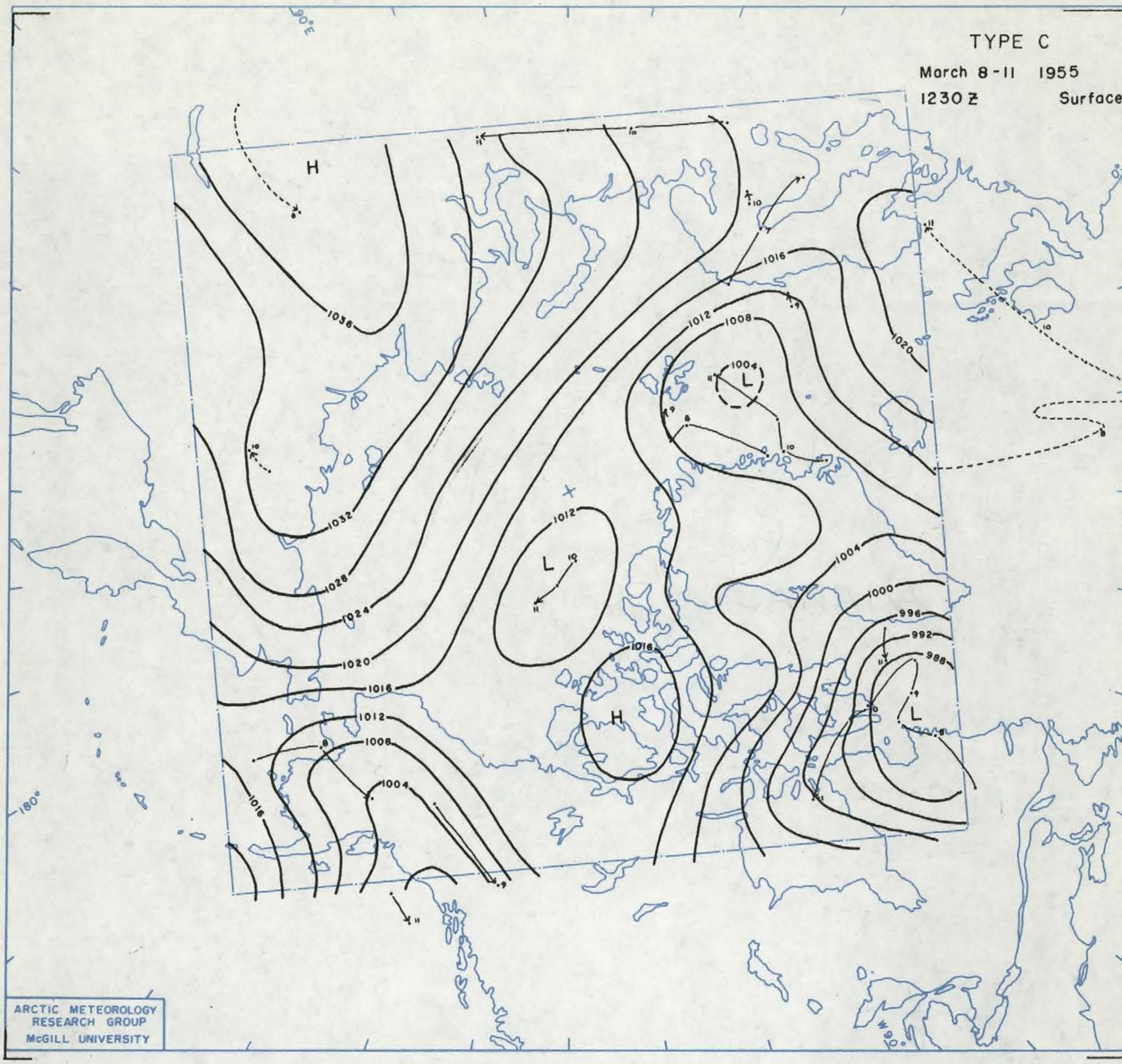

Map 6

Again the number of cells increases, and the patterns are continually changing until March 7 when there is a reinstatement of the Siberian high. From March 8 to 11 there is considerable synoptic change, especially over the Greenland area, where the ridge of high pressure extending from the archipelago to the Atlantic weakens, and the Atlantic high centre shifts eastwards. Cyclonic activity is in effect over Alaska and East Greenland below strong 500 mb. gradients. Over the Canadian Archipelago - Labrador area there is a major 500 mb. vortex. Following this period of persistence, the Siberian high once again breaks down as the flow at 500 mb. becomes more zonal and synoptic activity accelerates.

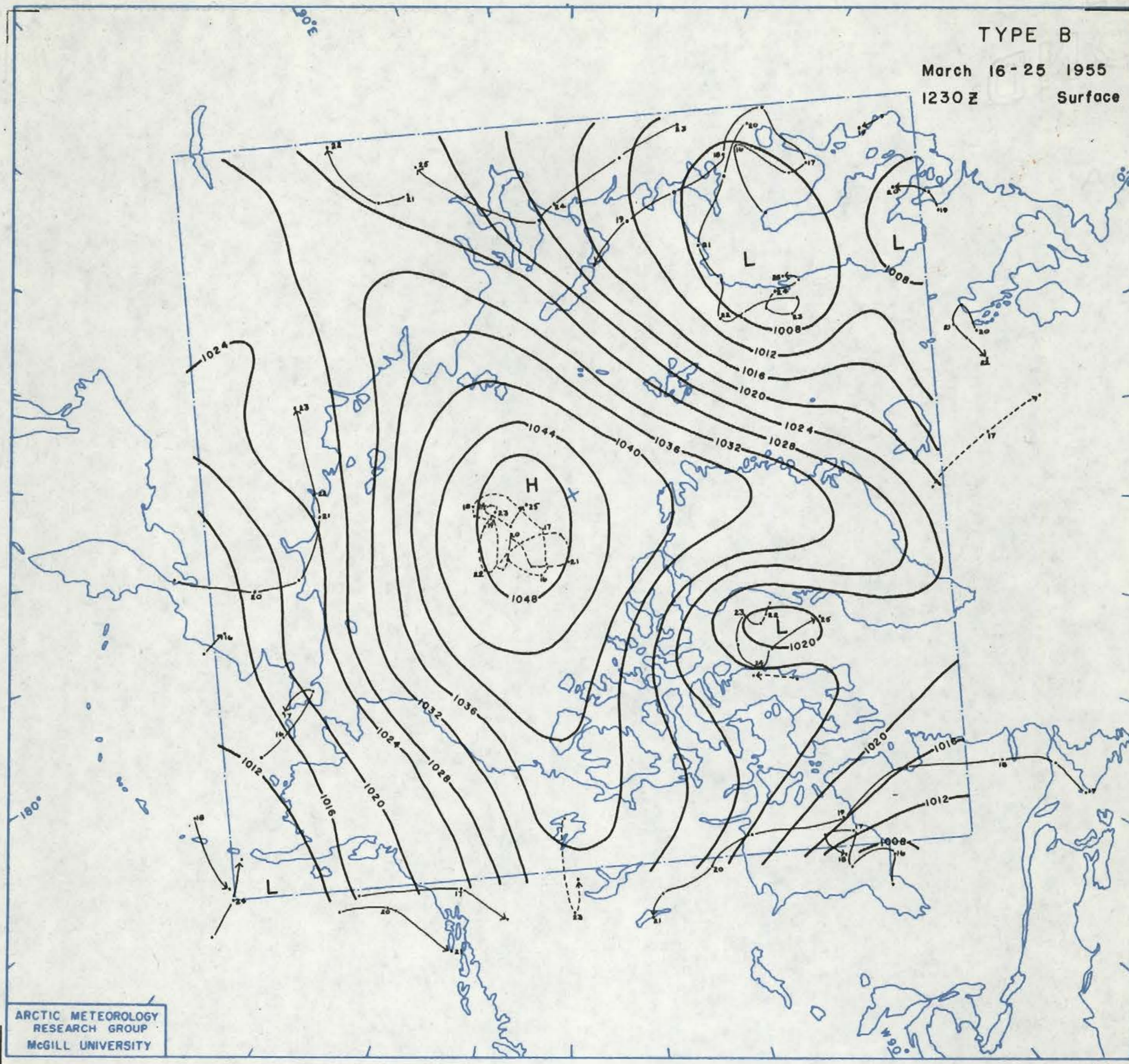

Map 7

About March 13 a high begins to build up over N. Alaska, under a ridge of warm air from the Pacific. By March 16 this centre has migrated polewards and has become firmly established over most of the area, extending into Siberia, over the Atlantic and into Canada. During these ten days the main feature is the stability of the anticyclone over the Arctic basin with peripheral synoptic activity. During the first few days a ridge of high from the Atlantic extends at 500 mb. over the Archipelago and develops a closed centre. Towards the end of the period a strong low vortex at the upper level is displaced to the west over Greenland and the Archipelago, and cyclogenesis takes place in the Thule area. By March 26 there is a change in the axis of the high, the Siberian ridge breaks down and lows move across into S.E. Siberia. The former low index conditions give way to more zonal flow, especially over the European-Asian Sector.

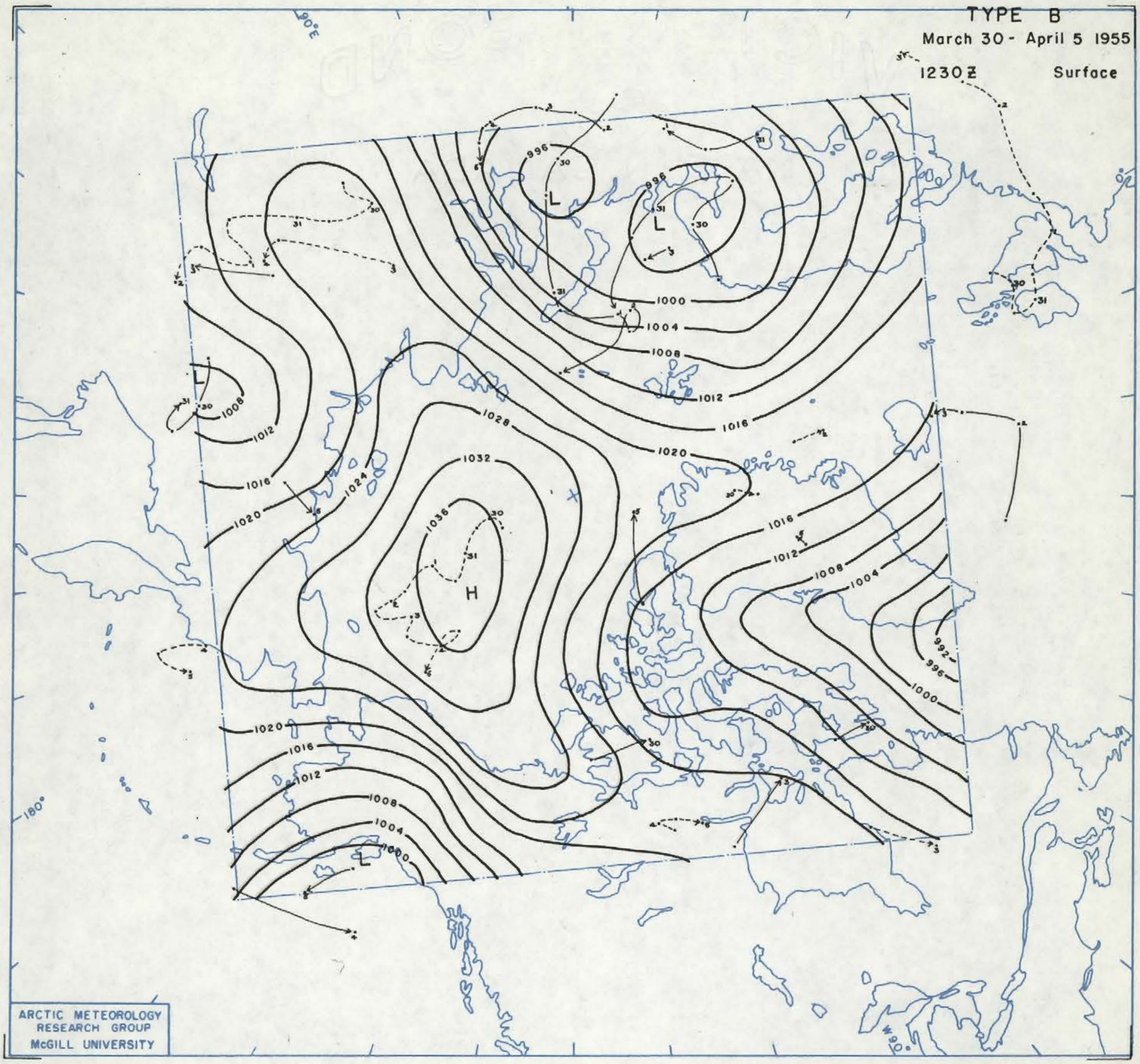

Map 8

The increased zonal flow relaxes, and the two continental and two oceanic ridges once again become prominent. The anticyclone over the Arctic basin expands and moves slowly towards the Alaskan coast. This very regular distribution of nighs and lows is almost a replica of patterns aloft.

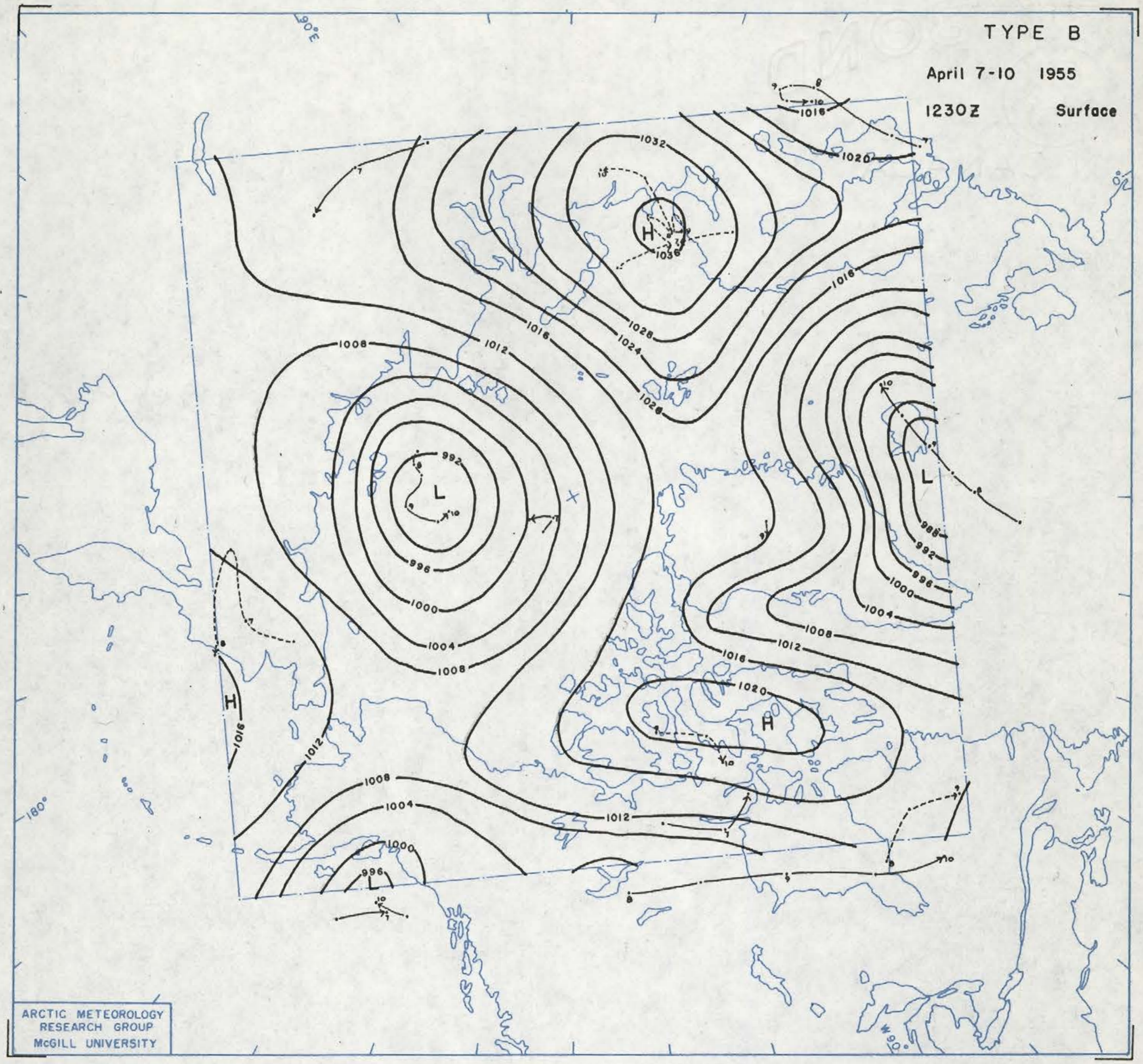

Map 9

April 4 to 7 shows a complete reversal of pattern from an intense Arctic high to a deep low which lasted well into mid-April. The charts for April 5 are highly cellular and intricate in design. A trough develops across the pole, breaking the polar high into two cells, one over Asia and the other over the American Arctic. Cyclogenesis occurs over the basin under a cold cyclonic vortex at 500 mb. Over the White Sea the Asian high centre intensifies. The upper air low over the Arctic remains steadfast throughout the four days and even longer. The drop in the correlation coefficient between April 10 and 11 appears to be due partly to the beginning of a change in the orientation of the large-scale systems to the east over the Atlantic and Asia.

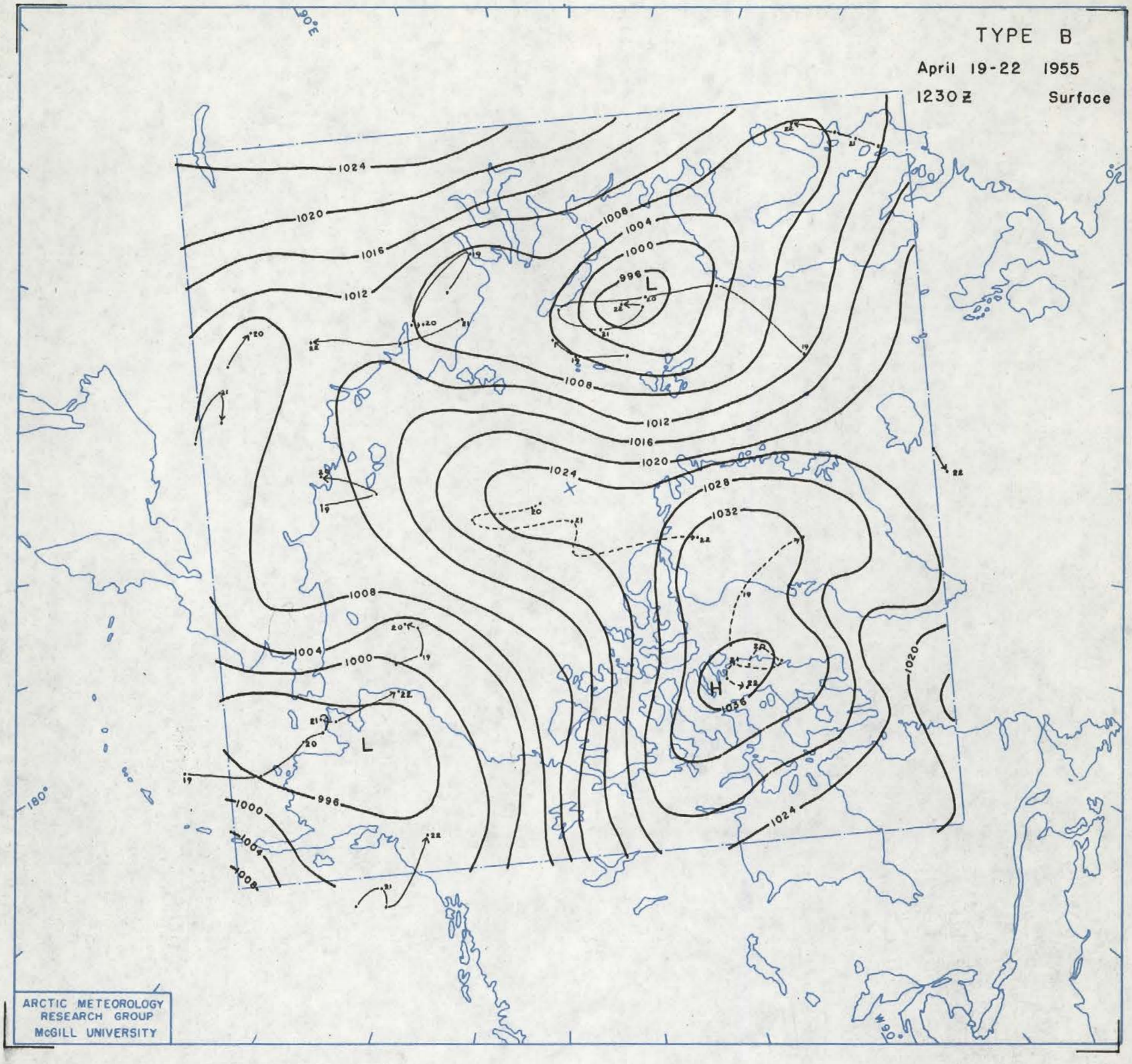

Map 10

Comparing Maps 9 and 10 there is a hint of a second reversal in pattern over much of the area. In the interim there has been a general eastward movement of the major centres of action. The high over the Archipelago and E. Canada has intensified beneath a ridge of warm air, and extended by April 19 to include a separate centre over the polar area. At 500 mbs. the axis of the major cyclonic vortex lies between Svalbard and Alaska and is associated with quite strong gradients. After April 22 the large-scale anticyclonic system breaks up and there is a polar extension of the Siberian high, preventing the passage of cyclones across Siberia.

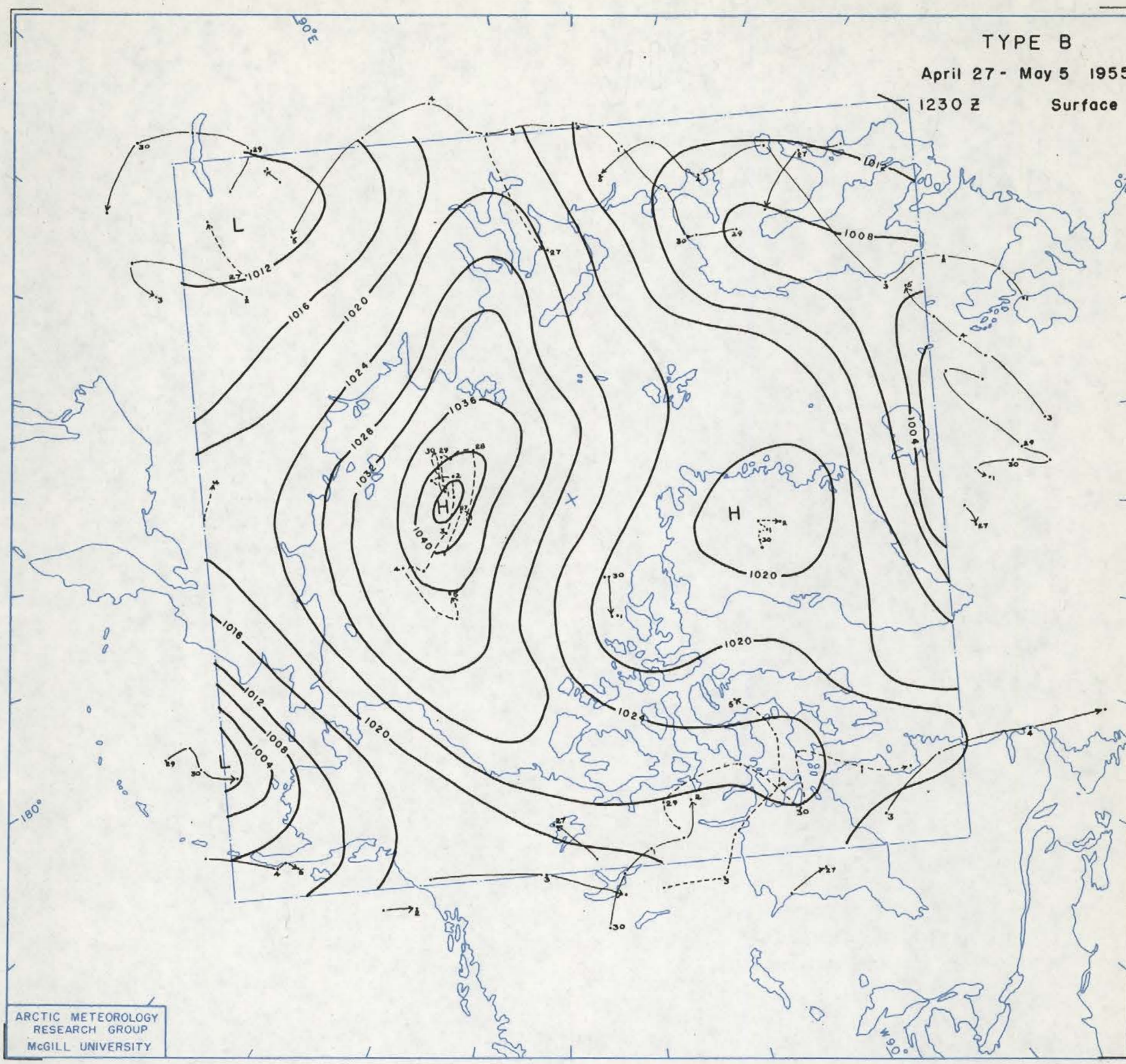

Map 11

A closed centre of high pressure develops over Alaska and moves into the Arctic basin to join up with the Siberian ridge. From April 27 the upper air flow pattern is becoming increasingly zonal, and by May 2 the Siberian ridge has given way to the passage of cyclones. This map has features in common with Map 7, with its dominating anticyclone and peripheral cyclonic activity. Persistence breaks down when the anticyclone begins to weaken and contract, and with increasing synoptic activity.

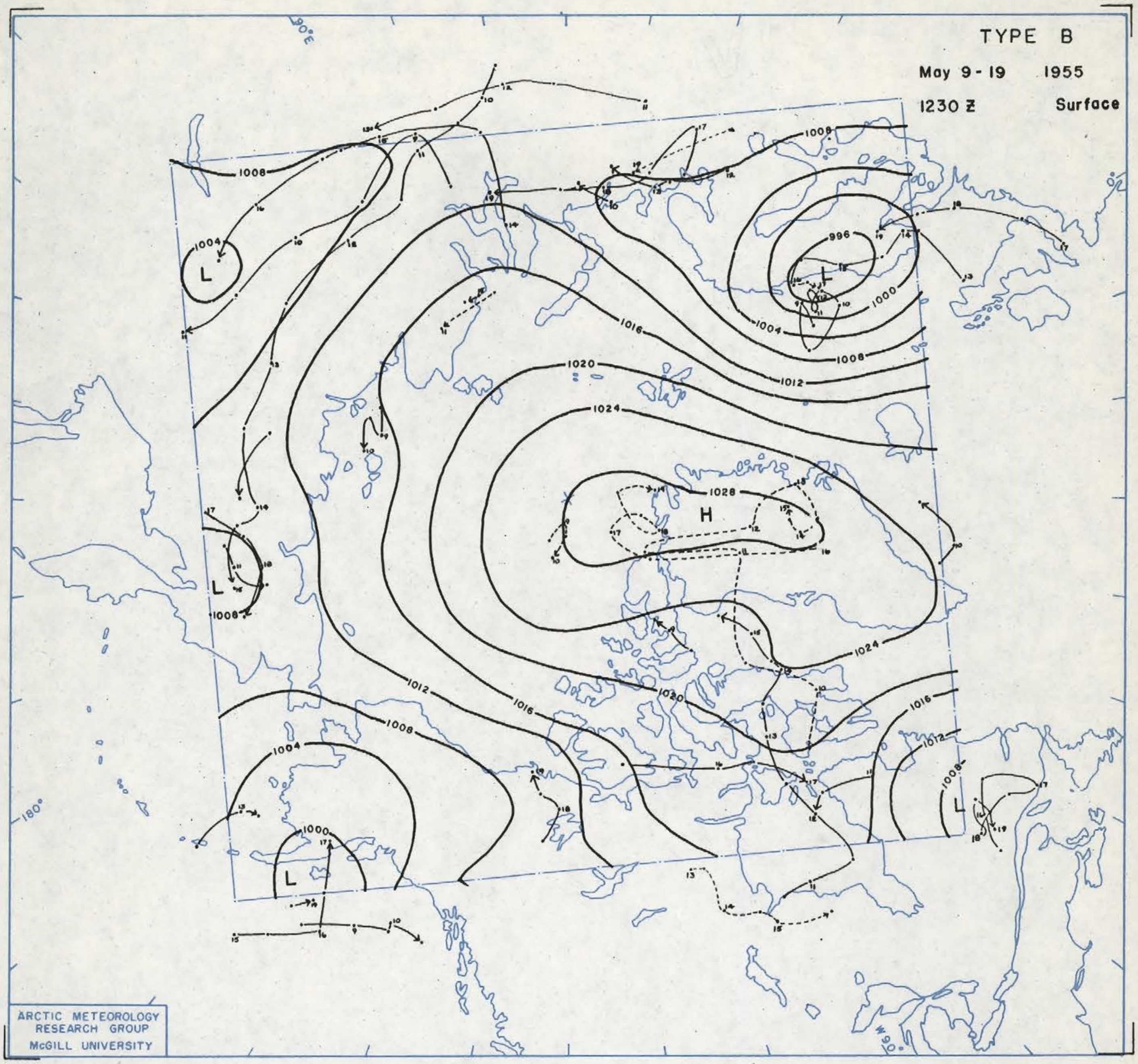

Map 12

The major anticyclonic system has moved towards N. Greenland. At 500 mb. the low over the western Archipelago appears to be steering surface storms into Baffin Bay. In general the major change has been one in orientation with the major anticyclone block recentred well to the east over the Atlantic and extending towards Siberia. There is considerable synoptic activity within this period associated with upper air lows and strong westerly flow, especially over Europe and Asia. Following May 19 the circulation over Asia slackens. There is an increase in the number of centres.

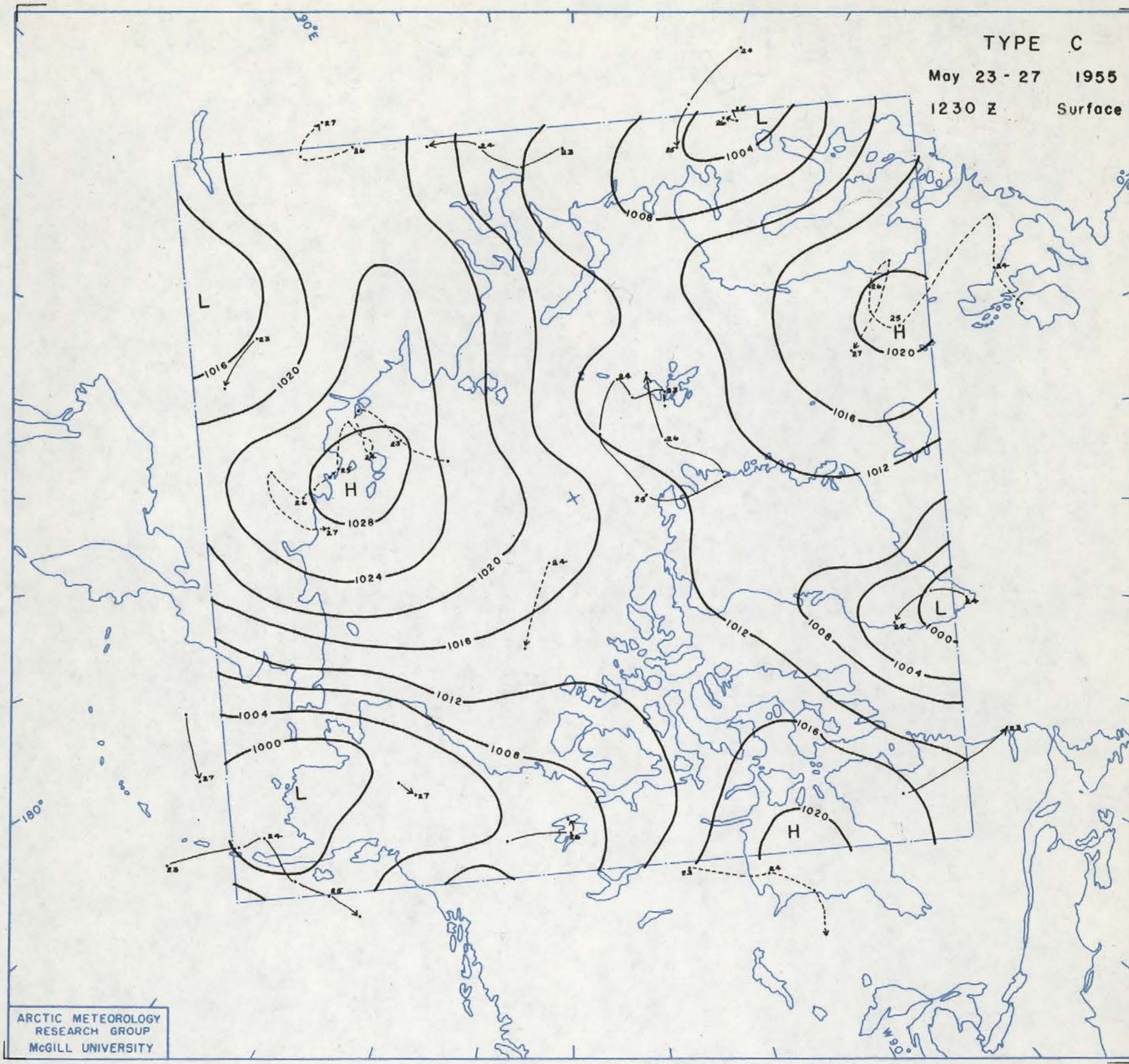

Map 13

There is a change from predominantly zonal to meridional flow from May 19 to 23 and this map shows the contrasting strongly cellular circulation pattern which persists from May 23 to 27. Once again this pattern closely reflects the upper air pattern where the polar vortex, centred over the Svalbard-Greenland area, has lobes with closed centres of low corresponding to the cyclonic centres at sea level.

On May 28 the circulation relaxes further and a number of weak centres of low occur in the polar area.

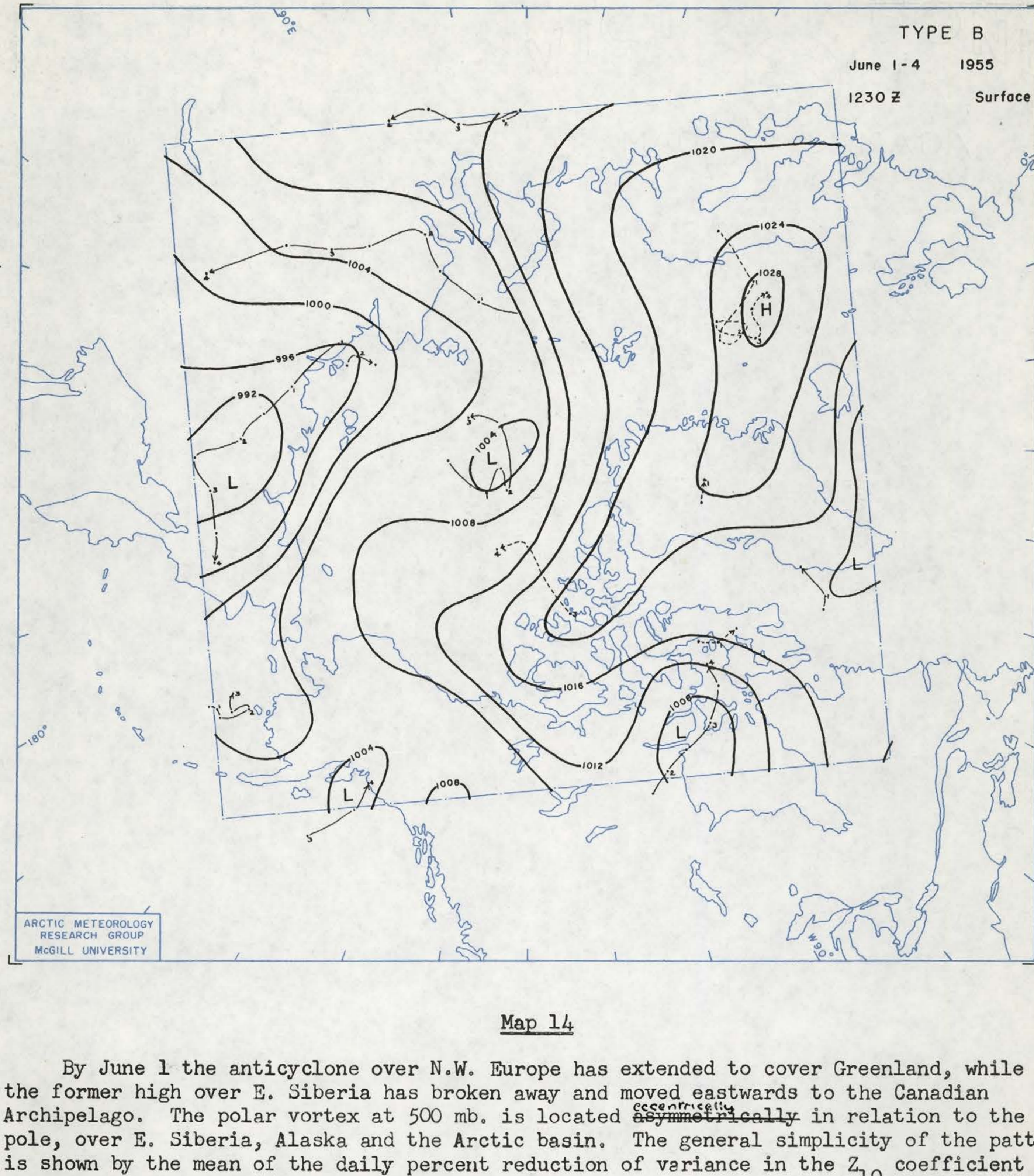

Map 14

By June 1 the anticyclone over N.W. Europe has extended to cover Greenland, while the former high over E. Siberia has broken away and moved eastwards to the Canadian Archipelago. The polar vortex at 500 mb. is located eccentrically ~~asymmetrically~~ in relation to the pole, over E. Siberia, Alaska and the Arctic basin. The general simplicity of the pattern is shown by the mean of the daily percent reduction of variance in the Z_{10} coefficient which is as high as 56%. Over much of the mean chart there has in fact been a complete reversal from Map 13. Synoptic activity is connected both with individual upper air centres of low pressure and with the strong gradients of the large-scale vortex.

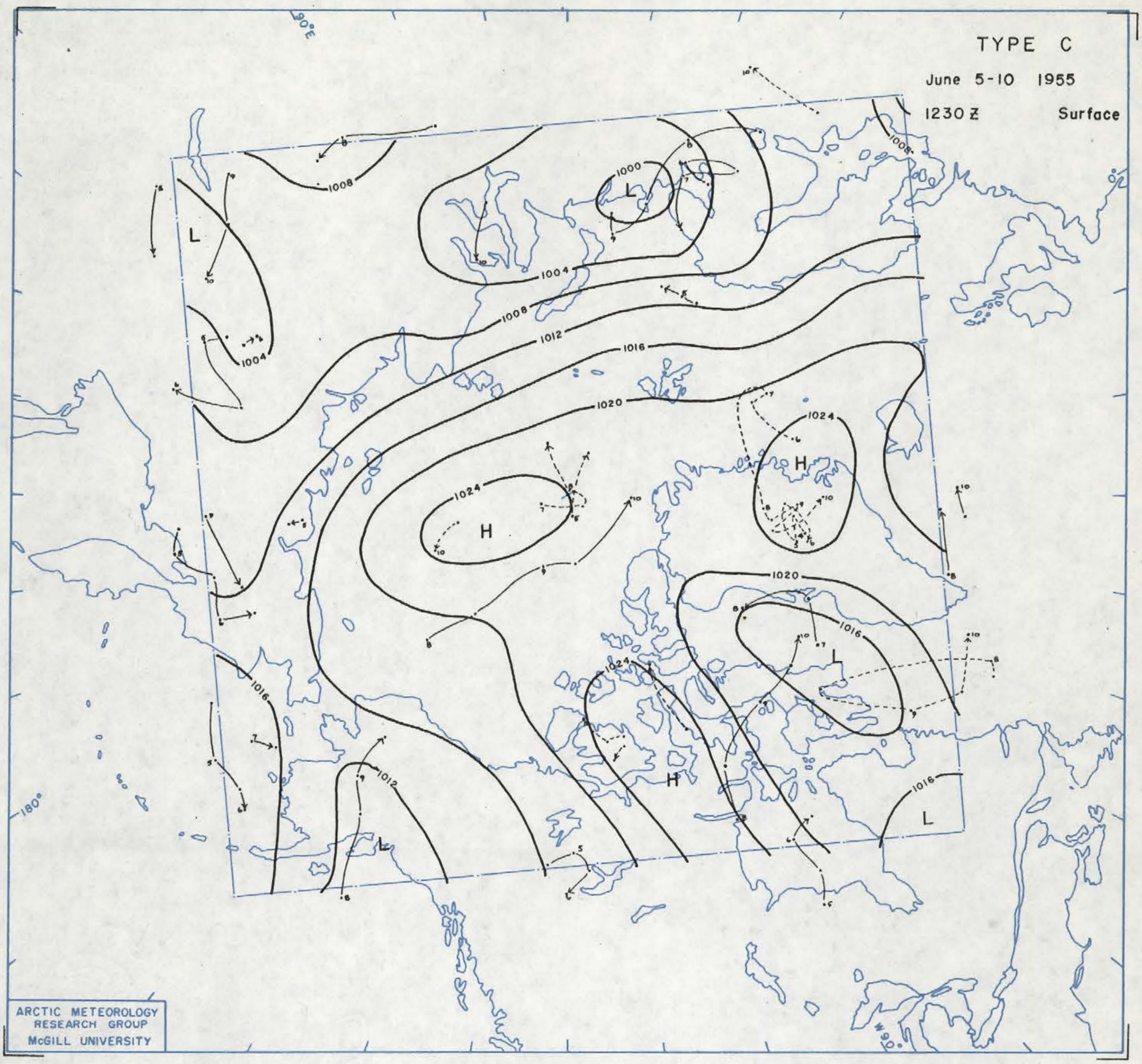

Map 15

The extensive anticyclonic system over the European-Greenland Sector on June 1-4 breaks down and the high extends over the Arctic basin. At 500 mb. there is a retrogression of the polar vortex during June 5-10 to an alignment from E. Siberia to W. Europe, and over Europe and Asia a corresponding tightening of the gradient. The surface lows associated with these strong upper air gradients are deep but elsewhere the systems are shallow and the circulation remains predominantly meridional. (The low which develops over the Arctic basin on June 8 has central values ranging from 1020 to 1015 mbs.) Between June 11 to 25 the circulation patterns become very amorphous. A number of shallow centres appear and disappear, comparable to the shifting patterns of a kaleidoscope. The variance of the whole chart remains throughout on the lowest level for the year.

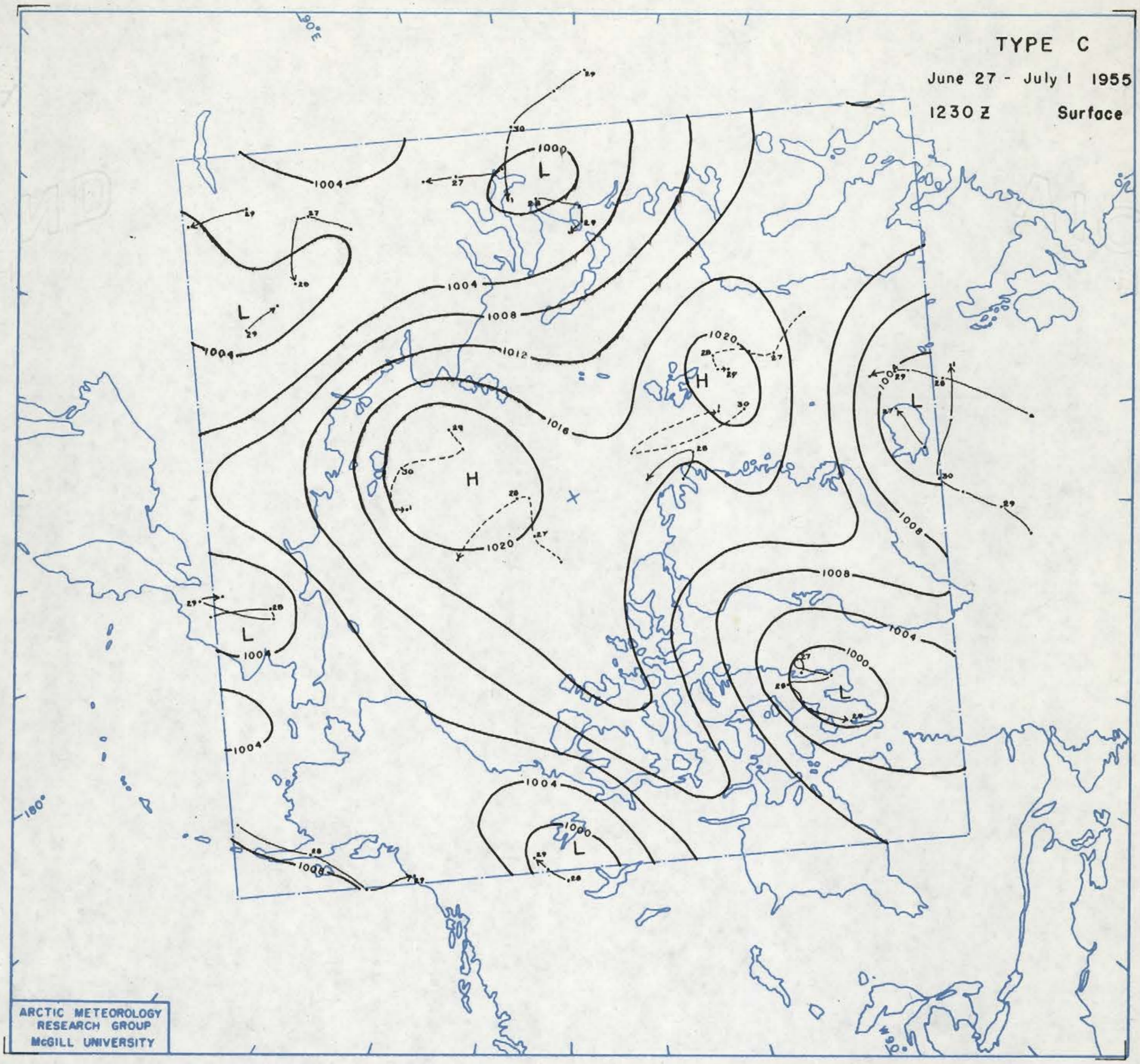

Map 16

After the restless quality of the circulation, by ~~July~~ June 27 the patterns have clarified once again and become more stable. In mid-June a low was centred over the Arctic basin much of the time, but by the end of June there has been a reversal to anticyclonic conditions. Map 16 is remarkably similar to Map 15 in spite of the changes which have taken place in the interval. During the middle of this period, the peripheral circulation becomes zonal, especially across the Atlantic, Eurasia and Alaska, but by July 2 it breaks down once again into a more meridional flow, and a trough deepens between Siberia and Baffin Bay below an upper air trough. Through the next six days the polar vortex at 500 mb. gradually becomes focused on the Greenland-Archipelago area and the gradients steepen.

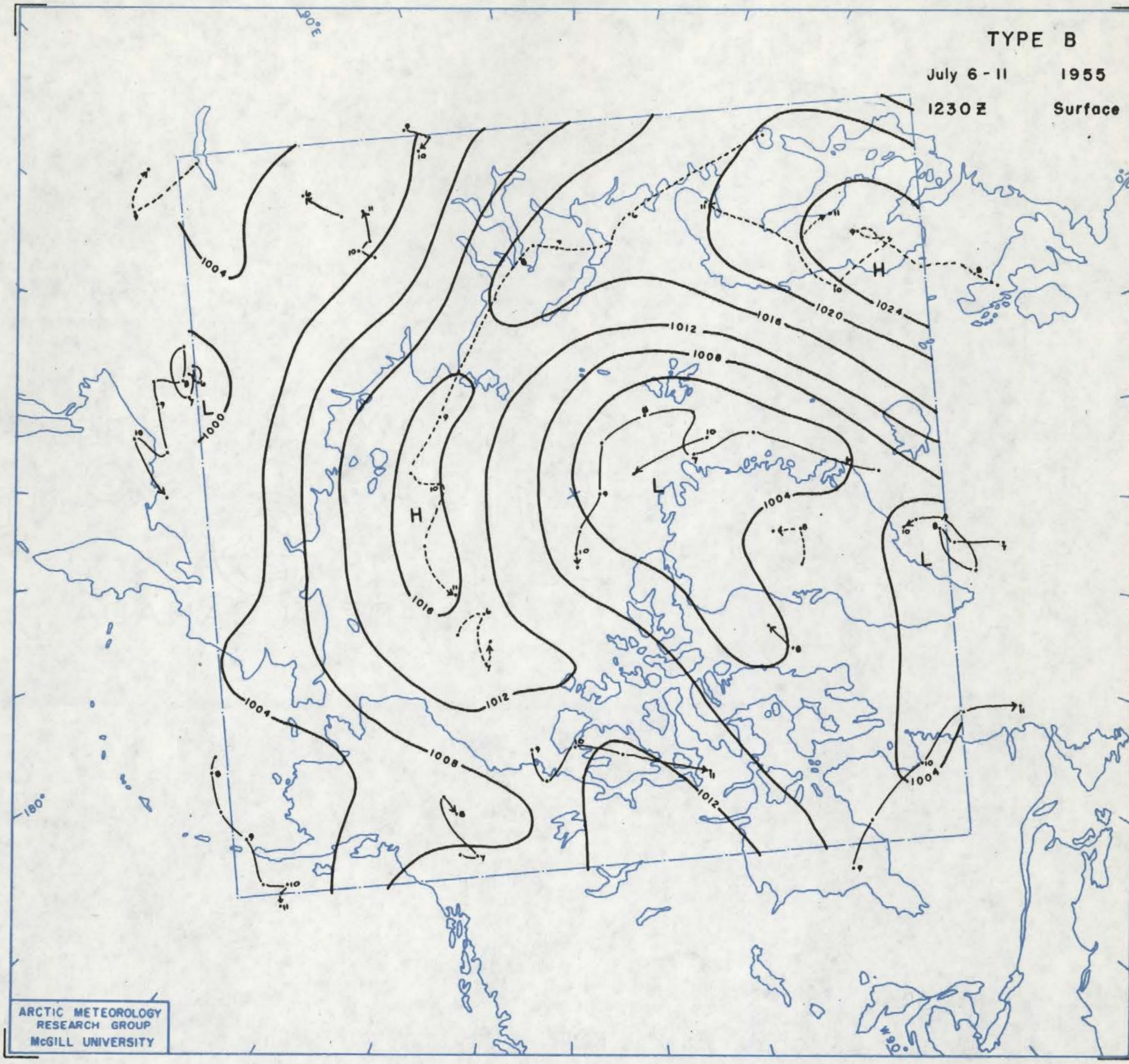

Map 17

By July 6 the anticyclone over N.W. Europe has extended a ridge to Novaya Zemlya, linking up with a centre of high over the polar basin. Cyclones are steered around the upper vortex over Greenland into the Arctic basin. Once again the surface map reflects the patterns of the 500 mb. surface. The charts for July 12 indicate the beginning of the breakdown of the ridge and the establishment of a low over the Arctic basin, associated with a shift of the upper air vortex to a more symmetrical position with respect to the pole.

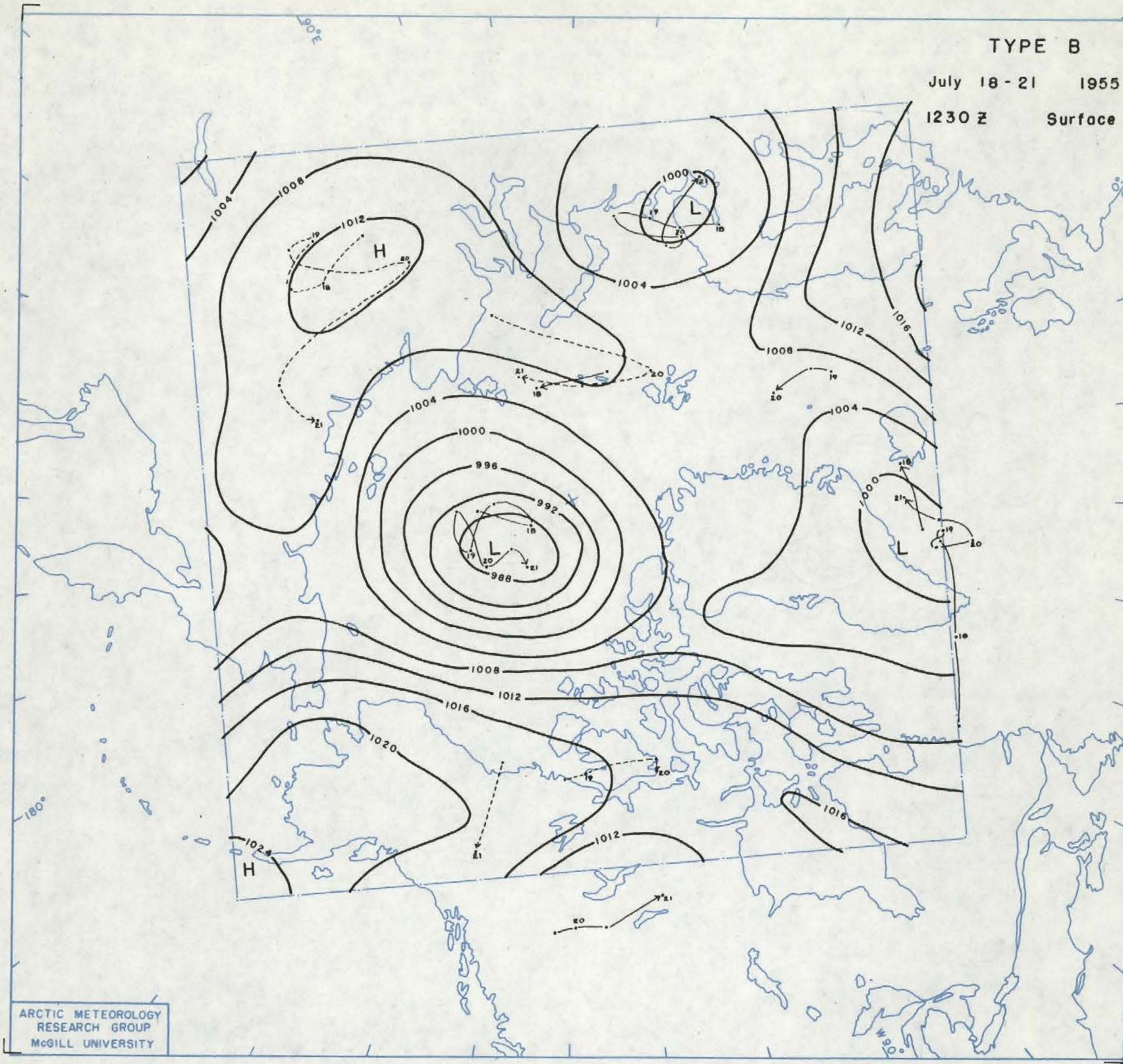

Map 18

By July 16 the polar vortex has contracted and there is strong zonal flow. Over Asia, however, there is a relaxation into meridional flow towards the end of the period. It is interesting that in spite of the high speed of the polar westerlies, synoptically the situation is very persistent. On the 22nd the polar vortex is centred eccentrically ~~asymmetrically~~ over Greenland and the Archipelago. The low over the Arctic basin moves to the W. Archipelago, and the anticyclone over Siberia extends into the Arctic basin.

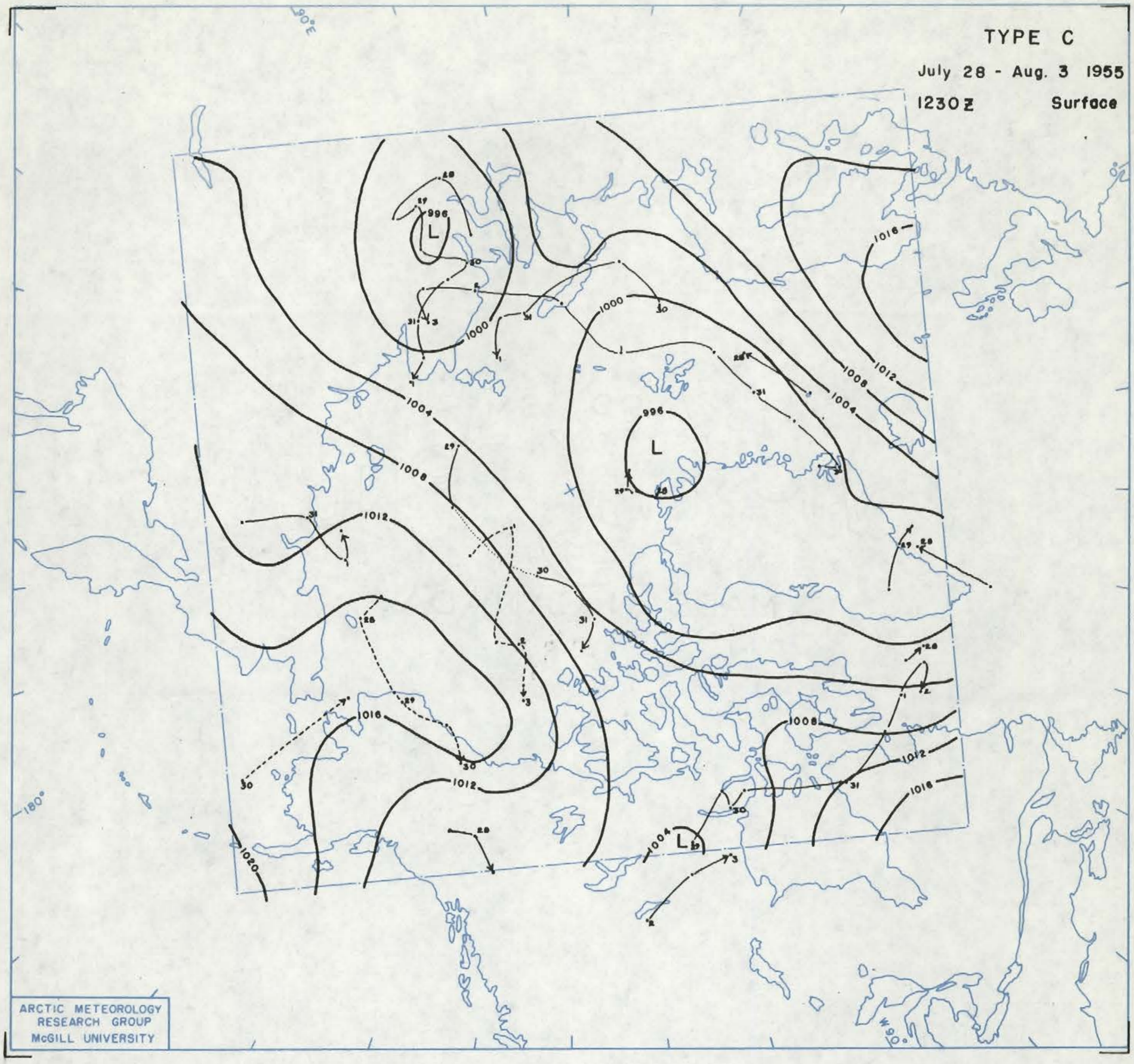

Map 19

By July 28 the 500 mb. polar vortex has become elongated from Siberia to S. Greenland. During this period there is considerable synoptic scale activity associated with the strong gradients of the vortex. Over E. Canada persistence is lower than elsewhere. In this area, there is an extension of high pressure on the first two days which gives way to the passage of cyclones during the remainder of the period. In spite of the C category of this map and the low variance, the large-scale systems appear to be adequately defined. The end of persistence is marked by the development of a number of centres and the patterns, although flat, become more complex.

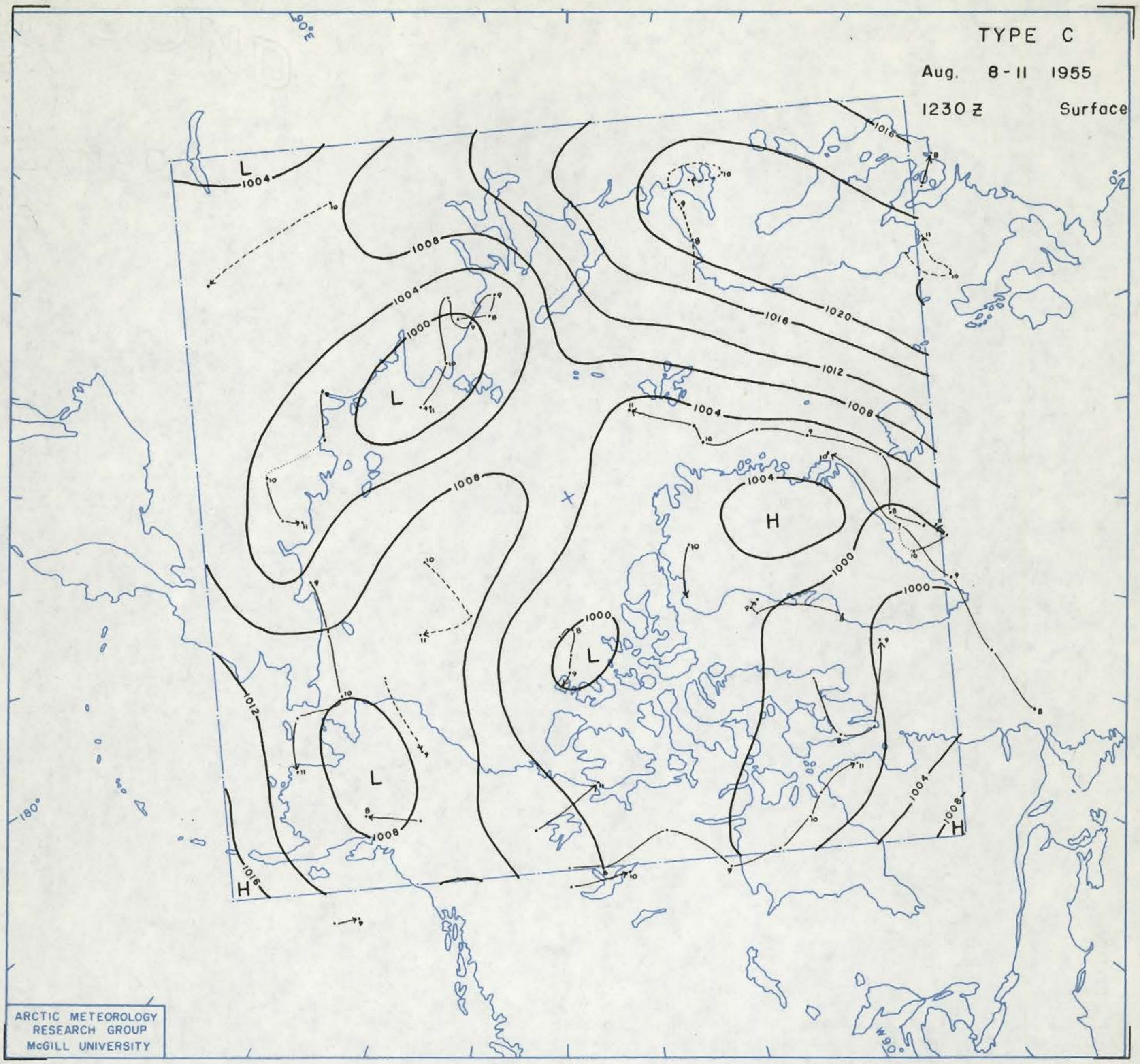

Map 20

The circumpolar jet continues to be further north than normal. There is considerable surface cyclonic activity connected with this flow and with the individual upper air low centres over the W. Archipelago, Tscheljuskin, and S. Baffin. A weak ridge extends over the Arctic basin linking the Scandinavian and Pacific highs. As persistence weakens on August 11 the wave length at 500 mb. shortens and the surface pattern increases in cellularity. A weak ridge develops between Greenland and Alaska, breaking the continuity of the large-scale system of lower pressure over this area.

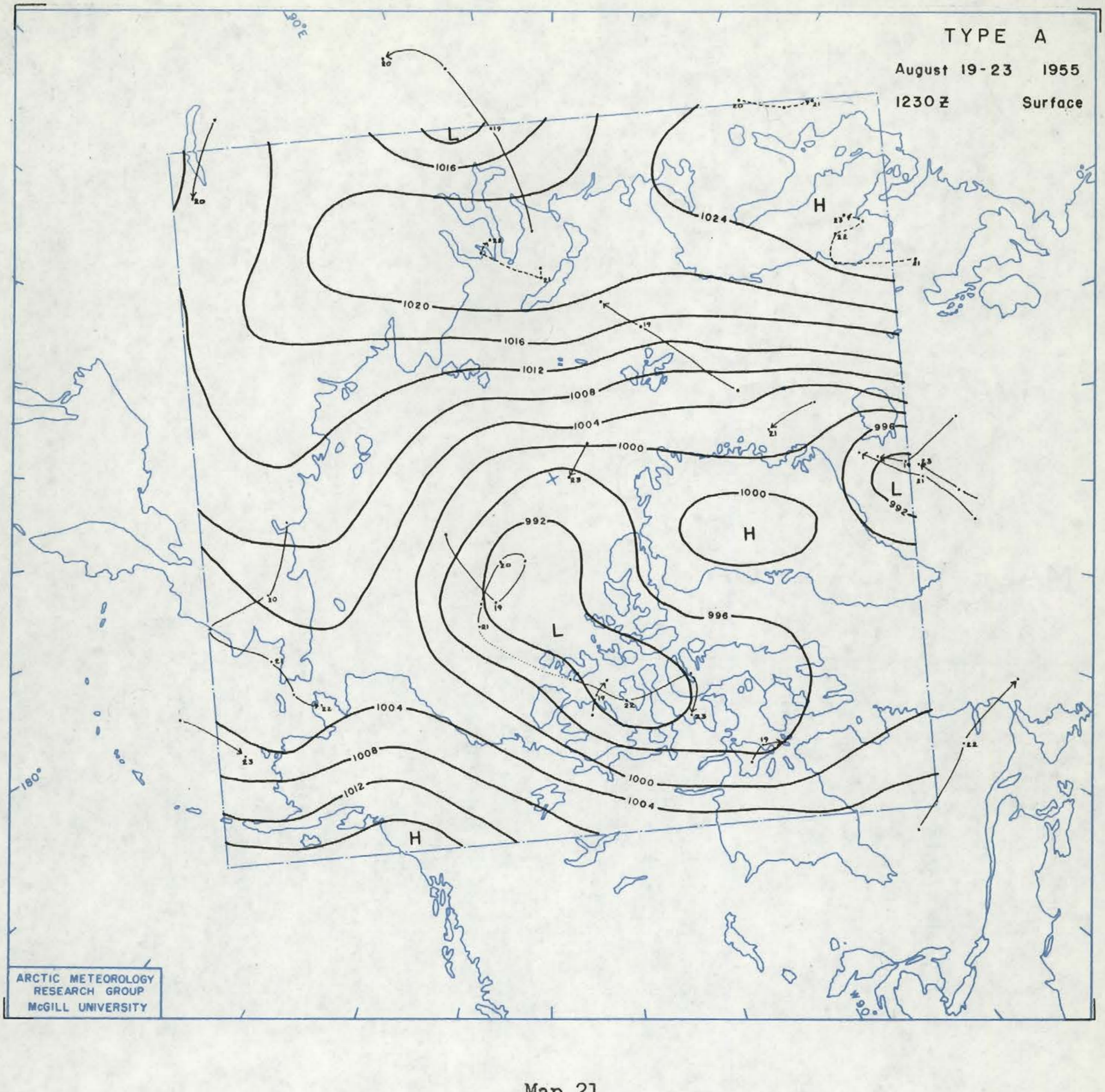

Map 21

After much fluctuation of ridge and trough, the wave lengthens at 500 mb. At sea level, lateral extensions of high pressure cover the continents, almost surrounding a central core of low pressure. Storms enter from the Atlantic and Pacific. The circulation patterns become highly stable from August 19 to 23. The upper air pattern is equally simple. Following these five days the persistence drops rapidly as the eastward progression speeds up, leading to a complication and reorientation of the pattern.

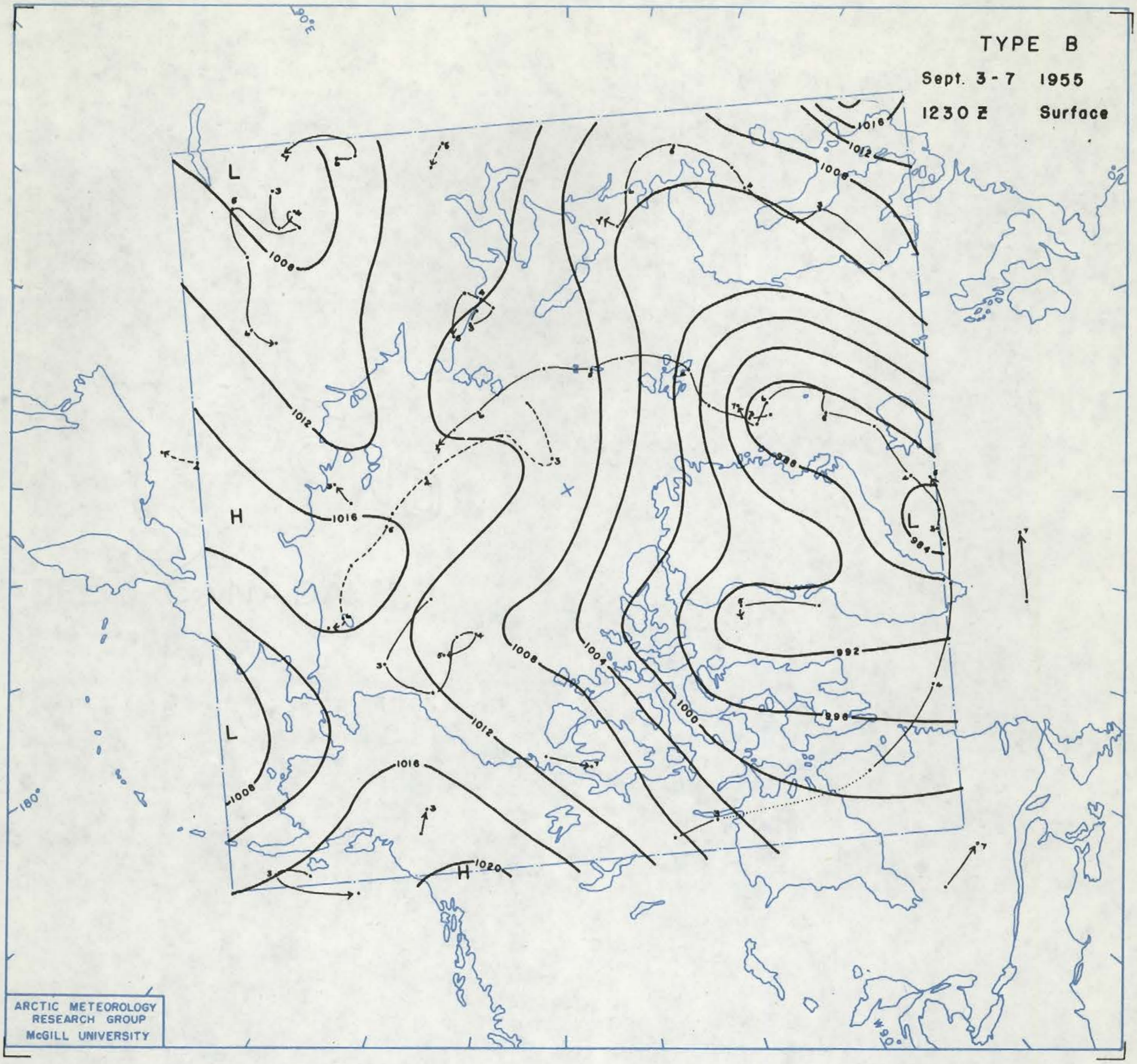

Map 22

At the end of August the polar westerlies weaken. On September 3 the main upper air vortex lies over Greenland and the E. Archipelago, with strong gradients from Hudson's Bay to Scandinavia. It is in this sector of the chart that persistence of the large-scale systems is most clearly marked. Over the Siberian-Alaskan Sector the amplitude of the upper air waves is greater and large-scale patterns are less well defined. A weak anticyclone crosses the Arctic basin in an easterly progression, the high over E. Siberia and Alaska weakens and a deep cyclone moves in from the Bering Sea. By September 8 the Scandinavian, Siberian and Pacific ridges extend northwards towards the pole and there is a slackening in the polar westerlies at 500 mb.

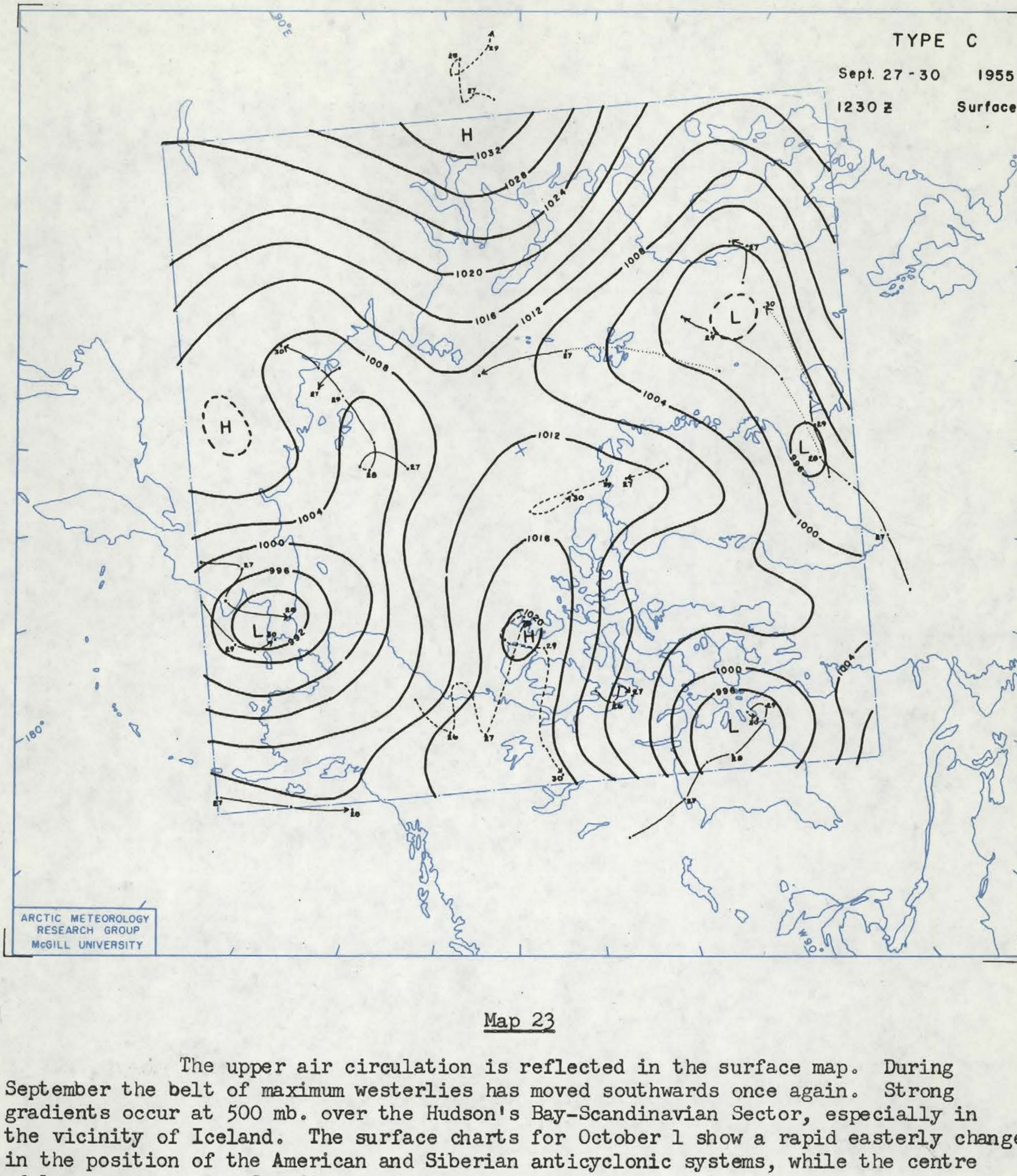

Map 23

The upper air circulation is reflected in the surface map. During September the belt of maximum westerlies has moved southwards once again. Strong gradients occur at 500 mb. over the Hudson's Bay-Scandinavian Sector, especially in the vicinity of Iceland. The surface charts for October 1 show a rapid easterly change in the position of the American and Siberian anticyclonic systems, while the centre of low pressure over Scandinavia deepens and extends.

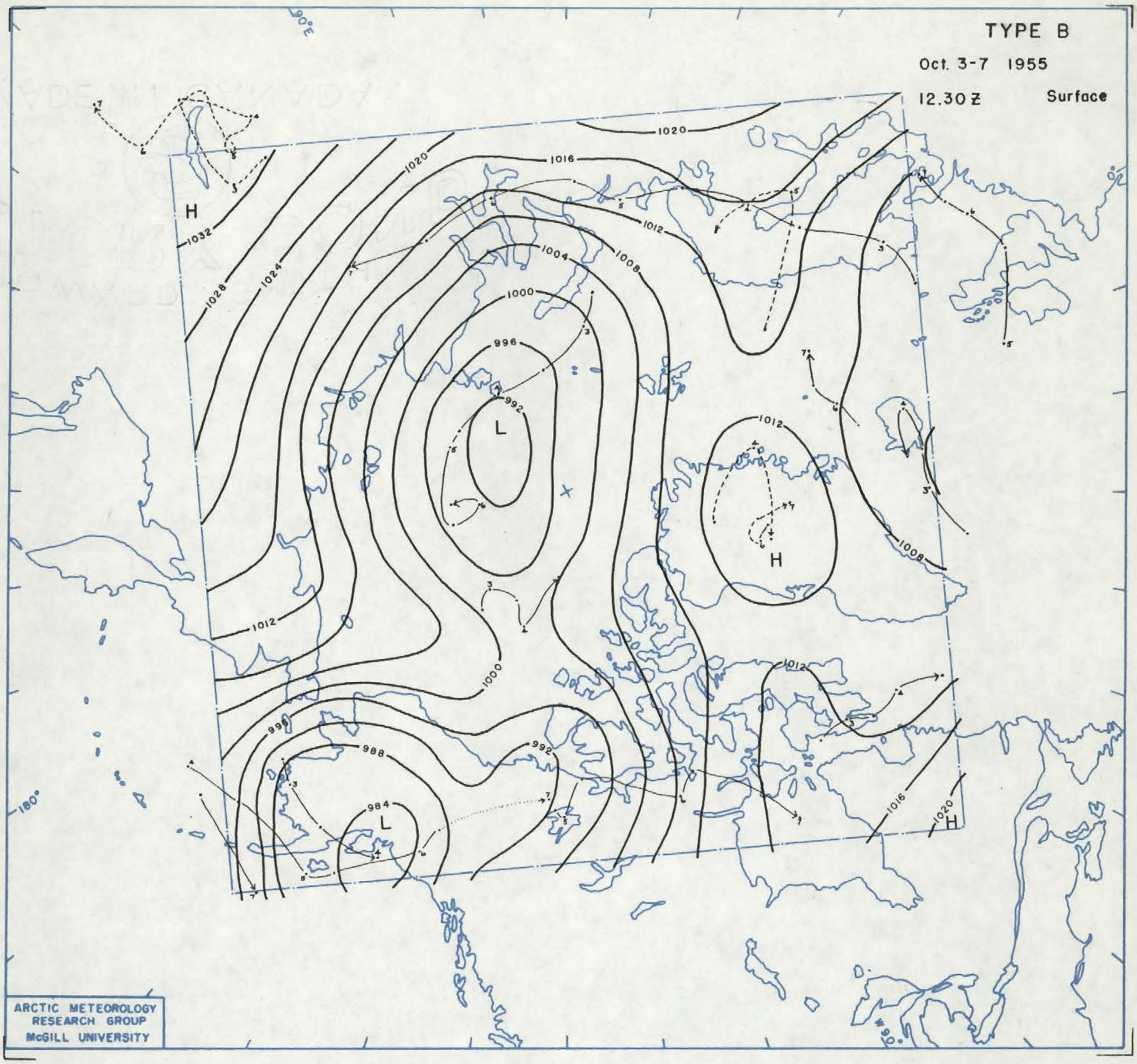

Map 24

Between October 2 and 3 there is a rapid change in the orientation of the 500 mb. low to a position from Svalbard to Alaska, and by October 4 a ridge has developed over Greenland linking the Scandinavian and American high pressure systems. During this period there is much synoptic activity associated with strong zonal flow aloft.

The charts for October 8 show a reversal from those for October 3 in several areas, owing to the eastward progression of both the Scandinavian high and the high over Labrador and the rapid eastward motion of the cyclones.

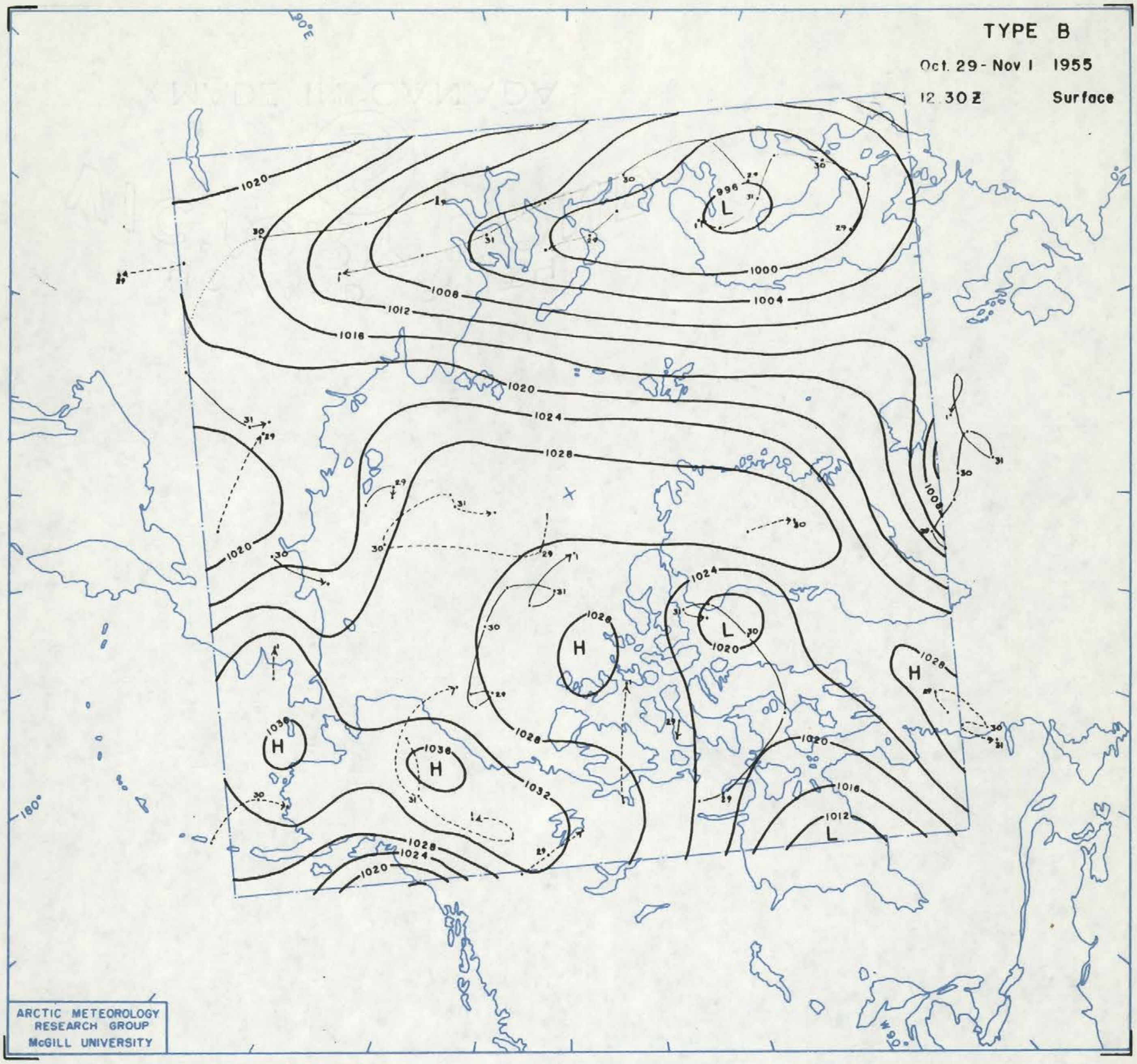

Map 25

At 500 mb. there is strong zonal flow ~~at 500 mb.~~ from Europe to Mongolia with the major cyclonic vortex elongated from Sakhalin to the Baltic Sea. Over the rest of the hemisphere flow is meridional. The breakdown in persistence at the beginning of November is connected with the slackening of the flow over Eurasia.

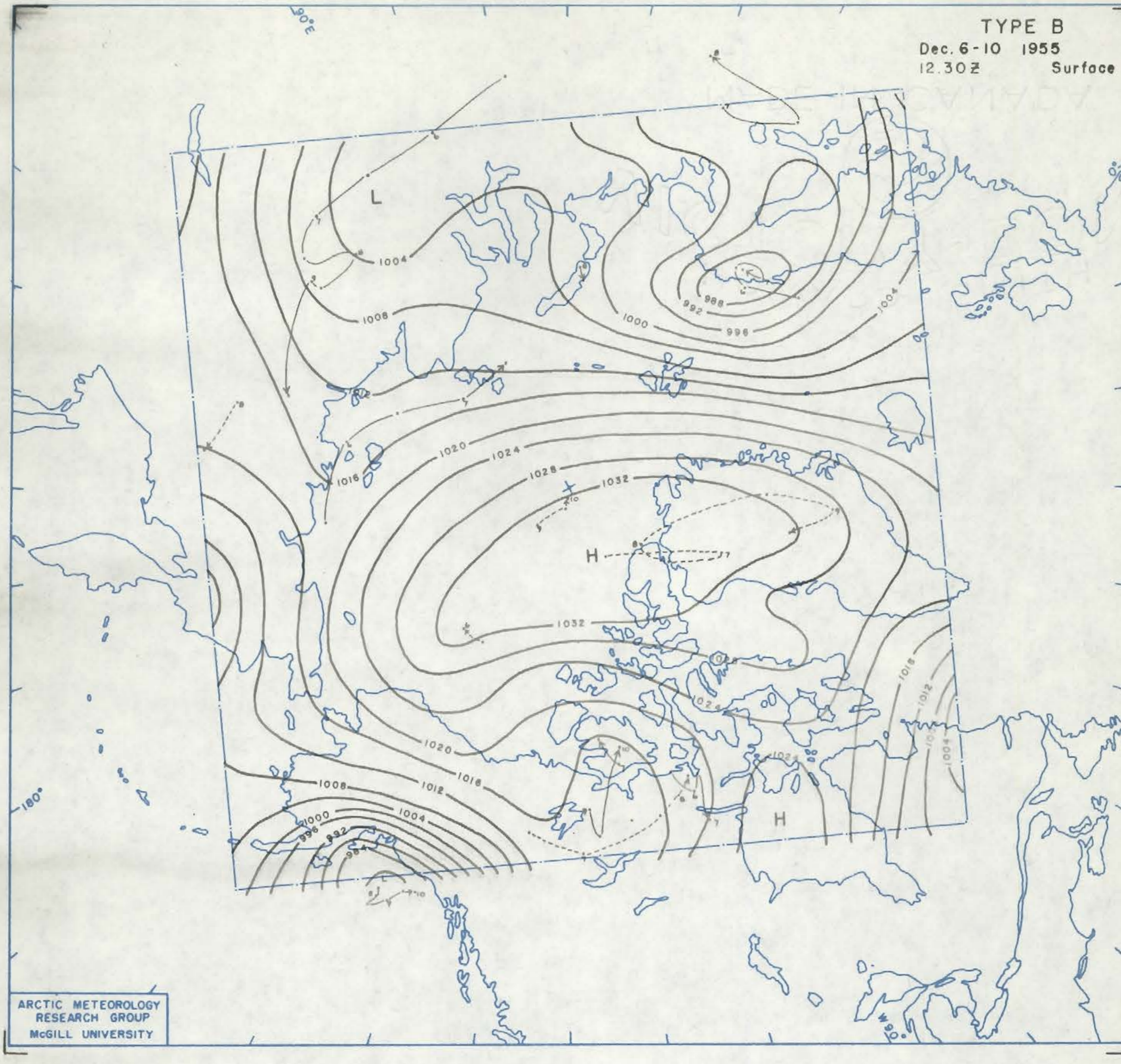

Map 26

The major cyclonic activity is associated with the strong upper air gradients around a large-scale low located between Baikal and the British Isles, while a similar system lies above the surface cyclones in the Alaska-Labrador area. Ridges of warmer air approach the Pole from the Pacific and Atlantic. The systems break down with the gradual poleward extension of ridges from Siberia, the gradual weakening of the N. Atlantic block, and strengthening of the Pacific ridge.

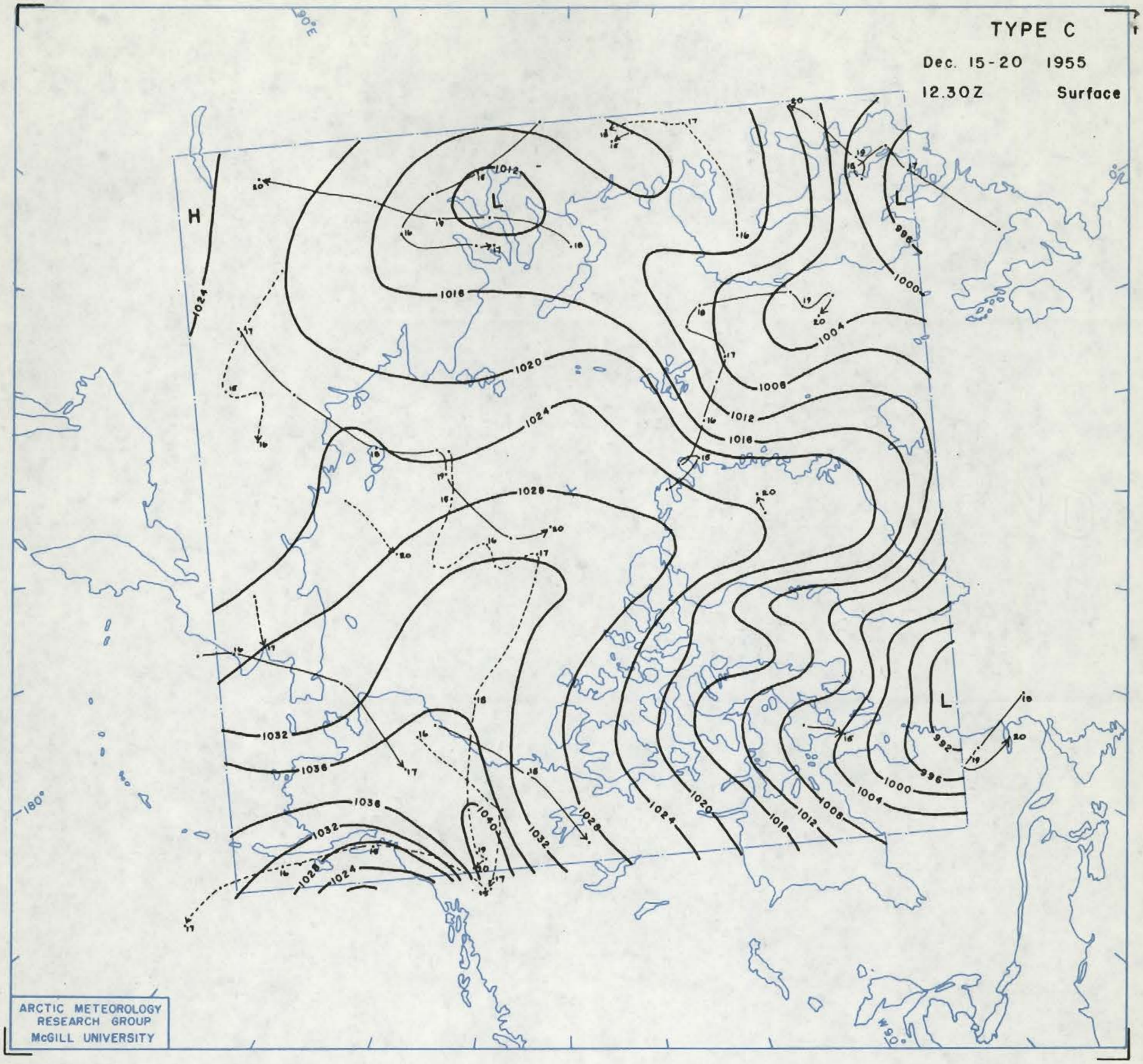

Map 27

This map is discussed in the text. The most remarkable feature is the degree of change over the Arctic basin as the centre of high pressure moves rapidly southwards over Alaska and a low pressure system replaces it, to remain almost to the end of December.

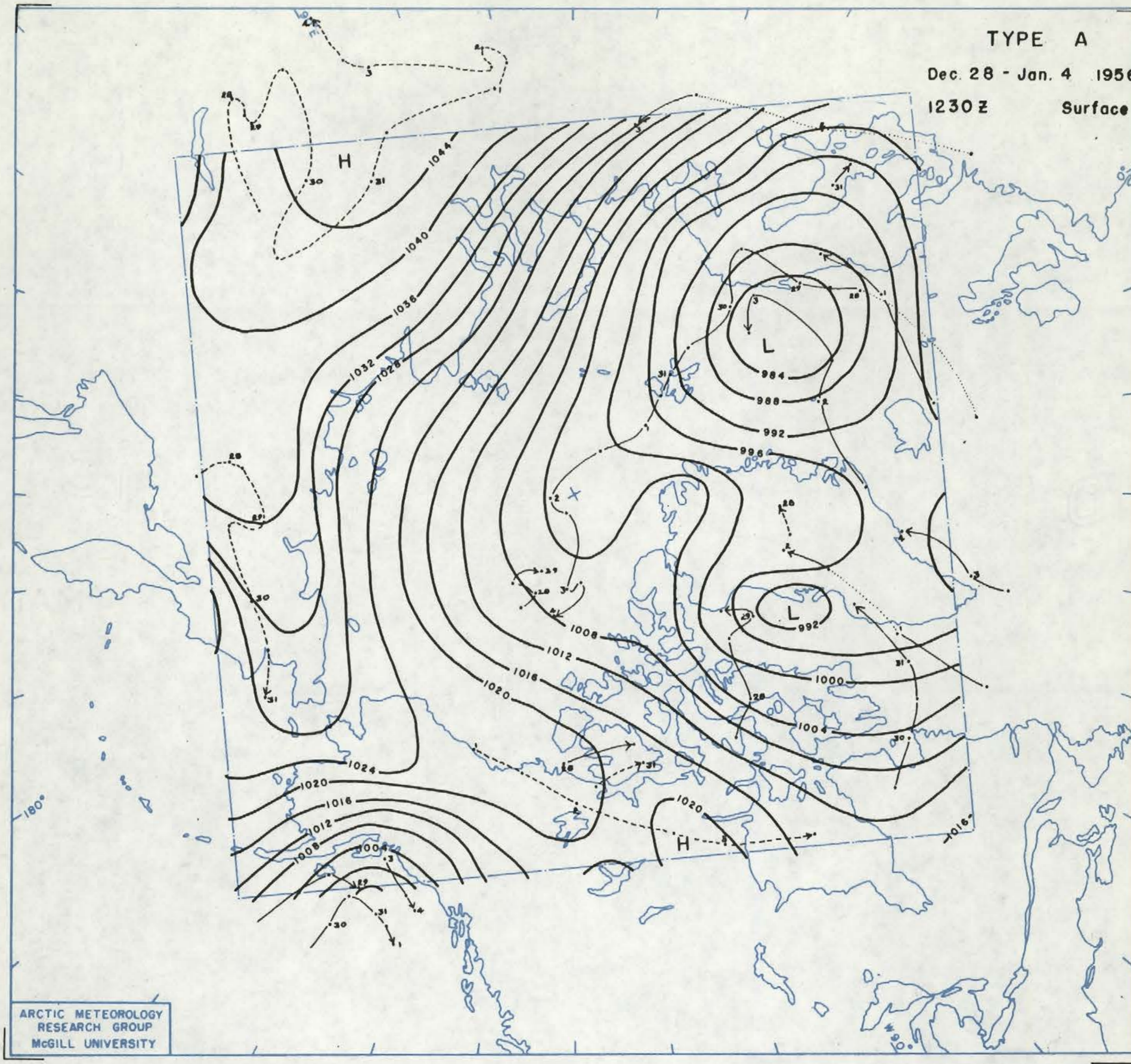

Map 28

During this period there is a gradual eastward change in the position of the main upper air low from the Arctic basin to E. Greenland. At the surface anticyclonic centres move across E. Siberia and Canada, while there is much cyclonic activity associated with strong upper air gradients. By January 5 this easterly progression has brought about a reorientation of the main systems sufficient to lower the level of persistence.

APPENDIX C

Surface Level

An Attempt to Relate Geomagnetic Indices

to Sea-Level Circulation Changes

DAY	$\bar{r}_1$	DAY	$\bar{r}_1$	DAY	$\bar{r}_1$
0		0		+13	.698
-1	.701	+1	.748	+14	.657
-2	.718	+2	.783	+15	.710
-3	.688	+3	.766	+16	.733
-4	.740	+4	.702	+17	.742
-5	.756	+5	.735	+18	.733
-6	.727	+6	.762	+19	.758
-7	.698	+7	.702		
-8	.718	+8	.772		
-9	.731	+9	.767		
-10	.692	+10	.752		
-11	.710	+11	.736		
-12	.755	+12	.739		

Mean Persistence Correlations (one-day lag) from 12 Days Before to 19 Days After the Key Days.

(These values were computed by means of Fisher's z' transformation.)

Table 2

KEY DAYS IN 1955

QUIET KEY DAYS				DISTURBED KEY DAYS			
January	10	July	4	January	9	July	2
	15		5		17		11
	24		19		18		12
	25		21		19		15
	26		28		20		26
February	1	August	1	February	4	August	4
	2		11		5		5
	10		22		22		6
	19		23		23		7
	27		25		28		28
March	1	September	11	March	7	September	5
	2		15		9		13
	3		21		22		27
	4		25		30		29
	29		26		31		30
April	16	October	12	April	5	October	5
	17		13		7		6
	18		18		27		25
	19		19		28		26
	23		24		29		31
May	17	November	3	May	6	November	4
	19		6		7		16
	21		7		8		18
	23		22		25		19
	24		23		26		20
June	5	December	13	June	8	December	1
	10		14		15		6
	21		18		16		25
	26		23		23		26
	30		29		24		27

Surface, 1955

Behaviour of $\bar{r}_1$ After the Five Quiet Days of Each Month   Table 3

KEY DAY − +	YEAR 60 Key Days	SUMMER 25 Key Days	WINTER 35 Key Days	JUNE/NOV 30 Key Days	DEC/MAY 30 Key Days
-3	.720	.722	.719	.694	.746
-2	.721	.720	.721	.692	.750
-1	.712	.704	.718	.666	.758
0					
1	.722	.709	.731	.678	.766
2	.720	.708	.729	.676	.764
3	.712	.694	.725	.663	.761
4	.717	.661	.744	.669	.766
5	.698	.661	.724	.642	.754
6	.684	.650	.708	.623	.744
7	.702	.684	.715	.658	.746
8	.703	.679	.720	.675	.731
9	.708	.689	.722	.669	.748
10	.709	.708	.710	.658	.760
11	.699	.682	.711	.671	.727
12	.719	.717	.721	.696	.743
13	.728	.721	.733	.709	.746
14	.735	.732	.737	.711	.758
15	.710	.683	.730	.664	.756
16	.719	.691	.738	.672	.766
17	.725	.662	.770	.672	.778
18	.730	.693	.757	.682	.779
19	.702	.673	.723	.659	.746

Surface, 1955

Behaviour of $\bar{\bar{r}}_1$ After the Five Disturbed Days of Each Month Table 4

KEY DAY − +	YEAR 60 Key Days	SUMMER 25 Key Days	WINTER 35 Key Days	JUNE/NOV 30 Key Days	DEC/MAY 30 Key Days
-3	.683	.678	.687	.660	.706
-2	.696	.687	.703	.674	.718
-1	.694	.635	.737	.647	.741
0					
1	.710	.636	.762	.662	.758
2	.701	.622	.757	.638	.764
3	.701	.640	.744	.645	.756
4	.719	.708	.727	.680	.758
5	.728	.722	.732	.684	.772
6	.719	.698	.733	.669	.768
7	.726	.713	.735	.691	.760
8	.728	.716	.738	.677	.780
9	.712	.702	.720	.660	.764
10	.707	.668	.735	.664	.749
11	.683	.644	.710	.628	.737
12	.688	.662	.706	.638	.737
13	.686	.682	.689	.639	.733
14	.708	.705	.711	.668	.748
15	.729	.724	.732	.702	.756
16	.734	.729	.738	.706	.763
17	.723	.714	.729	.691	.754
18	.704	.705	.703	.688	.720
19	.712	.690	.727	.698	.725